# FoxM1 in Liver Cancer

Akshay Pandey

B.Tech., Vellore Institute of Technology, 2008

**THESIS**

Submitted as partial fulfillment of the requirement for the degree of Doctor of Philosophy in Biochemistry and Molecular Genetics in the Graduate College of the University of Illinois at Chicago, 2017

Chicago, IL

**Defense Committee**

Pradip Raychaudhuri, Chair and Advisor

Angela Tyner

Karen Colley

Nissim Hay

Vadim Gaponenko

Deepak Shukla, Department of Microbiology, Ophthalmology, UIC

## Acknowledgements

At first, I would like to sincerely express my gratitude towards my advisor, Pradip, for his mentorship. Pradip's presence has been a very pivotal to my PhD training and to the successful completion of the presented work. I am very grateful to Dr Tyner, Dr Colley, Dr Hay, Dr Gaponenko and Dr Shukla for their guidance, inspiration and support throughout the course of this work. I would like to further extend my thanks to the Department of Biochemistry and Molecular Genetics for providing a superior educational experience and a scientifically stimulating environment

I would extend my thanks to my collaborators and friends; Dr Kopanja and Dr Chand for their significant contributions in the presented work. Working closely with Dr Kopanja and Dr Chand I gained insight into the intricacies of the experiments which helped me improve my scientific approach constantly. Without the help from the above-mentioned people it would have been much harder to render the project in the present form.

I would like to thank the past and present members of Raychaudhuri lab, esp., Dr Roy, Dr Carr, Dr Mukhopadhyay, Dr Wang, Dr Elangovan, Shuo Huang, Megan Kiefer, for their friendship and support.

Finally, I would like to thanks my grandparents, parents, family and friends for their belief in me to successfully complete this work. They have always been very supportive irrespective of the up and downs during this PhD.

## Author Contributions

The derivation of triple transgenic mice used in the study, FoxM1$^{fl/fl}$; HRasV12; MxCre and FoxM1$^{+/+}$; HRasV12; MxCre, and studies on CD90+ human HCC cells were carried out in collaboration with Dr. Dragana Kopanja, Research Assistant Professor, University of Illinois at Chicago. The human HCC patients tissue microarrays were kindly provided by Dr. Grace Guzman, Department of Pathology, University of Illinois at Chicago. Clonogenicity and soft agar assays were performed by Dr. Vaibhav Chand, Postdoctoral fellow, University of Illinois at Chicago.

Contents

## List of Figures

## List of Tables

## Summary

The work presented in this thesis elucidates the role of transcription factor FoxM1 in progression of hepatocellular carcinoma. In this work, I provide the genetic evidence that FoxM1 is important for progression and maintenance of liver tumors. Also, high FoxM1 expression leads to accumulation of poorly differentiated tumor cells by inhibition of liver differentiation factors.

I show here that deletion of FoxM1 from hepatocytes leads to regression of Ras induced liver tumors. This regression in number of tumor nodules was found to result from decreased proliferation, increased apoptosis and higher accumulation of reactive oxygen species in the HCC cells. Deletion of FoxM1 also leads to a disproportionate loss of liver cancer progenitor cells. The work also shows that the liver cancer stem cells are dependent on the expression of FoxM1.

Further, I show that FoxM1 inhibits the expression of liver differentiation genes FoxA1 and FoxA2 by silencing their promoters for transcription. This inhibition of FoxA factors leads to accumulation of poorly differentiated tumor cells and thus helps liver cancer progress to an aggressive phenotype.

# Abbreviations

| | |
|---|---|
| Ad | Adenovirus |
| Arf | Alternate reading frame |
| ChIP | Chromatin immunoprecipitation |
| DAPI | 4’,6-diamidno-2-phenylindole |
| DCFDA | 2’,7’ –dichlorofluorescin diacetate |
| DEN | Diethyl-N-nitrosamine |
| DNA | Deoxyribonucleic acid |
| DNMT3b | DNA methyltransferase 3b |
| FITC | Fluorescein isothiocyanate |
| FoxM1 | Forkhead box M1 |
| GAP | GTPase activating protein |
| GDP | Guanosine diphosphate |
| GFP | Green fluorescence protein |
| GTP | Guanosine triphosphate |
| HBV | Hepatitis B virus |
| HCC | Hepatocellular carcinoma |

| | |
|---|---|
| HCV | Hepatitis C virus |
| IHC | Immunohistochemistry |
| KO | Knock out |
| MAPK | Mitogen activated protein kinase |
| MEF | Mouse embryonic fibroblast |
| mRNA | Messenger RNA |
| NAFLD | Nonalcoholic fatty liver diseases |
| NASH | Nonalcoholic steatohepatitis |
| PCR | Polymerase chain reaction |
| Plk1 | Polo like kinase 1 |
| Rb | Retinoblastoma |
| ROS | Reactive oxygen species |
| siRNA | Small interfering RNA |
| WT | Wild type |

## Introduction

Cancer is one of the leading causes of death around the world. As documented in the year 2015, it caused 8.8 million deaths globally[1]. Liver cancer is 6$^{th}$ most common cancer type with a low 5-year survival rate[1]. There are projections by various health agencies that the number of new reported cases of liver cancer shall rise to 700,000 as well as the death toll due to liver cancer is projected to rise to 600,000 by the end of the year 2017. These numbers have almost increased by 200% since the 1980s and are projected to rise considerably in the coming years.

Several risk factors have been associated with development of liver cancer. Between both genders, liver cancer is much more common in males[2,3]. Liver cancer rates also vary with ethnicity, for example, in the United States, Asian Americans and Pacific Islanders have much higher incidence of liver cancer when compared with other ethnicities. People from African American and White ethnicities have the lowest incidence of liver cancer[2,3]. Chronic infections of hepatitis B virus (HBV) or hepatitis C virus (HCV) are the greatest risk factors associated with liver cancer [4–6]. The chronic infection leads liver cirrhosis from where liver cancer development becomes more plausible. The risk of liver cancer development becomes much greater when coupled with alcohol abuse (6 or more standard drinks per day). In fact, alcohol abuse is the leading cause of liver cirrhosis in the United States[7,8]. HCV is more prevalent in the United States whereas in the Asian countries HBV seems to be the major cause of infection [9]. Despite the advancements in treatment and prevention of hepatitis infections the incidences of HBV and HCV are on the rise. In the United States, as of 2016, more than 50% of liver cancer cases have also

been found to be positive for HCV whereas 15% of the cases were positive for HBV[5,10]. Hepatitis C and hepatitis B infections have also been on a rise (CDC). NAFLD (Non-Alcoholic Fatty Liver Disease) and NASH (Non-Alcoholic Steatohepatitis) have also been observed to contribute significantly to the development of the disease [7,8]. Contamination of food items with Aflatoxin, arsenic is associated with risk of liver cancer occurrence. Exposure to chemicals like vinyl chloride, thorium dioxide has also been associated with increased risk of liver cancer [11–13].

Cancer results from transformation of a normal cell into a tumor cell resulting in indefinite proliferation. In this multi stage process the cells, very often, acquire the ability migrate and colonize neighboring or distant tissue, thus becoming metastatic [14]. The deaths caused by cancer are primarily due to organ failure and metastasis, or the spread of primary tumor cells to other sites. Majority of deaths by liver cancer have been attributed to organ failure because of increased tumor load, however, incidence of metastasis leading to fatality has also been observed in liver cancer. The 5-year survival rate upon metastasis of liver cancer to distant parts is only 3% [1].

The rising numbers of liver cancer cases is very alarming and the disease must be understood at a molecular level to derive new therapeutic strategies for the cure. At this point no effective therapeutic is available – Sorafineb extends life only by around 3 months [15–18]. Dissection of the molecular basis involved in the disease progression will be impotant for understanding of how liver cancers acquire aggressive phenotype.

**RAS pathway activation in HCC**

Ras protein belongs to the family of small GTPases. Structurally, Ras protein has two conformations often referred to as 'ON' and 'OFF'. In the 'ON' state Ras is GTP bound and its intrinsic GTPase activity hydrolyses the gamma phosphate of the bound GTP and converts it to GDP. As Ras becomes bound to GDP it goes through a conformational change that switches it 'OFF'. Ras, when in 'ON' state, activates downstream signaling pathways that are involved in cell growth, differentiation and survival. Guanine nucleotide exchange factors (GEFs) and GTPase activating proteins (GAPs) facilitate the exchange of nucleotides. As the intrinsic GTPase activity of Ras is too low for physiological purposes, it is assisted by GAPs, that acts as a catalyst, to hydrolyze the gamma phosphate group[19–22].

Active or GTP bound 'ON' Ras activates signaling pathways involved in proliferation and survival, thus, over or constitutive activation of Ras can lead to the development of cancer[23–25]. This is true in the case multiple cancers such as pancreatic cancer, colon cancer[26,27]. Ras pathway is found to be ubiquitously active in hepatocellular carcinoma[23]. Mutations at multiple residues of Ras (such as G12 – common, Q61- rare, but observed) have been attributed with constitutive activation of this protein. Activating Ras mutations have been commonly observed in pancreatic adeno carcinoma, colorectal carcinoma, non-small cell lung carcinoma and others, however, they contribute to only 5% of HCC cases. Ras pathway is ubiquitously active in HCC either because of silenced Ras regulator proteins or attenuated GAPs levels [28].

RASSF1A (Ras associated domain containing protein - 1) and NORE1B (RASSF5 - Ras associated domain containing protein - 5), effector proteins for Ras and identified tumor suppressors, have been found to be silenced in majority (97%) of HCC cases [29–32]. These Ras effector proteins relay the signal downstream to signaling pathway that regulate cellular processes of mitosis, cell adhesion, cell cycle arrest, apoptosis etc. Epigenetic silencing of RASSF1A and NORE1B genes renders them transcriptionally inactive and is carried out by hyper methylation of CpG islands that mark the promoters of these genes [31,33,34].

Ras GTPase proteins (or GAPs) RASAL1 (Ras protein activator like - 1, GAP1 subfamily), DAB2IP (DAB Interacting Protein), NF1 (Neurofibromin) are found to be silenced in more than 70% of reported HCC cases [28,35,36]. This epigenetic silencing of the GAPs is a result of inappropriate promoter methylation. In about 40% of HCC cases, PITX1 (paired like homeo domain - 1 protein), a transcription factor that activates the expression of RASAL1 gene, is also epigenetically silenced by promoter hyper methylation [37,38].

The silencing of GAPs leads to increase in the active or GTP bound Ras protein leading to hyper activation of downstream signaling pathways. Since Ras effector proteins that are involved in the regulation of cell cycle arrest, apoptosis etc. are silenced in most HCCs (97%), hyperactivation of Ras signaling pathway leads to unchecked proliferation and cell growth leading ultimately to tumor development [35,39].

Hyperactive Ras signaling in multiple cancers makes it an attractive target for cancer therapy. Ras requires post translational modification by farnesyl transferase to localize to

the plasma membrane to relay the signals. Farnesyl transferase inhibitors or FTIs that mimic CAAX carboxy terminus motif of KRas compete for the binding with farnesyl transferase and prevent Ras signaling from being activated [40]. It has been observed that in absence of farnesyl transferase modification on Ras, geranylgeranyltransferase (GGT) modifies Ras to carry out its biological activity [41]. GGTs are also known to modify the CAAX motif. This is one of the reasons why the early potential of FTIs has not been observed [42]. The combinatory therapy involving both FTIs and GGTIs has shown some promise, but results in greater toxicity levels [43]. Inhibition of Ras signaling pathway has also utilized kinase inhibitor molecules both upstream and downstream of Ras protein. The most popular kinase inhibitor to date is Glivec and has provided a leap forward in chronic myeloid leukemia [44–46]. Kinase inhibitors of MEK1 and 2 have been developed and has shown to inhibit MAPK-ERK signaling [47]. Inhibition of receptor tyrosine kinases (upstream of Ras) esp, ERBB2 and EGFR has proven to be effective against hyperactivation of Ras signaling. Several small molecule inhibitors against the tyrosine kinases are in clinical trials, and antibodies targeting ERRB2 are used with partial success in breast cancer [48–50]. This targeting of ERRB2 only works for the cells harboring WT Ras protein; in case the protein is mutated for constitutive activation targeting ERRB2 shall not be therapeutic. Antisense oligonucleotides sequences targeting Ras and Raf have also been used in studies with a certain degree of success [51,52]. The delivery of the large oligonucleotides becomes very difficult in the solid tumors and decreases the efficacy significantly [51,53]. Despite targeting Ras pathway at multiple nodes, the downstream effector proteins in some cases have shown aberrant activation through alternative

mechanisms and has led to increase cell growth [42,43]. This makes successfully targeting Ras very difficult.

**Cancer Stem Cells**

Stem cells are characterized by their property to self-renew and differentiate; i.e., stem cell can give rise to a daughter cell (upon cell division) which is either identical – self-renewal, or can change its nature to serve a specialized function – differentiation [54]. The adult and embryonic stem cells are similar in this context. Adult stem cell niches are classified into quiescent and active subgroups; active subgroup is responsible for everyday tissue turnover and the quiescent subgroup helps in regenerative response to an injury [55,56].

Cancer cells that reflect these properties are termed as cancer stem cells (CSCs) [57]. These are also often considered to be the 'tumor initiating cells' as it has been shown in multiple studies that very few cancer stem cells can give rise to a tumor mass in mice [58–60]. This holds true even upon serial transplantations demonstrating the self-renewal property of cancer stem cells. Some scientists prefer to call these as 'tumor propagating cells' as opposed to 'tumor initiating cell' as per them the cancer stem cells are already 'initiated' and merely propagate the phenocopy of the primary tumor as determined by examination of the tumor heterogeneity in serial transplantation experiments [61].

First evidence of cancer stem cells was discovered in hematopoietic malignancies in the mid-90s, since then evidence of cancer stem cells have been found in multiple cancers [57,62]. The identification of these cells is based on the presence of certain cell surface

markers such as CD133, CD44 etc. The cell surface markers used to identify the group of CSCs vary from tissue to tissue, i.e., liver cancer stem cells markers may not be the same as the cell surface markers of colon cancer stem cells. Colon cancer stem cells (CCSCs) have been found to be positive for CD133, CD44 (Hyaluronic acid receptor), CD166 (adhesion molecule) and Aldh1 [63,64]. Pancreatic cancer stem cells (PCSCs) have been identified with CD24, CD44, ESA expression, and have been shown to give rise to tumor, however, another distinct subset of cancer stem cells has been identified which were found to be CD133 and CXCR4 positive [65]. Breast cancer stem cells (BSCSs) have been identified with an expression of CD44, CD24 and CD133, however, some BCSCs show the presence of a different cell surface marker – Aldh1 (Aldehyde dehydrogenase) [66–68]. This also demonstrates the existence of more than a single cancer stem cell niche within the same tumor type.

Studies have shown the presence of cancer stem cells in liver cancers. These liver CSCs have been well characterized in human and mice. CD90+ liver cancer cells have been found to mimic stem cell like properties in humans. A low number of CD90+ cells from multiples human HCC cell lines have been shown to generate tumor mass within a span of 1-4 months as shown in a study by Yang et.al. demonstrating the high tumorigenic capacity. Incidence of metastasis was also observed in some cases [69]. It was found that that the number of liver CSCs isolated from HCC cell lines directly correlated with the number of tumor incidences and metastatic potential. It was observed that inhibition of CD44 led to attenuation of the tumorigenic potential of CD90+ liver cancer cells as well as induced apoptosis of CD90+ cells [69].

Presence of cancer stem cells have been associated also with the incidence of metastasis. Studies have suggested that epithelial to mesenchymal transition (EMT), a process often required for tumor cells to disseminate from the primary site, can help differentiated tumor cells to de-differentiate to a cancer stem cell like state, so that the disseminating cells may propagate the tumor phenocopy at a distant site in the body[61,70–72]. Some studies have also associated certain sub populations in the CSC compartment directly with metastasis. In pancreatic cancer, the PanCSCs compartment identified with CD133 expression has a subpopulation that co-expresses CXCR4 (Chemokine receptor type 4, also known as fusin or CD184 is a receptor for SDF-1)[73]. This double-positive subpopulation has been shown to possess a high metastatic potential. These PanCSCs were shown to give rise to circulating tumor cells (CTCs) which later established metastatic lesions at a secondary site. Depletion of the CD133-CXCR4-double positive subpopulation by CXCR4 inhibitor prevented the formation of metastatic lesions in an *in vivo* orthotopic model of pancreatic cancer[65]. Similarly, in breast cancer, two different compartments of BCSCs identified with CD44, CD24 and Aldh1 cell surface markers, are found to be distributed differentially amongst the breast cancer subtypes. The $CD44^{+}CD24^{-}$ sub population in enriched in more than three fourth of basal-like breast cancer cases whereas the $Aldh1^{+}$ sub population was enriched in only around 35% of basal like subtype. The $Aldh1^{+}$ is also prevalent in Her-2 over expressing breast cancers[66,68]. These observations suggest that different CSCs subpopulations carry out different specialized functions.

Cancer stem cells have many features that help them evade the effects of chemotherapy and radiotherapy leading to relapse of the disease. In the case of breast cancer, the BCSCs have evolved various drug resistance mechanisms, e.g., these express some members of ABC family of proteins, such as glycoprotein P and MDR1 which are involved in multi drug resistance, at high levels leading to shunting out of the drug molecules before they can get metabolized thus protecting the cells from the effects of the drug[74,75]. Dysregulated expression of Aldh1 in BCSCs is indicative of radio resistance as is helps in keeping ROS in check and attenuates the oxidative stress[76]. High ROS scavenging and good DNA repair mechanisms, common traits amongst CSCs of different origin, are very helpful to CSCs in resisting the effects of the drugs[77–79]. Cancer stem cell targeted therapy has been suggested to prevent cancer metastasis and relapse of the disease, however, it has been proven to be a difficult problem thus far.

**FoxM1 in development and cancer**

FoxM1, a transcription factor belonging to the family of forkhead box proteins, is important for embryonic development[80–82]. FoxM1 is expressed liver development, however, its expression is highly diminished in adult livers. HCCs show a high expression of FoxM1, and over expression of FoxM1 also correlates with high grade progression of liver cancer[83].

FoxM1 transcriptionally activates expression of several genes that are directly involved in cell cycle phase transitions[81,84]. FoxM1 activates the expression of Cdc25A and Cdc25B involved in G1/S and S/G2 transitions respectively. It also regulates expression of proteins

involved in mitosis, such as Polo like kinase 1, AuroraB, Survivin etc. FoxM1 is expressed only by the dividing cells and its expression ranges from undetectable to low levels in adult cells; FoxM1 is highly expressed in embryonic tissues whereas its expression is reduced in adult tissues with exceptions of the tissues with high proliferative index such as testis, intestine etc. FoxM1, therefore, is referred to as a 'proliferation specific transcription factor'[85].

FoxM1 plays a very crucial role in early development. Knocking out FoxM1 in mice results in embryonic lethality attributed to multiple defects in development of several crucial organs such as heart, liver lungs etc. Conditional knocking out of FoxM1 from different tissues in mice has suggested that FoxM1's role is cell specific[80].

Knocking out the gene from hepatoblasts in mice using AFP-cre results in embryonic lethality by E18.5 due to several defects in the development of liver including improper development of hepatic chords, absence of proper intra hepatic bile duct network and defects in vasculature in the liver [80,83]. There was a 75% reduction in the hepatoblast population of embryonic livers deleted for FoxM1, mainly due to defects in DNA replication and mitosis [80]. This decrease in the population of hepatoblasts is the reason behind the multiple defects observed during liver development of FoxM1 knockout mice[83]. Conditional knocking out of FoxM1 from pancreas using Pdx-1 cre in mice does not result in embryonic lethality and shows a rather normal embryonic development of pancreas, however, these mice develop diabetes later in life as FoxM1 deletion causes post-natal defects in expansion of the beta cell mass leading to impaired islet functioning[86].

Though FoxM1 expression in dormant in the adult tissue, it can be activated upon an injury. Absence of FoxM1 expression in multiple organs has been studied in context of tissue regeneration upon injury. Deletion of FoxM1 in hepatocytes showed an impaired repair upon partial hepatectomy which was found to result from diminished proliferation of these cells[87]. FoxM1 deletion in endothelial cells resulted in decreased proliferation and reduced vascular repair in lungs following injury induced by LPS treatment[88]. Deletion in pancreatic epithelial cells led to decreased proliferation of alpha and beta cells but not acinal or ductal cells upon partial pancreatectomy[75]. Intuitively, induced expression of FoxM1 has shown to assist recovery upon injury as suggested by several studies. Expressing FoxM1 under Rosa26 promoter resulted in enhanced proliferation of respiratory epithelial and endothelial cells upon lung injury induced by BHT treatment[89]. Similarly, targeted expression of FoxM1 in hepatocytes (TTR-FoxM1b) resulted in increased proliferation of hepatocytes following carbon tetrachloride treatment[90]. FoxM1 overexpression in the same mouse model resulted in protection of mice from decline in liver regeneration capacity with age suggesting that FoxM1 is potential therapeutic target for age associated defects in liver regeneration.

FoxM1 is also important for the regulation of oxidative stress in transformed cells[91]. Regular metabolism of oxygen produces ROS in low concentrations in order for the cells to carry out physiological processes such as homeostasis[92]. Optimal level of ROS is also critical to self-renewability of stem cells[93,94]. Increased concentration of ROS is well known to lead the cell fate to necrosis, apoptosis or senescence, but this is checked by the expression a network of anti-oxidants genes or ROS scavenging genes such as MnSOD,

Catalase and PRDX3. The expression of FoxM1, which is known to directly regulate the expression of some of the ROS scavenging genes[91], is found to be activated by free radical species or ROS. Thus, increasing ROS concentrations in cells lead to increased levels of FoxM1, leading to increased expression of ROS scavengers, which in turn keep a check on rising ROS concentration in a feed-back loop[95]. High concentration of ROS is common in cancer cells; to counteract the oxidative stress produced by increased ROS concentrations, cancer cells depend on high expression of FoxM1, and thus are 'addicted' to high FoxM1 expression.

It has been observed that growth factors and oncogenes activate the expression of FoxM1 through the upstream proliferative signals, whereas, tumor suppressor proteins such P53, Rb and Arf have been shown to inhibit FoxM1's transcriptional activity[96–98]. Activated Ras increases FoxM1 expression by JNK1 which is activated by reactive oxygen species. P19Arf in mice has been shown to directly bind to FoxM1 protein and translocate it to the nucleolus, where it is rendered transcriptionally inactive. Use of small peptide that mimics the essential portion of Arf protein required for FoxM1 translocation has shown to inhibit FoxM1's transcriptional activity[99].

Increased expression of FoxM1 leads to increase in tumorigenicity and has been demonstrated in multiple *in vitro* and *in vivo* studies[100–102]. As FoxM1 is a critical regulator of the cell cycle and provides protection to cells from oxidative stress, its over expression enables the transformed cells to proliferate faster and thrive well even in the presence of oxidative stress, making them robust for survival and propagation. Attenuating the expression of FoxM1 using siRNA has resulted in decrease of the number soft-agar

colonies in multiple human cancer cell lines, whereas, it's over expression has led to increase in the number of soft agar colonies[100,103].

FoxM1 regulates the expression of matrix metalloproteinases MMP2, and MMP9 and vascular endothelial growth factor or VEGF, factors that are critical to cell invasion and vascularization of tissue[104]. These are also required by tumor cells to initiate their dissemination from primary tumor site. Thus, implicating FoxM1's requirement in early steps of metastasis. FoxM1 has also been shown to activate the expression of genes which regulate the process of EMT [95,105–108]. In different models of the disease including breast cancer, pancreatic cancer, glioma and others, over expression of FoxM1 has led to the acquiring of a mesenchymal phenotype by activation of mesenchymal markers such as ZEB1, ZEB2, Vimentin and Snail[95].

Once the tumor cells disseminate from the primary site and invade into the blood vessels, assisted by FoxM1 in early metastasis process, the circulating tumor cells (CTCs) need to establish a secondary colony which is dependent on several factors including a favorable microenvironment at the secondary site[95]. FoxM1 has been shown to help in establishing a pre-metastatic niche for CTCs in DEN induced mouse HCC. Park et.al. showed that by over expression of FoxM1 in Arf-/- HCC cells can lead to increased secretion of Lox (Lysyl Oxidase) and Lox2 (Lipoxygenase 2) enzymes, both of which have been previously implicated in establishment of pre-metastatic niche. These cells when injected subcutaneously in mice gave rise to metastatic lesions. Inhibition of the enzymes did not lead to metastasis, however, had no effect on the tumorigenic potential of the cells. The genes LOX and LOX2 have been found to be under direct regulation of FoxM1[109]. Since

presence and involvement of FoxM1 is important to the multiple steps of metastasis such as cell migration, EMT, pre-metastatic niche formation, it is referred to as a 'Master Regulator of Metastasis'.

Pathological examination of metastatic tumors possessing an aggressive phenotype reveals that the aggressive tumors have a much higher accumulation of poorly differentiated cancer cells in comparison to non-aggressive tumors. In fact, presence of higher number of poorly differentiated cells in tumor biopsies of patients is indicative of poor prognosis[110,111]. Poorly differentiated tumor cells have mesenchymal properties that make them more motile as compared to well differentiated tumor cells which are more epithelial in nature. To metastasize, the tumor cells often need to acquire a mesenchymal phenotype which is induced by the process of epithelial to mesenchymal transition of differentiated tumor cells, also regulated by FoxM1 as mentioned above. These poorly differentiated tumor cells have stem cell like properties and express high levels of pluripotency genes. FoxM1 has been shown to directly regulate the expression several stemness genes such as Sox2, Bmi1, Nanog, c-Myc etc., indicative of regulating de-differentiation of tumor cells[95,100].

FoxM1 was shown to directly regulate the differentiation in mammary gland using *in vivo* model[112]. Over expression of FoxM1 in the mammary gland of mice led to higher accumulation of mammary luminal progenitor cells ($CD61^+$, CD29lo) and lower abundance of differentiated mammary luminal cells ($CD61^-$, CD29lo) leading to morphological defects in the duct formations as found by analysis of mammary gland tissues using immunohistochemistry. Deletion of FoxM1 led to increase in the differentiated luminal

cell numbers in the same study suggesting that FoxM1 expression, by itself, can regulate the process of differentiation. It was discovered that FoxM1 acts as a transcriptional repressor for well characterized mammary luminal differentiation factor GATA3, also known as master regulator of mammary gland luminal differentiation and is also considered a tumor suppressor[113–115].

FoxM1 binds to the GATA3 promoter and recruits retinoblastoma (Rb) and DNA methyl transferase 3B (DNMT3B). The complex was shown to carry out the methylation of GATA3 promoter rendering it transcriptionally inactive[112]. This leads to fall in GATA-3 protein levels and inhibits the downstream signaling required for differentiation of mammary luminal progenitor cells leading to their accumulation. That study was the first study to suggest a transcriptional repression ability of FoxM1. The methylation of the promoter carried out by this complex is dependent on Rb recruitment on the GATA-3 promoter. Induction of FoxM1 expression in absence of Rb fails to hyper methylate the GATA-3 promoter. This inverse correlation between expression of FoxM1 and GATA-3 has found to hold true in breast cancer samples. Analysis of breast cancer patients' mRNA expressions from *Oncomine* shows clearly that grade 1 tumor samples, less aggressive kind, express high levels of GATA-3 and very low levels of FoxM1 mRNAs[112]. In contrast, the aggressive breast cancer samples showed high expression of FoxM1 mRNA and diminished levels of GATA-3 mRNA suggesting that high levels of FoxM1 may lead to more aggressive tumor phenotype by inhibiting the process of differentiation or carrying de-differentiation of tumor cells. The Rb-dependent repression of GATA-3 by FoxM1 in breast cancer is indicative of a counterintuitive role of Rb in which Rb supports the progression

of tumor. As in the case of high grade breast cancer progression, FoxM1 expression correlates with high grade progression of liver cancer, with grade 3 showing very robust expression of FoxM1, suggesting that FoxM1 may be regulating the accumulation of poorly differentiated tumor cells leading to aggressive phenotype.

**Results**

I. FoxM1 deletion causes regression of Ras induced liver hepatocellular carcinoma
   - (i) Introduction
   - (ii) Ras induced liver tumors have high FoxM1 expression
   - (iii) FoxM1 deletion results in regression of tumor nodules.
   - (iv) FoxM1 deletion leads to lower proliferation, higher apoptosis and accumulation of ROS in tumor cells

II. FoxM1 inhibition leads to loss of liver cancer stem like cells
   - (i) Introduction
   - (ii) Deletion of FoxM1 causes a disproportionate loss of the EpCAM+ and the CD44+ HCC cells in the H-ras12V model
   - (iii) FoxM1 activates expression of CD44 in HCC cells
   - (iv) Inhibition of FoxM1 preferentially eliminates the cancer cells with stem cell features

III. FoxM1 inhibits the expression of liver differentiation factors FoxA1 and FoxA2
   - (i) Introduction
   - (ii) Opposite expression patterns of FoxM1 and FoxA1/A2 in hepatocellular carcinoma
   - (iii) FoxM1 inhibits FoxA1/A2 in HCC cells
   - (iv) FoxM1 recruits DNMT3b and Rb onto the FoxA1/A2 promoters
   - (v) FoxM1 induces methylation of CpGs in the FoxA1/A2 promoters requiring Rb
   - (vi) Deletion of FoxM1 in a Ras-transgenic model for HCC causes accumulation of FoxA1/A2, coinciding with decreased promoter methylation
   - (vii) FoxA1/A2 inhibit FoxM1b-induced clonogenicity and soft agar colony formation

## I. FoxM1 deletion causes regression of Ras induced liver hepatocellular carcinoma

*(Previously published: 'Essential Roles of FoxM1 in Ras induced liver cancer', Kopanja D, Pandey A, Kiefer M, Wang Z, Chandan N, Carr JR, Franks R, Yu DY, Guzman G, Maker A, Raychaudhuri P., J Hepatol. 2015 Aug;63(2):429-36)*

### (i) Introduction

The Ras-signaling pathway is frequently activated in HCC. To investigate the role of FoxM1 in Ras induced HCC, we utilized a previously described mouse transgenic mouse model that expresses constitutively active form of Hras (HrasG12V) under the albumin promoter. This results in constitutive expression of active form of Ras protein and thus keeps the Ras signaling pathway constitutively active. Consequently, these mice develop several abnormalities in the liver as they age [116]. These mice are a good model for Ras induced HCC development, primarily because these mice are not embryonically lethal, unlike previous Ras transgenic models; these mice have a high reproducibility in terms disease onset and penetration of the disease; these mice have a long-term survival, this allows a good timeline for studying the gradual progression of liver cancer; these mice show a male dominant prevalence of HCC formation with around 90% incidence of HCC, this is the same trend as observed in humans [116].

These mice were crossed with FoxM1$^{fl/fl}$; Mx-Cre transgenic mice, that were already available in our lab. In this transgenic mouse model the Cre recombinase gene is under the regulation Mx-1 promoter that is activated in the hepatocytes by double stranded RNA molecule [117,118]. This allows for conditional deletion of FoxM1 from the hepatocytes.

These mice develop multiple HCC nodules by the age of 9 months, as expected. At the age of nine months we induced the expression of Cre recombinase by treating the mice with 250 μg pIpC or polyinosinic-polycytidylic (which is a synthetically produced double stranded RNA molecule) delivered using intraperitoneal injections every day. Cre was induced in groups of 25 mice (FoxM1 $^{fl/fl}$) and 21 mice (FoxM1$^{+/+}$) with 5 i.p. injections of pIpC; also, a group of 7 mice (FoxM1 $^{fl/fl}$) and 6 mice (FoxM1$^{+/+}$) with 10 i.p. injections of pIpC.

### (ii) Ras induced liver tumors have high FoxM1 expression

Consistent with the previous findings [116], we observed higher expression of the H-ras12V mRNA in the tumor tissue of the transgenic mice in comparison to the non-tumor tissue sections (Fig. 1A). The H-ras12V induced HCC exhibited much higher expression of FoxM1 mRNA (Fig. 1B). To delete FoxM1 in the tumor we injected the male mice at eight months of age with polyIpolyC (five injections every other day) that activates expression of Cre recombinase from the Mx promoter. Mice were sacrificed and organs were harvested 3 weeks post the last injection. Total RNAs from the tumor tissues of FoxM1 deleted ($FoxM1^{fl/fl}$) and undeleted ($FoxM1^{+/+}$) were compared. We detected a significant reduction of the FoxM1 mRNA in the tumors from the FoxM1 deleted samples. However, the reduction of the FoxM1 mRNA was not very quantitative (Fig. 1C). The reason for a partial loss of FoxM1-mRNA became clear from immunohistochemical staining for FoxM1. In the undeleted samples ($FoxM1^{+/+}$), clear FoxM1 expression in the nucleus was detected in the HCC cells as well as in the fibroblast-like cells in the tumor nodules (See arrow in Fig. 2). In the FoxM1 deleted samples ($FoxM1^{fl/fl}$), we observed clear loss of FoxM1 signals from the HCC cells (arrow head), but not from the other cells. Therefore, it appears that there is some specificity in the expression of Cre in this system that allows specific deletion of FoxM1 in the HCC cells. Interestingly, loss of FoxM1 expression had negligible effect on the expression of H-ras12V mRNA in the tumors (Fig 1D).

**Figure 1**

**Loss of FoxM1 expression in the HCC cells following MxCre induced deletion in transgenic mice expressing H-ras12V.**

Total RNA from ($FoxM1^{+/+}$) normal liver, transgenic non-tumor and tumor tissues were assayed for expression of (A) H-ras12V and (B) FoxM1. (C) FoxM1-mRNA and (D) HRas12V-mRNA levels without ($FoxM1^{+/+}$) and with deletion of FoxM1 ($FoxM1^{fl/fl}$) were compared. The RNAs were assayed by quantitative RT-PCR.

**Figure 1**

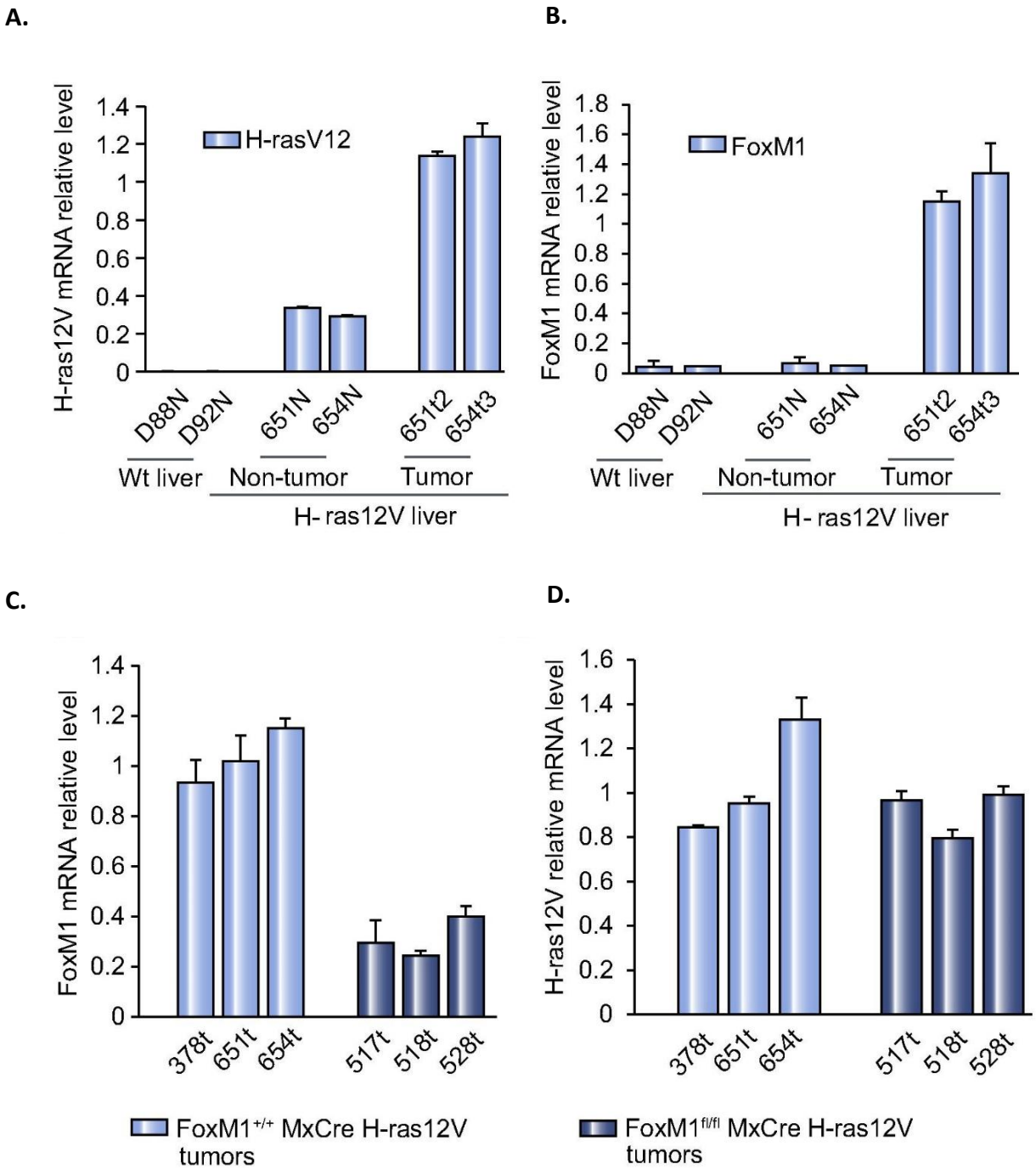
A.
H-ras12V mRNA relative level
H-rasV12
D88N
D92N
651N
654N
651t2
654t3
Wt liver
Non-tumor
Tumor
H- ras12V liver
B.
FoxM1 mRNA relative level
FoxM1
C.
FoxM1 mRNA relative level
378t
651t
654t
517t
518t
528t
FoxM1+/+ MxCre H-ras12V tumors
D.
H-ras12V relative mRNA level
FoxM1fl/fl MxCre H-ras12V tumors

**Figure 2**

**Loss of FoxM1 expression in the HCC cells following MxCre induced deletion in transgenic mice expressing H-ras12V.**

Tumor sections from FoxM1 undeleted ($FoxM1^{+/+}$) and FoxM1 deleted ($FoxM1^{fl/fl}$) samples were compared by immunohistochemical staining for FoxM1. Arrows indicate fibroblast-like cells in tumor sections and arrowheads indicate the HCC cells.

**Figure 2**

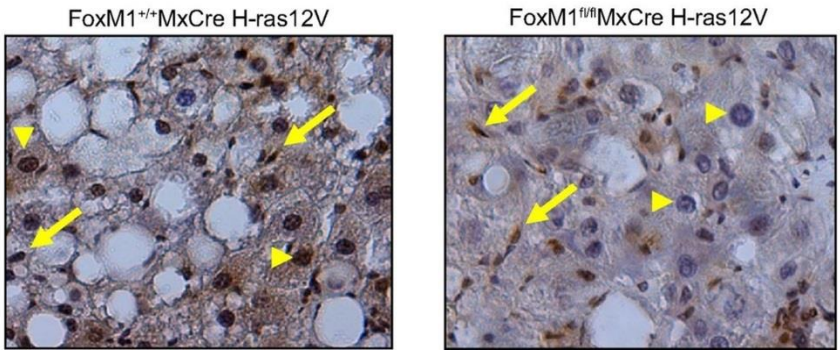

### (iii) FoxM1 deletion leads to regression of tumor nodules

The transgenic mice described above grow multiple tumor nodules by the age of nine months. The sizes of these tumors vary significantly from animal to animal with tumor sizes ranging from 0.1cm to 2.5cm or more in diameter. To measure an effect of FoxM1 deletion we analyzed the tumor nodules from large cohorts of mice following five i.p. injections of polyIpolyC. Total number of HCC nodules were counted irrespective of the nodule size. Deletion of FoxM1 resulted in a significant decrease in the number of tumor nodules as can been seen in the representative pictures (Fig. 3). We also compared number of tumors in mice after inducing deletion of FoxM1 with ten injections of pIpC and observed a significantly greater decrease in the latter set of $FoxM1^{fl/fl}$ mice (Fig. 4), in fact, 2 out of 7 livers from the $FoxM1^{fl/fl}$ were completely HCC free. The decrease in the number of tumor nodules has been quantified and presented as box plots below the representative liver pictures (Fig. 3 and 4).

**Figure 3**

**Decrease in the number of tumor nodules following deletion of FoxM1.** Transgenic male mice (Alb-H-ras12V FoxM1+/+ MxCre and Alb-Hras12V FoxM1fl/fl MxCre) at eight months of age were injected with five doses of polyIpolyC. The numbers of the tumor nodules were compared four weeks after the last injection. Box plots for the numbers are shown along with p values.

**Figure 3**

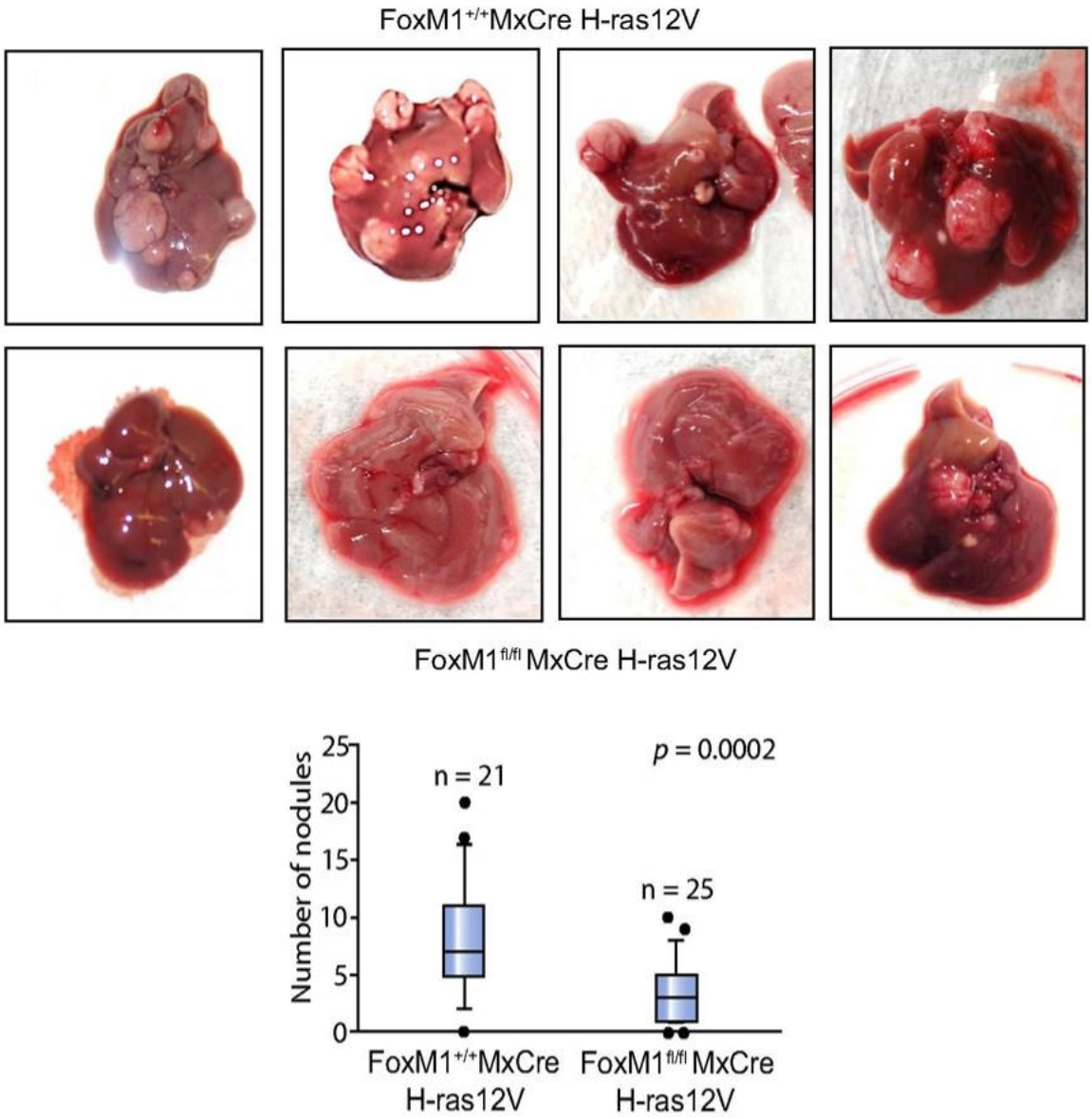
FoxM1+/+MxCre H-ras12V
FoxM1fl/fl MxCre H-ras12V
Number of nodules
25
20
15
10
5
0
n = 21
n = 25
p = 0.0002
FoxM1+/+MxCre H-ras12V
FoxM1fl/fl MxCre H-ras12V

**Figure 4**

**Decrease in the number of tumor nodules following deletion of FoxM1.** Transgenic male mice (Alb-H-ras12V FoxM1+/+ MxCre and Alb-Hras12V FoxM1fl/fl MxCre) at eight months of age were injected with ten doses of polyIpolyC. The numbers of the tumor nodules were compared four weeks after the last injection. Box plots for the numbers are shown along with p values.

**Figure 4**

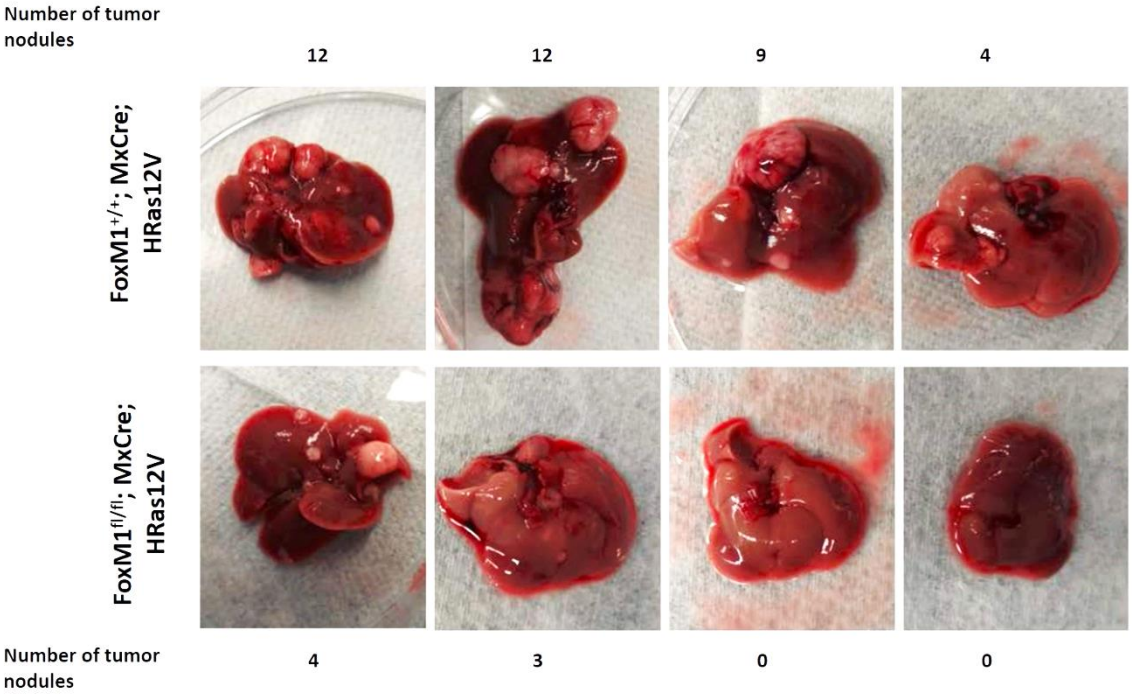
Number of tumor nodules
12
12
9
4
FoxM1+/+; MxCre; HRas12V
FoxM1fl/fl; MxCre; HRas12V
Number of tumor nodules
4
3
0
0

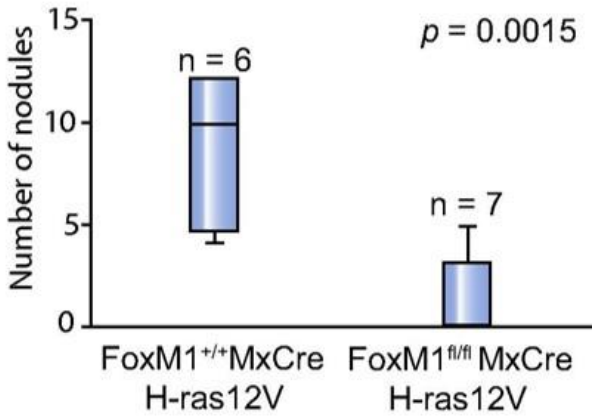
p = 0.0015
n = 6
n = 7
Number of nodules
15
10
5
0
FoxM1+/+MxCre H-ras12V
FoxM1fl/fl MxCre H-ras12V

**(iv) FoxM1 deletion leads to lower proliferation, higher apoptosis and accumulation of ROS in tumor cells**

We saw a reduction in the number of total HCC nodules upon FoxM1 deletion and wanted to investigate the molecular mechanisms that led to tumor regression. Similar sized tumor nodules were chosen from $FoxM1^{+/+}$ and $FoxM1^{fl/fl}$ groups for analysis. Tissue sections were stained for proliferation marker PCNA (proliferation cell nuclear antigen) and significant reduction in PCNA positive cells was observed in tumor section from $FoxM1^{fl/fl}$ group (Fig. 5). This change in PCNA positive cells from both groups has been quantified in the bar graph below and shows a significant decrease. Since FoxM1 is crucial to cell cycle we looked at the expression of FoxM1 targets that are involved in cell cycle progression. Tissue sections from both the groups were analyzed for the expression of Polo Like Kinase-1 (Plk1) and Cyclin E using immunohistochemical analysis. A significant decrease was observed in the Plk1 and Cyclin E positive cells (Fig. 6A and 6B). Further, we analyzed the mRNA expression and found a significant decrease in the expression of Plk1, Aurora B, Cdc25b mRNAs upon FoxM1 deletion (Fig. 7) which made it clear how deletion of FoxM1 was causing a decrease in proliferation.

The HCC cells in the tumor sections were analyzed also for TUNEL. In addition, we looked at the active caspase3 positive cells. Clearly, deletion of FoxM1 caused a significant increase in the TUNEL and active caspase3 positive cells, indicating an increased apoptosis (Fig. 8A and B). To investigate the cause of increased apoptosis in the FoxM1 deleted tumors, we stained tumors for the anti-apoptotic protein Survivin

whose expression is regulated by FoxM1. The results clearly show decrease in the percentage of Survivin expressing cells in FoxM1 deleted tumor samples (Fig. 9). Previous cell culture studies indicated that the oncogenic Ras expressing cells depends upon FoxM1 to regulate the levels of the ROS [91]. Consistent with that, we observed increased ROS in the tumor sections from the FoxM1 deleted samples compared to the undeleted samples (Fig 10). Together, these observations on decrease in the number of tumor nodules and increased apoptosis along with loss of proliferation in the remaining tumors upon deletion of FoxM1 provide genetic evidence that targeting FoxM1 inhibits H-ras12V-induced HCC progression. It is possible that MxCre might have deleted FoxM1 in other cells in the tumor nodules, such as the macrophages, that contributed to the apoptosis of HCC cells. But, that is expected also from a therapeutic agent that would target FoxM1 in liver cancer. In that regard, the inhibition of HCC progression is significant because there were no noticeable side effects of the MxCre mediated deletion of FoxM1 in the adult mice.

**Figure 5**

**Decreased proliferation in tumors following deletion of FoxM1.** Tumor sections from mice (Alb-H-ras12V FoxM1+/+ MxCre and Alb-H-ras12V FoxM1fl/fl MxCre) following five injections of polyIpolyC were compared for PCNA expression by immunohistochemical staining. Quantification of PCNA+ nuclei is shown below. Percentage in positive cells was calculated from 3 to 5 different fields of 5 tumors per genotype. Statistically significant changes were indicated with asterisks (*, $p< 0.05$; **, $p < 0.01$, ***, $p<0.001$).

**Figure 5**

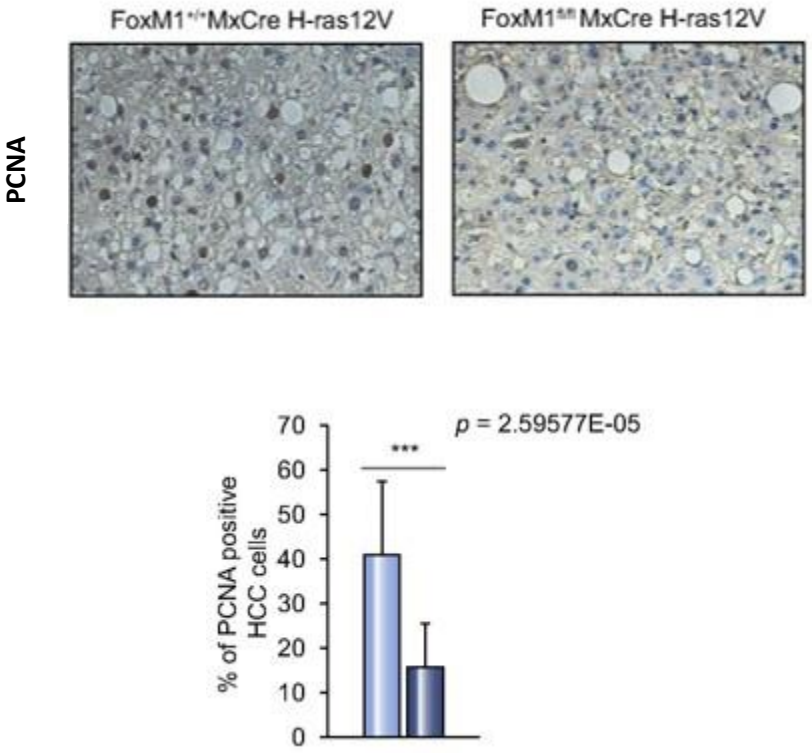
PCNA
FoxM1+/+MxCre H-ras12V
FoxM1fl/flMxCre H-ras12V
p = 2.59577E-05
***
% of PCNA positive HCC cells
70
60
50
40
30
20
10
0

**Figure 6**

**Decrease in the percentage of Plk1 and Cyclin E positive cells after FoxM1 deletion in H-ras12V-driven HCCs.** FoxM1 $^{+/+}$ MxCre H-ras12V and FoxM1 $^{fl/fl}$ MxCre H-ras12V tumor sections were stained with, Plk1 (A) and CyclinE (B) antibodies. Percentage in positive cells was calculated from 3 to 5 different fields of 5 tumors per genotype. Quantifications are shown on the right side of the panels. Statistically significant changes were indicated with asterisks (*, $p< 0.05$; **, $p < 0.01$, ***, $p<0.001$).

**Figure 6**

**A.**

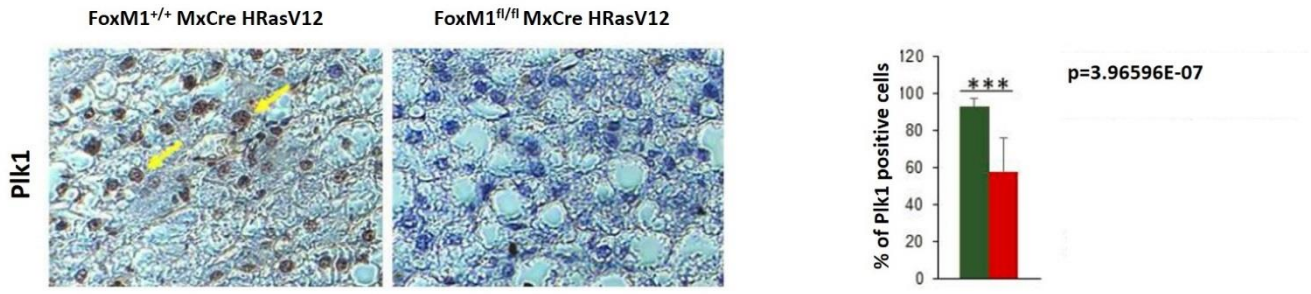
FoxM1+/+ MxCre HRasV12
FoxM1fl/fl MxCre HRasV12
Plk1
% of Plk1 positive cells
120
100
80
60
40
20
0
***
p=3.96596E-07

**B.**

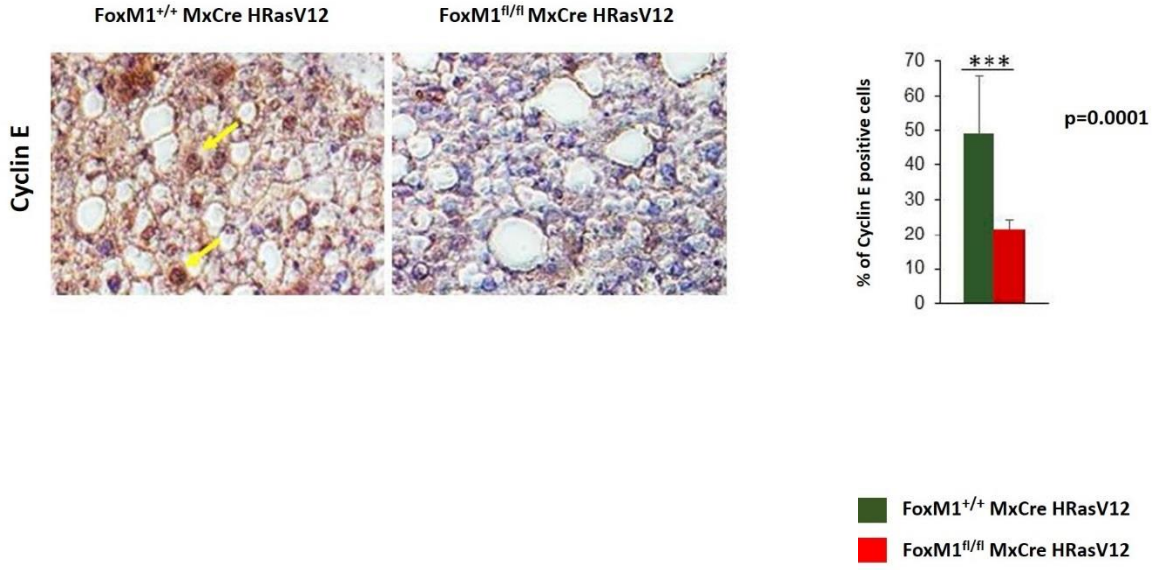
FoxM1+/+ MxCre HRasV12
FoxM1fl/fl MxCre HRasV12
Cyclin E
% of Cyclin E positive cells
70
60
50
40
30
20
10
0
***
p=0.0001
FoxM1+/+ MxCre HRasV12
FoxM1fl/fl MxCre HRasV12

**Figure 7**

**FoxM1 is critical for expression of proliferative genes in H-ras12V driven HCCs.** Four weeks after the last of five injections of polyIpolyC, FoxM1 $^{+/+}$ MxCre H-ras12V and FoxM1 $^{fl/fl}$ MxCre H-ras12V mice were sacrificed, tumors harvested and RNA isolated using Trizol. Total RNAs of two different pairs of mice (upper and bottom panel) were analyzed by quantitative RT-PCR. mRNA levels were normalized to GAPDH and control mice were set as 1. Statistically significant changes were indicated with asterisks (*, $p< 0.05$; **, $p < 0.01$, ***, $p<0.001$).

**Figure 7**

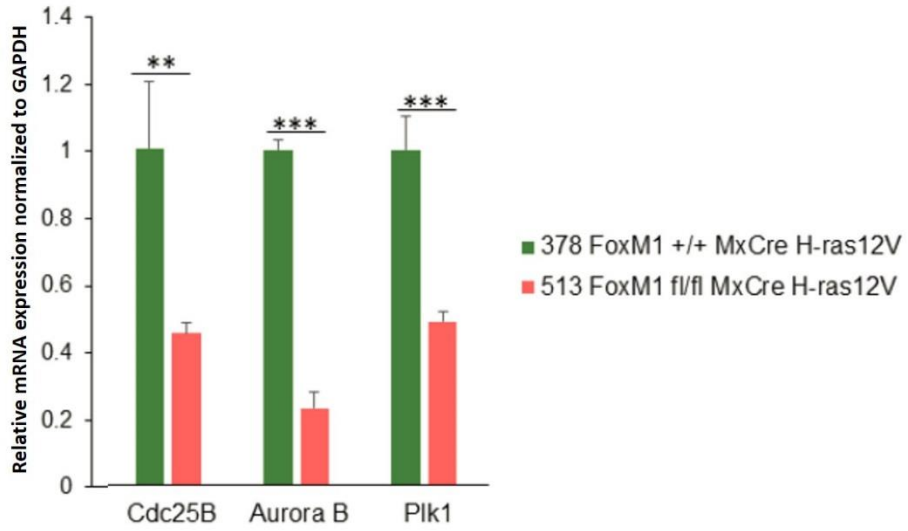
Relative mRNA expression normalized to GAPDH
1.4
1.2
1
0.8
0.6
0.4
0.2
0
**
***
***
Cdc25B
Aurora B
Plk1
378 FoxM1 +/+ MxCre H-ras12V
513 FoxM1 fl/fl MxCre H-ras12V

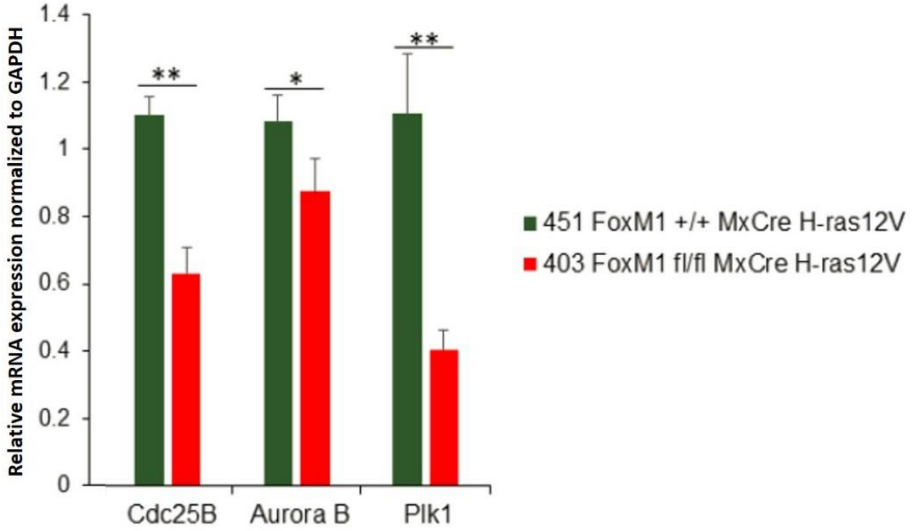
Relative mRNA expression normalized to GAPDH
1.4
1.2
1
0.8
0.6
0.4
0.2
0
**
*
**
Cdc25B
Aurora B
Plk1
451 FoxM1 +/+ MxCre H-ras12V
403 FoxM1 fl/fl MxCre H-ras12V

**Figure 8**

**Increase in apoptosis after FoxM1 deletion.** (A) The tumor sections were also subjected to TUNEL assays; (B) Single cell suspensions (CD45-) of the tumor tissues were compared for active caspase3+ cells by flow cytometry.

**Figure 8**

**A.**

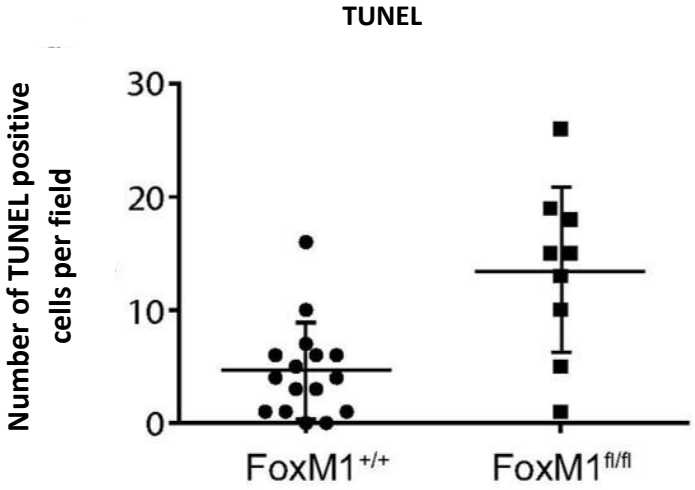
TUNEL
Number of TUNEL positive cells per field
30
20
10
0
FoxM1+/+
FoxM1fl/fl

**B.**

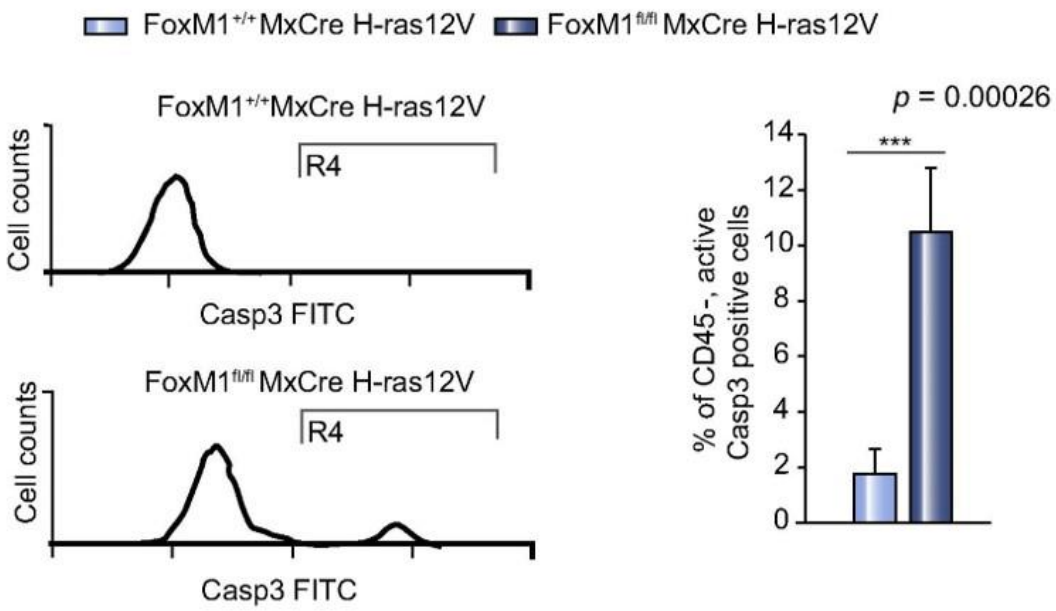
FoxM1+/+MxCre H-ras12V
FoxM1fl/fl MxCre H-ras12V
FoxM1+/+MxCre H-ras12V
R4
Cell counts
Casp3 FITC
FoxM1fl/fl MxCre H-ras12V
R4
Cell counts
Casp3 FITC
p = 0.00026
***
% of CD45-, active Casp3 positive cells
14
12
10
8
6
4
2
0

**Figure 9**

**Decrease in the percentage of Survivin positive cells after FoxM1 deletion in H-ras12V-driven HCCs.** FoxM1 +/+ MxCre H-ras12V and FoxM1 fl/fl MxCre H-ras12V tumor sections were stained with Survivin antibody. Percentage in positive cells was calculated from 3 to 5 different fields of 5 tumors per genotype. Quantifications are shown on the right side of the panel. Statistically significant changes were indicated with asterisks (*, $p< 0.05$; **, $p < 0.01$, ***, $p<0.001$).

**Figure 9**

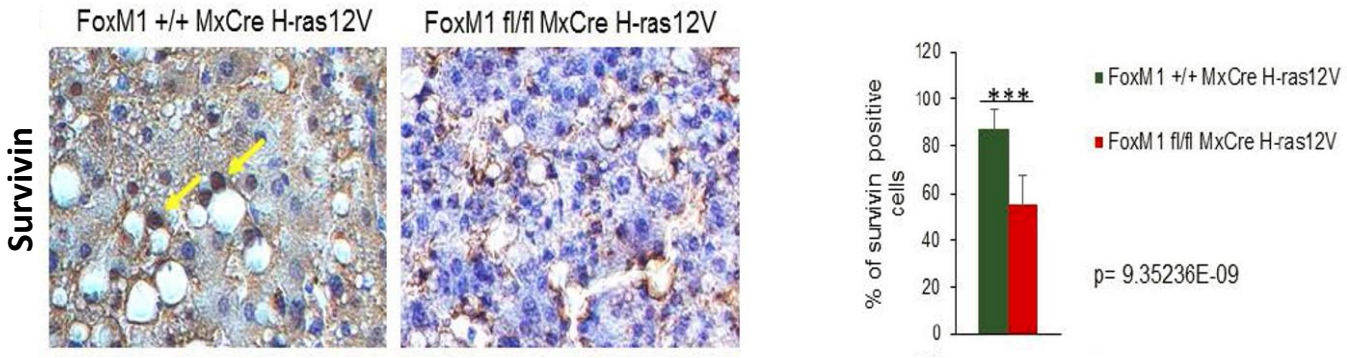
FoxM1 +/+ MxCre H-ras12V
FoxM1 fl/fl MxCre H-ras12V
Survivin
% of survivin positive cells
120
100
80
60
40
20
0
***
FoxM1 +/+ MxCre H-ras12V
FoxM1 fl/fl MxCre H-ras12V
p= 9.35236E-09

**Figure 10**

**FoxM1 deletion leads to higher accumulation of ROS in tumor cells**

Frozen sections of the tumor tissues were compared for accumulation of ROS following treatments with DCFDA. The sections were treated with 10 μM 5-(6)-chloromethyl-2-dichlorodihydrofluorescein diacetate (CM-$H_2$DCFDA) (Invitrogen, Carlsbad, CA) for 30 min at 37 deg C and counterstained with DAPI. Images were taken using a fluorescent microscope at 20X magnification.

**Figure 10**

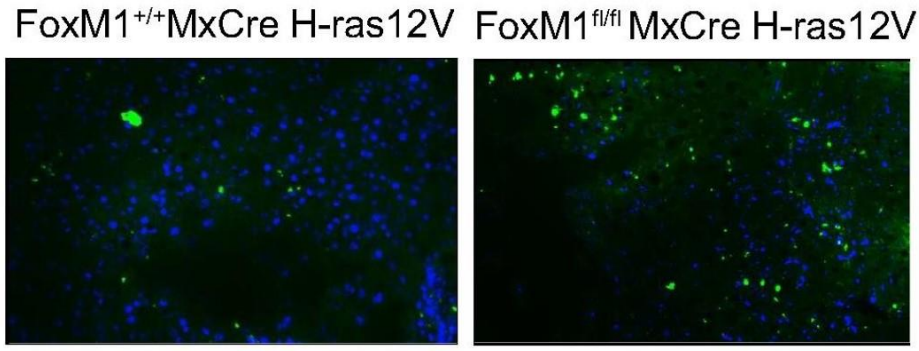
FoxM1+/+MxCre H-ras12V
FoxM1fl/fl MxCre H-ras12V

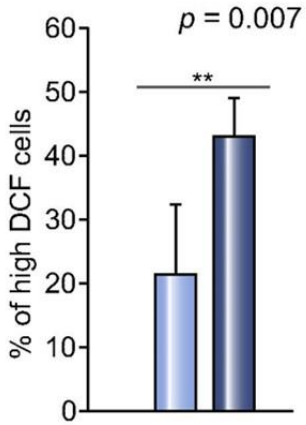
p = 0.007
**
% of high DCF cells
60
50
40
30
20
10
0

## II. FoxM1 inhibition leads to loss of liver cancer stem like cells

*Previously published: 'Essential Roles of FoxM1 in Ras induced liver cancer', Kopanja D, Pandey A, Kiefer M, Wang Z, Chandan N, Carr JR, Franks R, Yu DY, Guzman G, Maker A, Raychaudhuri P., J Hepatol. 2015 Aug;63(2):429-36*

### Introduction

Several studies have described the presence of cancer cells with stem cell like features. These cells are considered to be tumor initiating cells and have shown to exhibit high metastatic potential. CD90 (Thy-1), CD44 (HCAM-homing cell adhesion molecule) and EpCAM (Epithelial cell adhesion molecule) have been described as markers for liver cancer stem cells [69]. In human cell lines- Huh7, Hep3B, HepG2, $CD90^+$ and not $CD90^-$ cell were shown to possess tumorigenic potential. This potential was higher for cells expressing CD44 along with CD90 indicating that presence of CD44 modulates biological activity of $CD90^+$ cell. Inhibition of CD44 in the double positive population led to decrease in the aggressiveness and metastatic potential of $CD90^+$ cells [69].

Another study identified liver cancer progenitor cells in mice using the DEN model. DEN injected mice were sacrificed at the age of 3 or 5 months and their livers were subjected to collagenase digestion. It was observed that a certain population of cells was resistant to collagenase digestion and existed as aggregates. The cells from the aggregates showed higher expression of HCC markers such as alpha feto protein (AFP), Ly6D, glypican 3 (Gpc3) as compared to the non-aggregated cells [119]. These cells when injected in MUP-uPA mice using intrasplenic injections gave rise to 18 tumors per mouse liver as compared to less than one tumor per mouse liver when non-aggregated cells were injected. These cells were found to be positive for cell surface markers CD44 and EpCAM [119].

**(i) Deletion of FoxM1 causes a disproportionate loss of the EpCAM+ and the CD44+ HCC cells in the H-ras12V model**

We analyzed for the presence of $CD44^+$ and $EpCAM^+$ cells in the H-ras12V-induced HCC with and without deletion of FoxM1. Immunohistochemical staining of tumor section, derived from comparable size nodules, with EpCAM antibody indicated that a significant population of the HCC cells, about 40%, were positive for EpCAM. Interestingly, deletion of FoxM1 caused a severe reduction in the EpCAM expressing HCC cells (Fig. 11). Next we examined tumors for the CD44+ cells and observed significant loss of these cells in FoxM1-deleted tumors compared to the control tumors (Fig. 12A). We compared six tumors of each genotype by immunohistochemical staining, and counted CD44 expressing HCC cells. While percentage of CD44+ cells in control tumor sections averaged to 28.9%, the percentage of those cells in the FoxM1 deleted tumor sections was significantly lower, with an average of 12.2%. The reduction in EpCAM and CD44 was evident also in a western blot assay (Fig. 12B). Together, these observations on decrease in the percentages of the EpCAM+ and CD44+ HCC cells over the total number of the HCC cells in the FoxM1 deleted tumors suggest that those cells are more dependent upon FoxM1 in comparison to the other HCC cells. We speculate that these cells originated from the liver cancer progenitor cells known to be CD44 and EpCAM positive, or these cells are bona fide liver cancer cells with stem cell features. Interestingly, the FoxM1 deleted tumor specimens also exhibited decrease in expression of ‘‘stemness’’ genes Bmi1, Nanog and c-Myc (Fig. 13).

**Figure 11**

**Loss of the EpCAM+ HCC cells in the tumors following deletion of FoxM1.** Tumor sections from mice (Alb-H-ras12V FoxM1$^{+/+}$ MxCre and Alb-H-ras12V FoxM1$^{fl/fl}$ MxCre) following five injections of polyIpolyC were compared for HCC cells that are positive for EpCAM. Quantification of the percentages of the EpCAM+ HCC cell over the total number of HCC cells are shown. For EpCAM+ cells, we quantified HCC cells from nine different fields. For CD44+ cells, we quantified HCC cells from 16 different fields and six different tumors per genotype. (C) Protein extracts (150 μg) from tumor fragments were assayed by western blot.

**Figure 11**

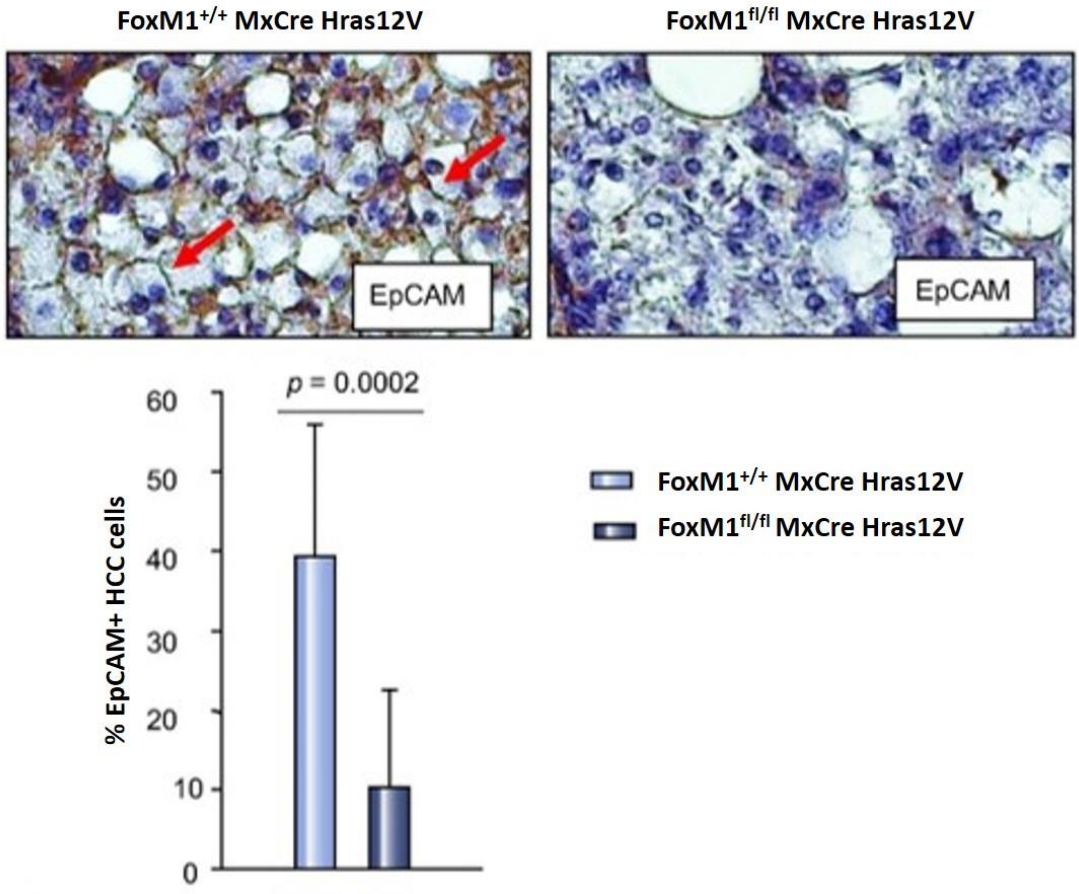
FoxM1+/+ MxCre Hras12V
FoxM1fl/fl MxCre Hras12V
EpCAM
EpCAM
p = 0.0002
% EpCAM+ HCC cells
60
50
40
30
20
10
0
FoxM1+/+ MxCre Hras12V
FoxM1fl/fl MxCre Hras12V

**Figure 12**

**Loss of the CD44+ HCC cells in the tumors following deletion of FoxM1.** Tumor sections from mice (Alb-H-ras12V FoxM1$^{+/+}$ MxCre and Alb-H-ras12V FoxM1$^{fl/fl}$ MxCre) following five injections of polyIpolyC were compared for HCC cells that are positive for CD44. Quantification of the percentages of the CD44 + HCC cell over the total number of HCC cells are shown (A). For CD44+ cells, we quantified HCC cells from nine different fields. For We quantified HCC cells from 16 different fields and six different tumors per genotype. (B) Protein extracts (150 μg) from tumor fragments were assayed by western blot.

**Figure 12**

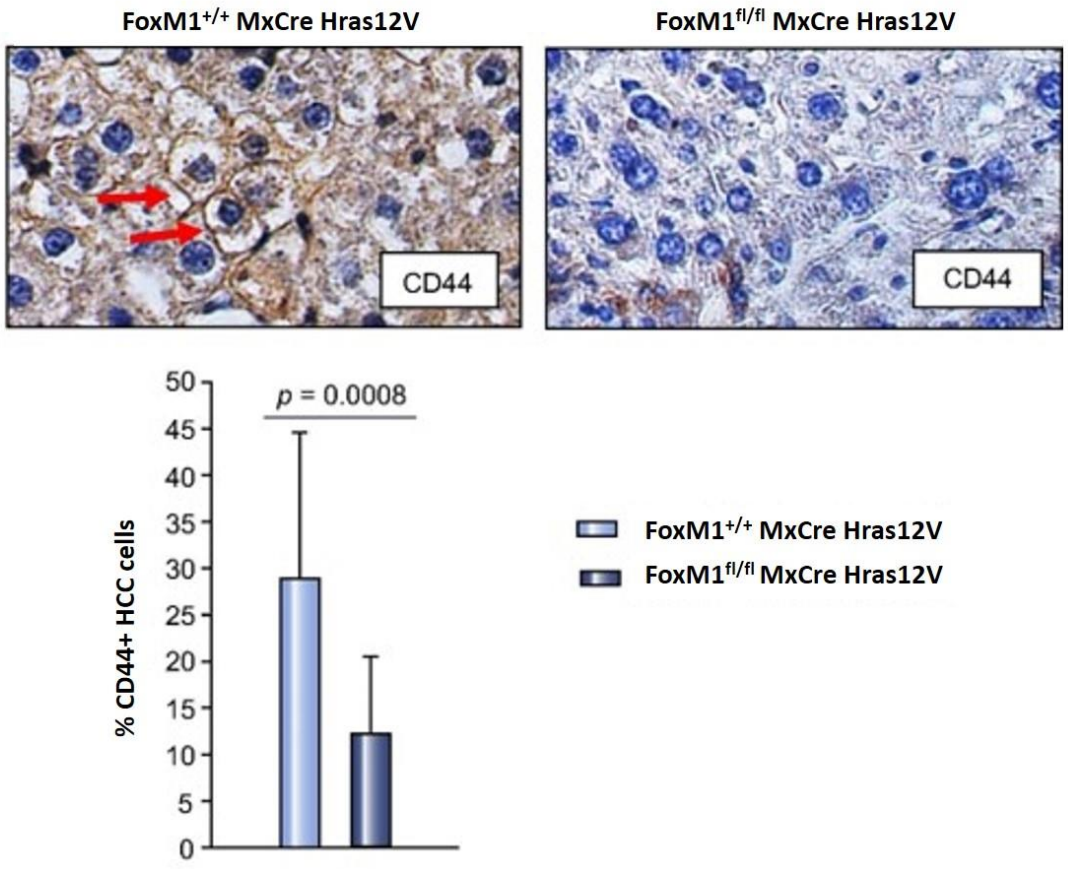
FoxM1+/+ MxCre Hras12V
FoxM1fl/fl MxCre Hras12V
CD44
CD44
p = 0.0008
% CD44+ HCC cells
50
45
40
35
30
25
20
15
10
5
0
FoxM1+/+ MxCre Hras12V
FoxM1fl/fl MxCre Hras12V

**C.**

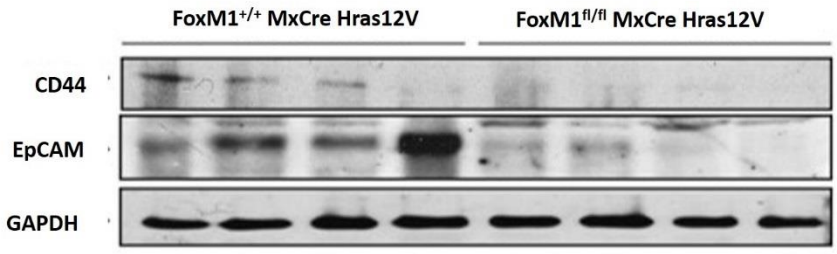
FoxM1+/+ MxCre Hras12V
FoxM1fl/fl MxCre Hras12V
CD44
EpCAM
GAPDH

**Figure 13**

**FoxM1 is critical for expression of "stemness" genes in H-ras12V driven HCCs.**

Four weeks after the last of five injections of polyIpolyC, FoxM1 $^{+/+}$ MxCre H-ras12V and FoxM1 $^{fl/fl}$ MxCre H-ras12V mice were sacrificed, tumors harvested and RNA isolated using Trizol. Total RNAs of two different pairs of mice (upper and bottom panel) were analyzed by quantitative RT-PCR. mRNA levels were normalized to GAPDH and control mice were set as 1. Statistically significant changes were indicated with asterisks (*, $p< 0.05$; **, $p < 0.01$, ***, $p<0.001$).

**Figure 13**

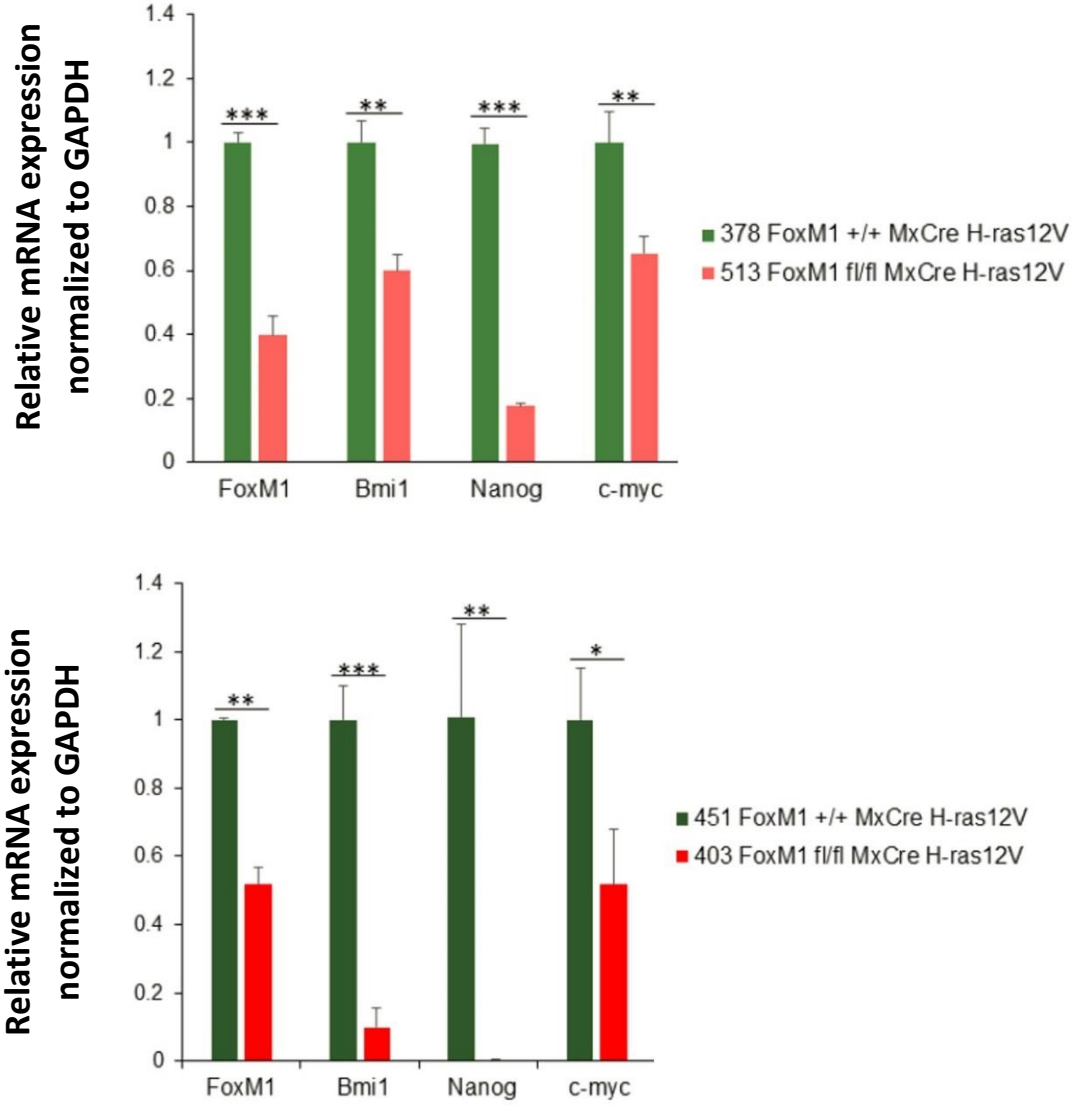
Relative mRNA expression normalized to GAPDH
1.4
1.2
1
0.8
0.6
0.4
0.2
0
***
**
***
**
FoxM1
Bmi1
Nanog
c-myc
378 FoxM1 +/+ MxCre H-ras12V
513 FoxM1 fl/fl MxCre H-ras12V
Relative mRNA expression normalized to GAPDH
1.4
1.2
1
0.8
0.6
0.4
0.2
0
**
***
**
*
FoxM1
Bmi1
Nanog
c-myc
451 FoxM1 +/+ MxCre H-ras12V
403 FoxM1 fl/fl MxCre H-ras12V

### (ii) FoxM1 activates expression of CD44 in HCC cells

CD44 was shown to be important for the liver cancer cells with stem cell features [69,120]. Inhibition of CD44 leads to apoptosis of those cells in HCC [69]. We observed that both mouse and human CD44 promoters contain FoxM1-binding sites. Therefore, we considered the possibility that CD44 might be a downstream transcriptional target of FoxM1. To test that, we analyzed human HCC cell lines HuH7 and Hep3B. The Ras-signaling pathway is active in these cell lines, as inhibition of that pathway reduces viability of the cells [121]. We employed siRNA to deplete FoxM1. Depletion of FoxM1 caused a significant loss in the levels of CD44 mRNA (Fig. 14A). In a reciprocal experiment, we transfected a plasmid expressing FoxM1 into both HuH7 and Hep3B cell lines. Expression of FoxM1 caused an increase in the expression of CD44, indicating that FoxM1 regulates the mRNA levels of CD44 (Fig. 14B and C). Also, we performed chromatin immunoprecipitation (ChIP) in HuH7 cells to see an interaction of FoxM1 with the putative binding sites in the CD44 promoter (Fig. 15). The results show that FoxM1 could associate with the CD44 promoter in the HCC cells and stimulate its expression.

**Figure 14**

**FoxM1 regulates the expression of CD44 in human HCC cell lines.** (A) Human HCC cell line HuH7 was transfected with control or FoxM1-siRNA #1. Seventy-two hours after transfection, total RNAs were assayed for FoxM1 and CD44 by quantitative RT-PCR. (B and C) HuH7 cells and Hep3B cells were transfected with control plasmid (pcDNA3) or plasmid expressing FoxM1. Forty eight hours after transfection, total RNAs were compared for FoxM1 and CD44 mRNAs by semi-quantitative PCR assays. Cyclophilin mRNA was assayed as loading control.

**Figure 14**

**A.**

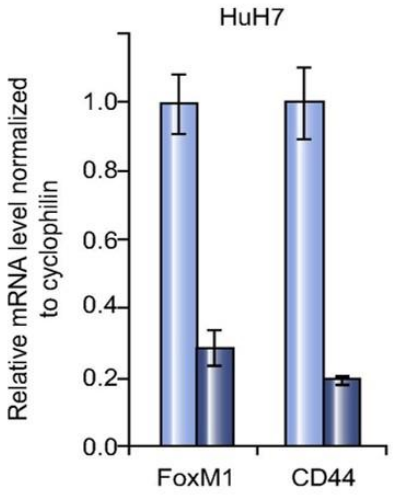


**B.**

**C.**

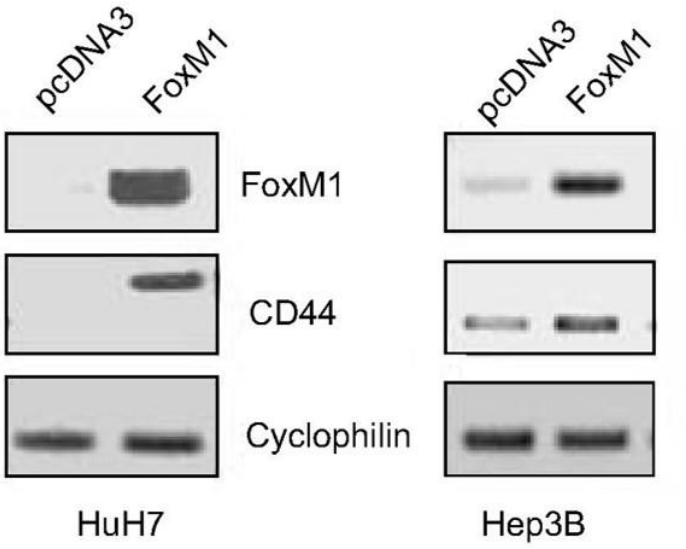

**Figure 15**

**FoxM1 binds to the promoter of CD44 and activates its expression.** Left panel - putative FoxM1-binding sites on the human CD44 promoter are shown. The schematic also includes the location of the PCR primers (arrows) used in the chromatin-IP assays. Chromatin-IP assays indicating FoxM1 binding to the two proximal sites are shown.

**Figure 15**

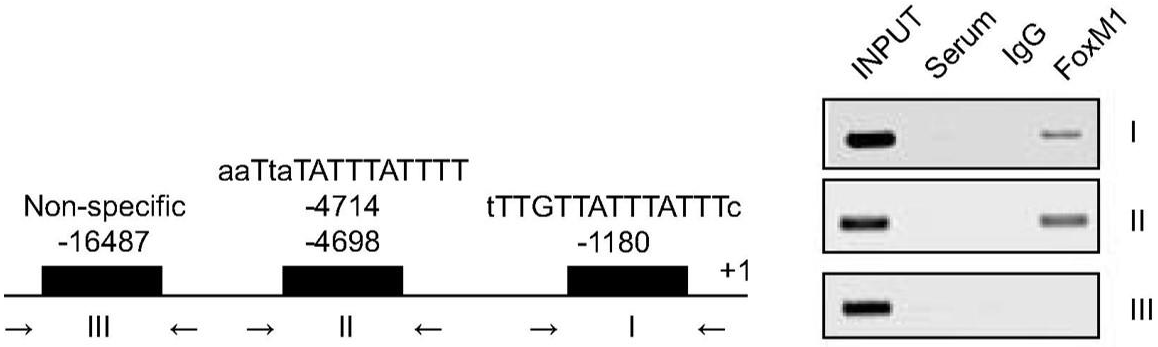
aaTtaTATTTATTTT
-4714
-4698
Non-specific
-16487
tTTGTTATTTATTTc
-1180
+1
III
II
I
INPUT
Serum
IgG
FoxM1
I
II
III

### (iii) Inhibition of FoxM1 preferentially eliminates the cancer cells with stem cell features

FoxM1 has been shown to stimulate expression of the ‘‘stemness’’ genes, including Sox2, Oct4, Nanog, c-Myc, Bmi1 and others [100,122]. We investigated whether expression of those genes in HCC cells involve FoxM1. Using siRNA mediated knockdown of FoxM1, as well as by overexpression of FoxM1, we observed evidence that expression of the ‘‘stemness’’ genes in HCC involves FoxM1 (Fig. 16). Interestingly, several studies characterized cell surface markers for cells with stem cell properties in HCC [123]. To investigate the effects of FoxM1 depletion in those cells, HuH7 cells were transfected with two independent siRNA against FoxM1 (FoxM1 siRNA #1 or FoxM1 siRNA #2) or control siRNA (Fig. 17). The depletion of FoxM1 had only a marginal effect on cell growth (Fig. 18). The transfected cells were then analyzed for the CD90+, CD133+ and CD44+ cells by flow cytometry. We observed significant decreases in the CD90+, CD44+ and CD133+CD44+ cells, while FoxM1 deletion did not have a statistically significant effect on the total CD133+ cell population. Consistent with the loss of the stem-like cancer cells, the FoxM1-depleted cells failed to generate tumor when injected subcutaneously in athymic nude mice (Fig. 19A). Lack of tumorigenicity was observed also in soft agar colony formation assay using other HCC lines (Fig. 19B). Together these results provide evidence that FoxM1 is critical for the survival of the cells with stem cell features in HCC. It is noteworthy that EpCAM was suggested as another marker for human liver cancer cells with stem cell properties. However, most the HuH7 cells are EpCAM+ and depletion of FoxM1 had very little effect on the population of the EpCAM+ cells. It remains possible that they underwent

differentiation because the FoxM1-depleted HuH7 cells failed to generate xenograft tumors.

**Figure 16**

**FoxM1 is required for expression of "stemness" genes in HCC cell lines.** (A) Huh7 cells were transfected with control and FoxM1 siRNA. Expression of Sox2, Bmi1, Nanog, Oct4, cmyc, AFP and CD44 was investigated using qRT PCR; mRNA expression was normalized with GAPDH mRNA levels. Protein levels upon FoxM1 knockdown are shown below. Hep3B cells were transfected with FoxM1 and mRNA for the above genes were assessed using semi quantitative PCR.

**Figure 16**

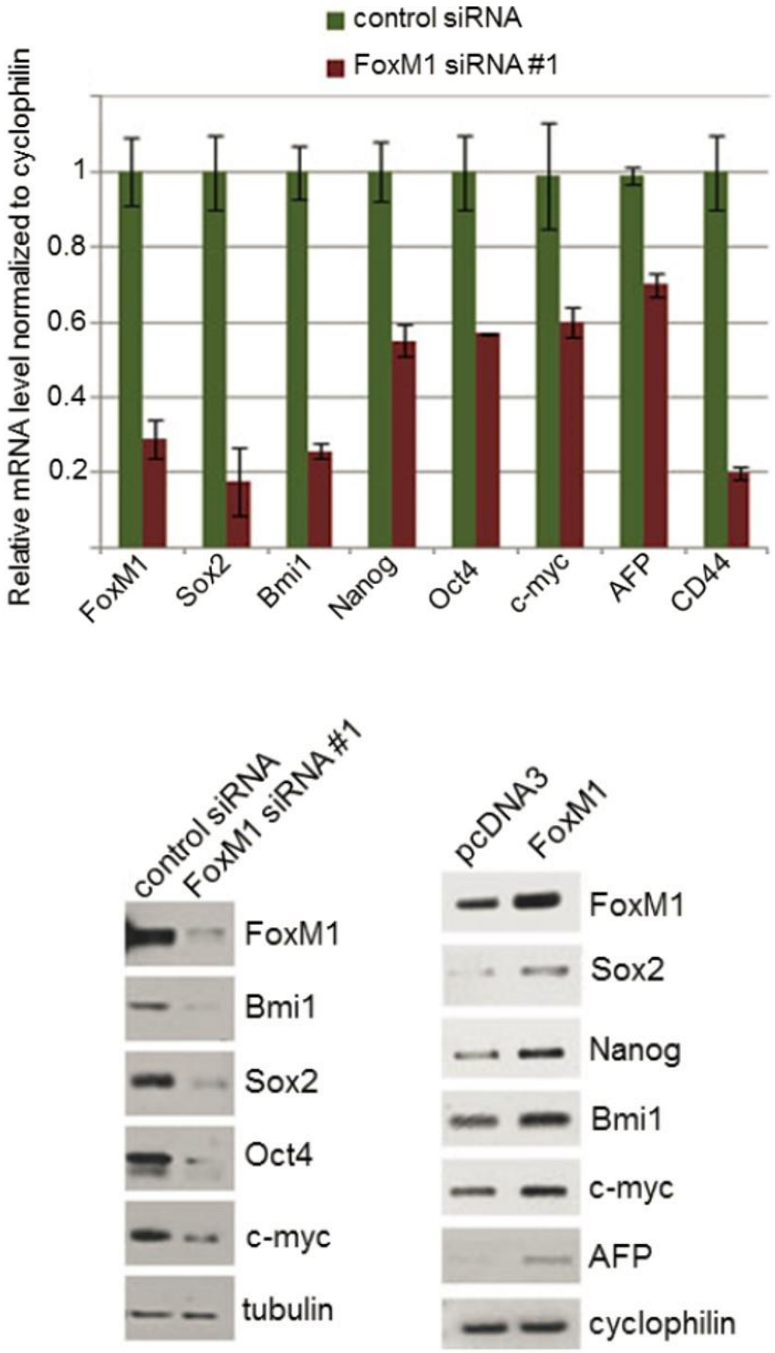
control siRNA
FoxM1 siRNA #1
Relative mRNA level normalized to cyclophilin
1
0.8
0.6
0.4
0.2
FoxM1
Sox2
Bmi1
Nanog
Oct4
c-myc
AFP
CD44
control siRNA
FoxM1 siRNA #1
FoxM1
Bmi1
Sox2
Oct4
c-myc
tubulin
pcDNA3
FoxM1
FoxM1
Sox2
Nanog
Bmi1
c-myc
AFP
cyclophilin

**Figure 17**

**Depletion of FoxM1 in HuH7 cells leads to specific loss of the cancer cells with stem cell features**. HuH7 cells were transfected with control siRNA, FoxM1-siRNA#1 and FoxM1 siRNA #2. 72 h after transfection, total RNAs were assayed by quantitative RT-PCR. mRNA levels were normalized to cyclophilin mRNA and control groups were set as 1. Protein levels after FoxM1 silencing are shown. Total RNAs from Hep3B cells, 48 h after pcDNA3 or FoxM1 transfection were analyzed by semiquantitative PCR. Western blots show the extent of FoxM1 depletion. The siRNA-transfected cells were treated with PE-tagged CD90-ab, FITC-tagged CD44-ab and PE-tagged CD133-ab and analyzed using a cell sorter.

**Figure 17**

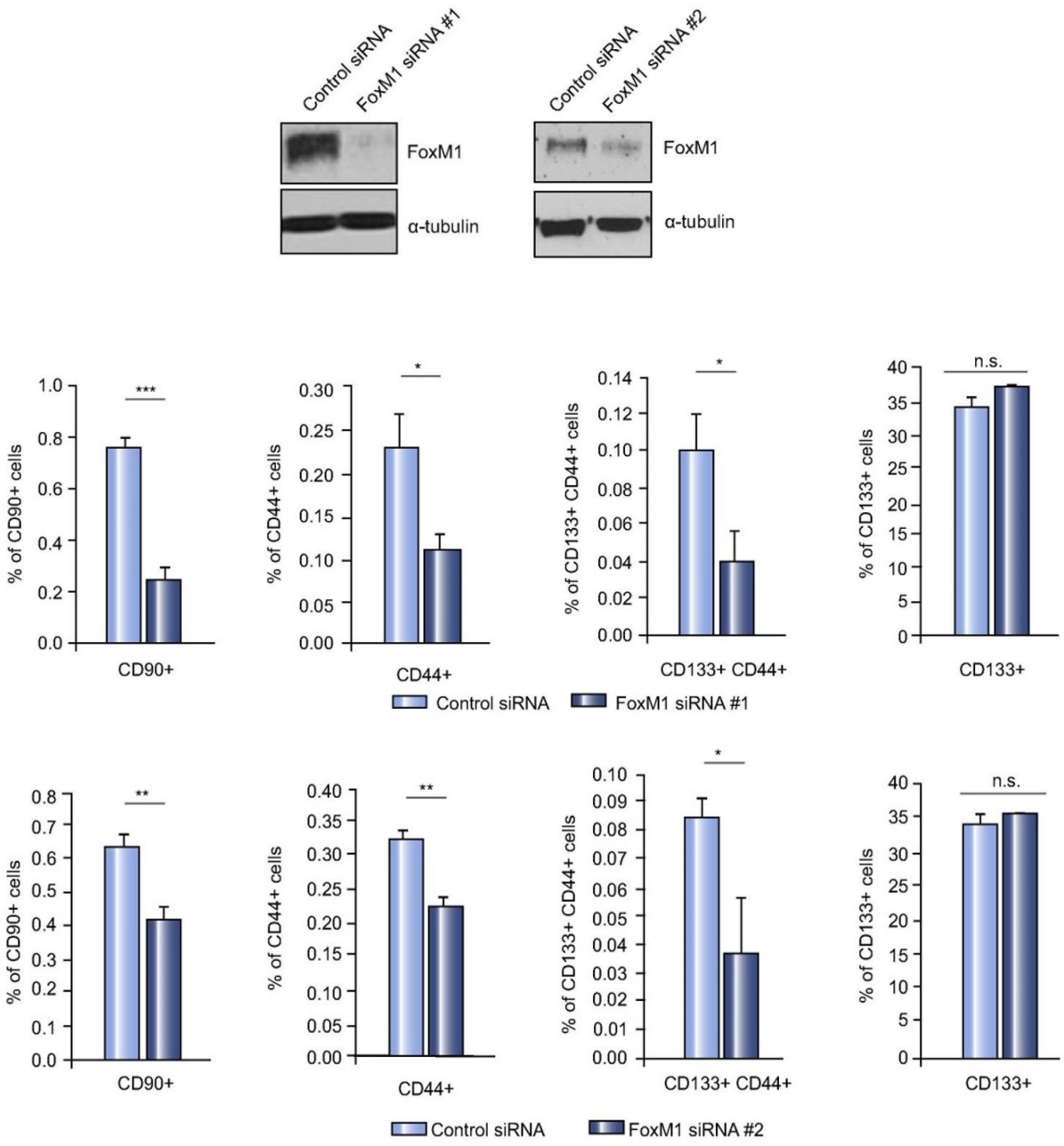
Control siRNA
FoxM1 siRNA #1
FoxM1
α-tubulin
Control siRNA
FoxM1 siRNA #2
FoxM1
α-tubulin
% of CD90+ cells
CD90+
% of CD44+ cells
CD44+
% of CD133+ CD44+ cells
CD133+ CD44+
% of CD133+ cells
CD133+
n.s.
Control siRNA
FoxM1 siRNA #1
Control siRNA
FoxM1 siRNA #2

**Figure 18**

**Depletion of FoxM1 had a marginal effect on cell proliferation.** Equal number of cells were plated with or without FoxM1 depletion. Cell growth was monitored by direct counting of cells every for 5 days.

**Figure 18**

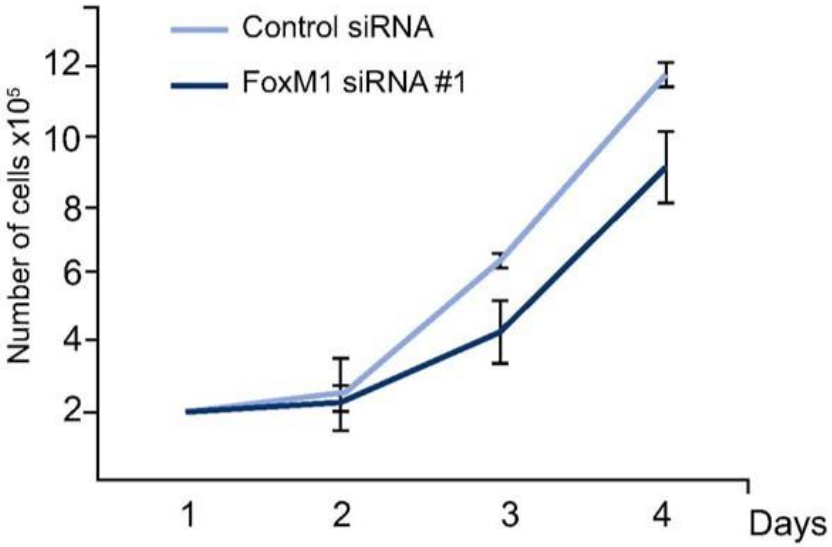
Control siRNA
FoxM1 siRNA #1
Number of cells x10⁵
12
10
8
6
4
2
1
2
3
4
Days

**Figure 19**

**FoxM1 attenuation leads to loss of tumorigenicity in HCC cells.** Twenty four hours after control or FoxM1 siRNA transfection, $10^6$ cells were subcutaneously injected into nude mice. The control siRNA transfected cells were injected on the left side and the FoxM1-siRNA #1 transfected cells on the right side of five different mice. A picture of three mice after six weeks is shown (A). Quantification of the tumor mass from all five mice is plotted. For soft agar assay, Huh7, HepG2 and Hep3B cells were counted and plated in 6-well plates in 0.35% agarose on a 0.7% agarose bed in triplicate (B). Colonies were stained with crystal violet and counted after 3 weeks. Representative pictures and quantification are shown. Huh7 cells, Hep3B and HepG2 cells. Statistically significant changes were indicated with asterisks (*p <0.05; **p <0.01, ***p <0.001.).

**Figure 19**

**A.**

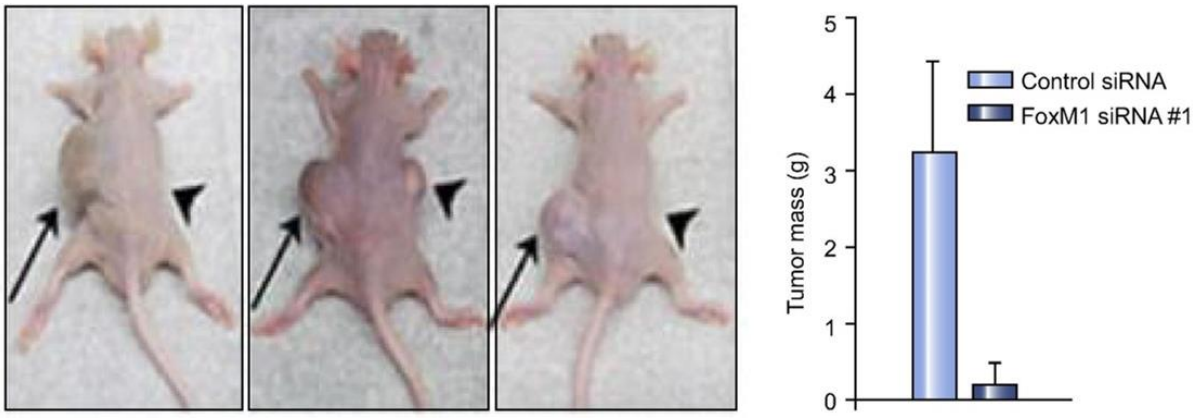
Tumor mass (g)
0
1
2
3
4
5
Control siRNA
FoxM1 siRNA #1

**B.**

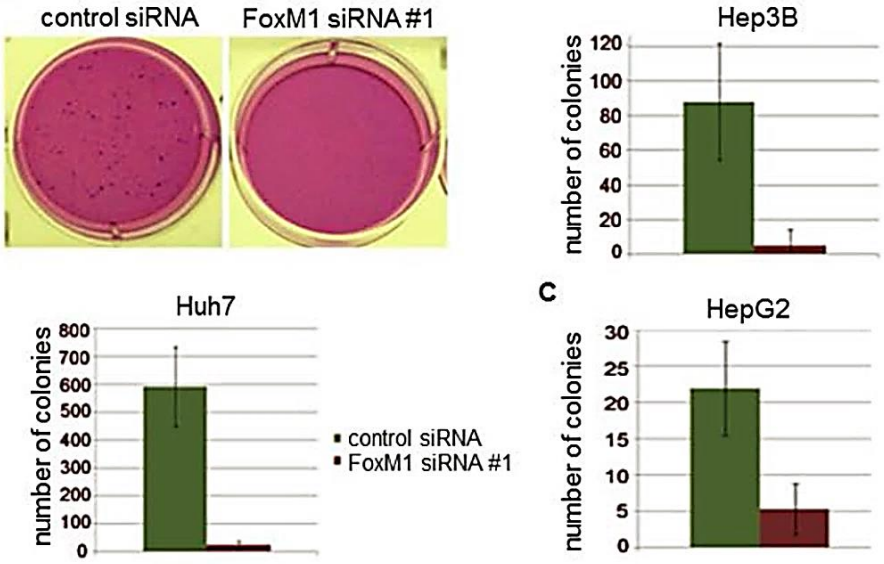
control siRNA
FoxM1 siRNA #1
Hep3B
number of colonies
0
20
40
60
80
100
120
Huh7
number of colonies
0
100
200
300
400
500
600
700
800
control siRNA
FoxM1 siRNA #1
C
HepG2
number of colonies
0
5
10
15
20
25
30

### (iv) FoxM1 supports survival of the cells with stem-like features by regulating the levels of ROS

We investigated apoptosis of the CD90+ and the CD90- population in HuH7 cells. Forty-eight hours after transfection of siRNA, the cells were incubated with PE-tagged CD90-ab as well as a FITC-tagged active caspase3 detection reagent. The cells were separated using a cell sorter, gating for the $CD90^+$/active caspase3+ and $CD90^-$/active caspase3+ cells. Depletion of FoxM1 caused a significant increase in the $CD90^+$/active caspase3+ cells (Fig. 20). The $CD90^-$ population did not exhibit any significant increase in caspase3+ cells, indicating that the $CD90^+$ cells undergo preferential apoptosis following depletion of FoxM1. Interestingly, the increase in the active caspase3+ $CD90^+$ population was stunted in experiment where cells were incubated with the ROS scavenger N-acetyl cysteine (NAC) for 24 h before analysis (Fig. 21), suggesting that ROS accumulation plays a role in the apoptosis of the $CD90^+$ cells. We measured the levels of ROS following depletion of FoxM1. The cells were incubated with PE-tagged CD90-ab as well as the ROS detection reagents DCF-DA, and the cells were then analyzed by flow cytometry. We observed increases in ROS mainly in the $CD90^+$ population (Fig. 22A). Moreover, when the $CD90^+$ and $CD90^-$ sorted populations were analyzed for MnSOD mRNA, we observed a stronger dependence of the $CD90^+$ cells on FoxM1 for MnSOD expression in comparison to that in the $CD90^-$ population (Fig. 22B). These observations indicate an important role of the FoxM1 induced expression of the antioxidant genes in the survival of the cells with stem cell features in HCC.

**Figure 20**

**Depletion of FoxM1 causes ROS-dependent apoptosis of CD90+ HCC cells.** HuH7 cells were transfected with control or FoxM1-siRNA #1 (all panels). Forty-eight hours after transfection, the cells were incubated with PE-tagged CD90-ab and FITC-tagged active caspase 3 detection reagents followed by separation of the CD90+ and active caspase 3+ cells using a cell sorter. Active Caspase 3+ CD90+ and the active caspase 3+ CD90- cells are plotted. Statistically significant changes were indicated with asterisks (*p <0.05; **p <0.01, ***p <0.001.).

**Figure 20**

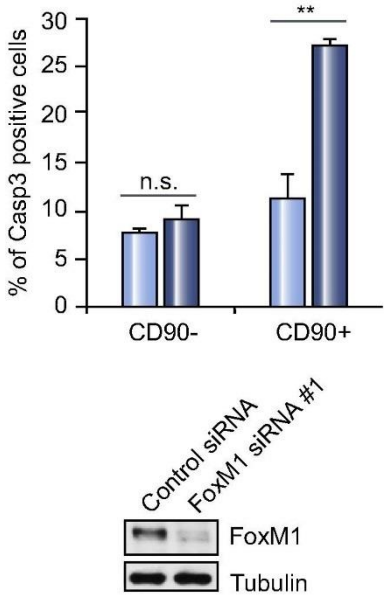
% of Casp3 positive cells
30
25
20
15
10
5
0
n.s.
**
CD90-
CD90+
Control siRNA
FoxM1 siRNA #1
FoxM1
Tubulin

**Figure 21**

**Depletion of FoxM1 ROS-dependent apoptosis of CD90+ HCC cells.** Twenty four hours after siRNA transfection, the cells were treated with NAC for 24 h followed by incubation with PE-tagged CD90-ab and FITC-tagged active caspase 3-detection reagent. The CD90+ and active caspase 3+ cells were quantified using a cell sorter. Statistically significant changes were indicated with asterisks (*p <0.05; **p <0.01, ***p <0.001.).

**Figure 21**

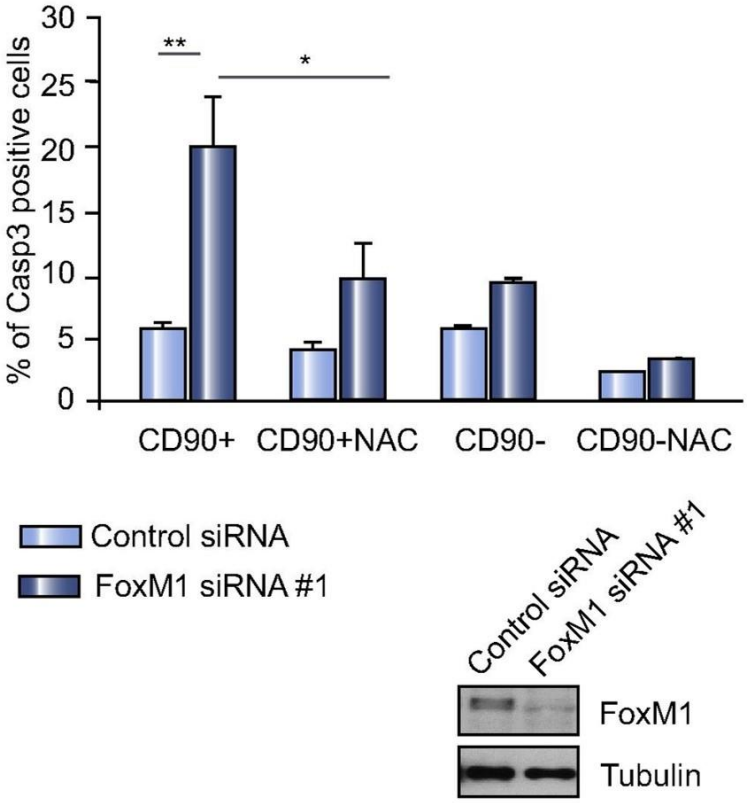
% of Casp3 positive cells
30
25
20
15
10
5
0
**
*
CD90+
CD90+NAC
CD90-
CD90-NAC
Control siRNA
FoxM1 siRNA #1
Control siRNA
FoxM1 siRNA #1
FoxM1
Tubulin

**Figure 22**

**CD90+ HCC cells are more sensitive to FoxM1 depletion.** (A) Forty-eight hours after transfection, the cells were incubated with PE-tagged CD90-ab and DCF-DA followed by separation of the CD90+ and CD90- cells using a cell sorter. (B) Forty-eight hours after transfection, the cells were incubated with PE-tagged CD90-ab followed by separation of the CD90+ and the CD90- cells using a cell sorter. Total RNAs isolated from the fractionated cells were analyzed for MnSOD mRNA expression by quantitative RT-PCR. Statistically significant changes were indicated with asterisks (*p <0.05; **p <0.01, ***p <0.001.).

**Figure 22**

**A.**

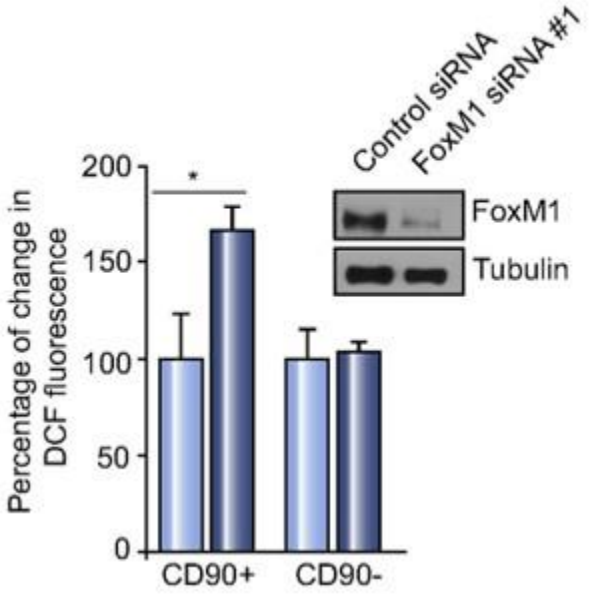
Control siRNA
FoxM1 siRNA #1
FoxM1
Tubulin
Percentage of change in DCF fluorescence
200
150
100
50
0
*
CD90+
CD90-

**B.**

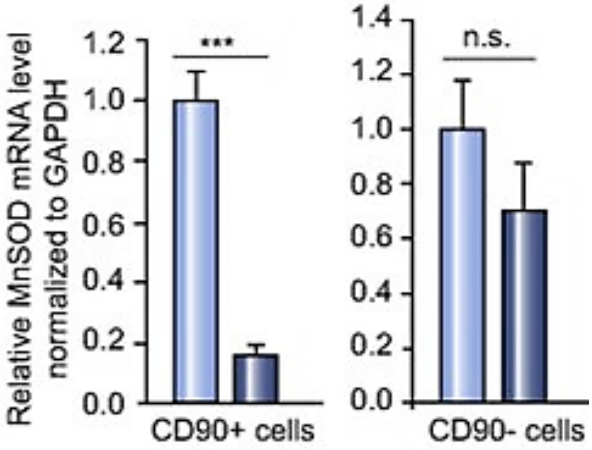
Relative MnSOD mRNA level normalized to GAPDH
1.2
1.0
0.8
0.6
0.4
0.2
0.0
***
CD90+ cells
1.4
1.2
1.0
0.8
0.6
0.4
0.2
0.0
n.s.
CD90- cells

## (III) FoxM1 inhibits the expression of liver differentiation factors FoxA1 and FoxA2

### (i) Introduction

Recent studies have linked aggressive progression of HCC to over-expression of the forkhead box transcription factor FoxM1. For example, over-expression of FoxM1 has been shown to strongly correlate with poor prognosis and high-grade progression of HCC[124,125]. Studies with mouse models provided strong causal link between FoxM1 and aggressive progression of HCC. It was shown that FoxM1 is essential for development of HCC in a chemical carcinogenesis model[126]. Deletion of FoxM1 in the adult liver blocked Diethylnitrosamine (DEN)-induced HCC development. Moreover, in the same model of chemical carcinogenesis, deregulated FoxM1 drives highly aggressive, metastatic progression of HCC [109]. In the absence of p19Arf, FoxM1 stimulates all steps of metastatic progression [109]. Consequently, inhibition of FoxM1 impedes metastatic progression of HCC [95,109].

As described above in the HRasV12 mouse model, conditional deletion of FoxM1 after HCC development causes inhibition of cancer progression and results in loss of HCC progenitor cells identified by presence of CD44 and EpCAM cell surface markers. Moreover, the hepatic cancer stem cells in human HCC lines are dependent upon FoxM1, as deletion of FoxM1 causes a preferential loss of the cancer stem cells. In that regard, it

is noteworthy that FoxM1 is a critical downstream factor of a variety of cancer signaling pathways, including Wnt/b-catenin signaling, that promote cancer stem cells[127].

FoxM1 stimulates expression of the pluripotency genes c-Myc, Oct4, Sox2 and Nanog[128,129]. In P19 embryonic carcinoma cells, knockdown of FoxM1 causes the cells to undergo differentiation with concomitant loss of expression of the pluripotency genes. Also, expression of FoxM1 induces expansion of human epithelial stem cells and increases expression of the pluripotency genes[122]. In human neuroblastoma cells, depletion of FoxM1 induces expression of differentiation markers with a loss of tumorigenicity and inhibition of the pluripotency genes[100]. Similar results were observed also in HCC. Expression of FoxM1 in human HCC cells, Huh7 and Hep3B, increases expression of the pluripotency genes, whereas knockdown of FoxM1 reduces expression of those genes. Also, in the mouse model of HRas-induced HCC, deletion of FoxM1 causes a reduction in the expression of those genes as described above. It is, therefore, likely that FoxM1 by increasing expression of the pluripotency genes supports high-grade progression of HCC. However, it is unclear whether activation of the pluripotency genes is sufficient to generate undifferentiated cancer cells that drive aggressive progression.

FoxM1 also possesses transcriptional repression activities. In the mammary gland, FoxM1 is expressed at high levels in the stem/progenitor cells to regulate their differentiation[112]. Deletion of FoxM1 decreases the population of the stem/progenitor cells and increases the population of differentiated luminal cells, and the scenario is opposite when FoxM1 is over-expressed in the mammary gland[112]. FoxM1 regulates the luminal differentiation by repressing expression of the luminal transcription factor GATA3. Here we show that

the repression function of FoxM1 is critical for aggressive HCC progression. FoxM1 represses the liver specification genes FoxA1/A2 in HCC by promoter CpG-methylation involving DNMT3b and Rb. The involvement of Rb in the FoxM1-mediated repression of FoxA1/A2 also reveals a new function of Rb in the context of FoxM1 over-expression and high-grade progression of HCC.

### (ii) Opposite expression patterns of FoxM1 and FoxA1/A2 in hepatocellular carcinoma

The FoxA genes, FoxA1 and FoxA2, are essential for liver development. Deletion of these genes in early mouse embryo inhibited development of the liver bud from foregut endoderm[130,131]. Interestingly, FoxA1/A2 have been implicated also in a chemical carcinogen-induced development of hepatocellular carcinoma in mice[132]. However, a recent study indicated that expression of FoxA2 is down-regulated in metastatic HCC[133]. Since deregulation of FoxM1 in HCC drives metastasis[109], we investigated whether FoxM1 and FoxA2 have opposite effects on aggressive progression of HCC. An analysis of the publicly available datasets revealed significant opposite correlation between the RNA levels of FoxM1 and FoxA2 in HCC (Fig. 23). In that dataset, FoxA1 RNA did not show any correlation. However, since it was possible that other FoxA1 expressing cell types present in HCC samples could confound the RNA data, we decided to analyze their expression by immunohistochemistry. We carried out immunohistochemical staining for the FoxM1 and FoxA2 proteins using tissue microarrays derived from consecutive sections of HCC specimens. FoxA1 expression also was assayed in the same cores but from distal sections. The microarrays contained grade I, grade II and grade III HCC samples. There was an obvious difference in the expression pattern of FoxM1 and FoxA1/A2. In the grade I samples, FoxA1/A2 are vividly detectable, whereas the nuclear expression of FoxM1 is low (Fig. 24A). On the other hand, in the grade III specimens, expressions of FoxA1/A2 are low, but there was abundant expression of FoxM1. Quantification of the stains further

confirmed the opposite expression patterns of FoxM1 and FoxA1/A2 in HCC. Immunohistochemical assays for FoxM1, FoxA1 and FoxA2 in normal human liver sections are shown (Fig. 24B).

**Figure 23**

**Expression of FoxM1 and FoxA2 in Roessler Liver 2 dataset (Oncomine), expression of FoxM1, FoxA1, and FoxA2 in human HCC tumor tissue microarrays**

220 normal and 225 HCC samples were analyzed for RNA expression. Expressions of FoxM1 and FoxA2 are shown (p value cut off for differential expression was selected at <0.00001). Human HCC tissue microarrays containing grade1 (n= 25), grade 2 (n= 19) and grade 3 (n= 27) were subjected to immunohistochemical staining using FoxM1, FoxA1 and FoxA2 antibodies.

**Figure 23**

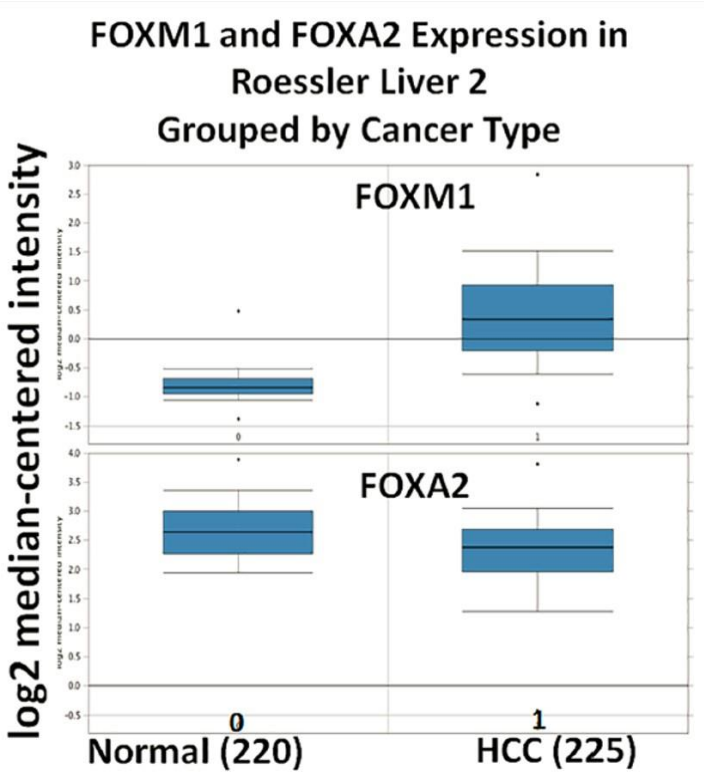
FOXM1 and FOXA2 Expression in
Roessler Liver 2
Grouped by Cancer Type
log2 median-centered intensity
FOXM1
FOXA2
0
1
Normal (220)
HCC (225)

**Figure 24**

**Expression of FoxM1, FoxA1, FoxA2 in human HCC patients.** (A)The representative tissue cores from grades 1, 2 and 3 are shown. Quantification of the imunohistochemical stains in the tissue cores corresponding to each of the grades was performed. Statistical calculations were performed using GraphPad. All images are in same scale as shown in grade 3 FoxA2 panel. (B) IHC shows the expression level of FoxM1, FoxA1 and FoxA2 in human normal liver.

**Figure 24**

**A.**

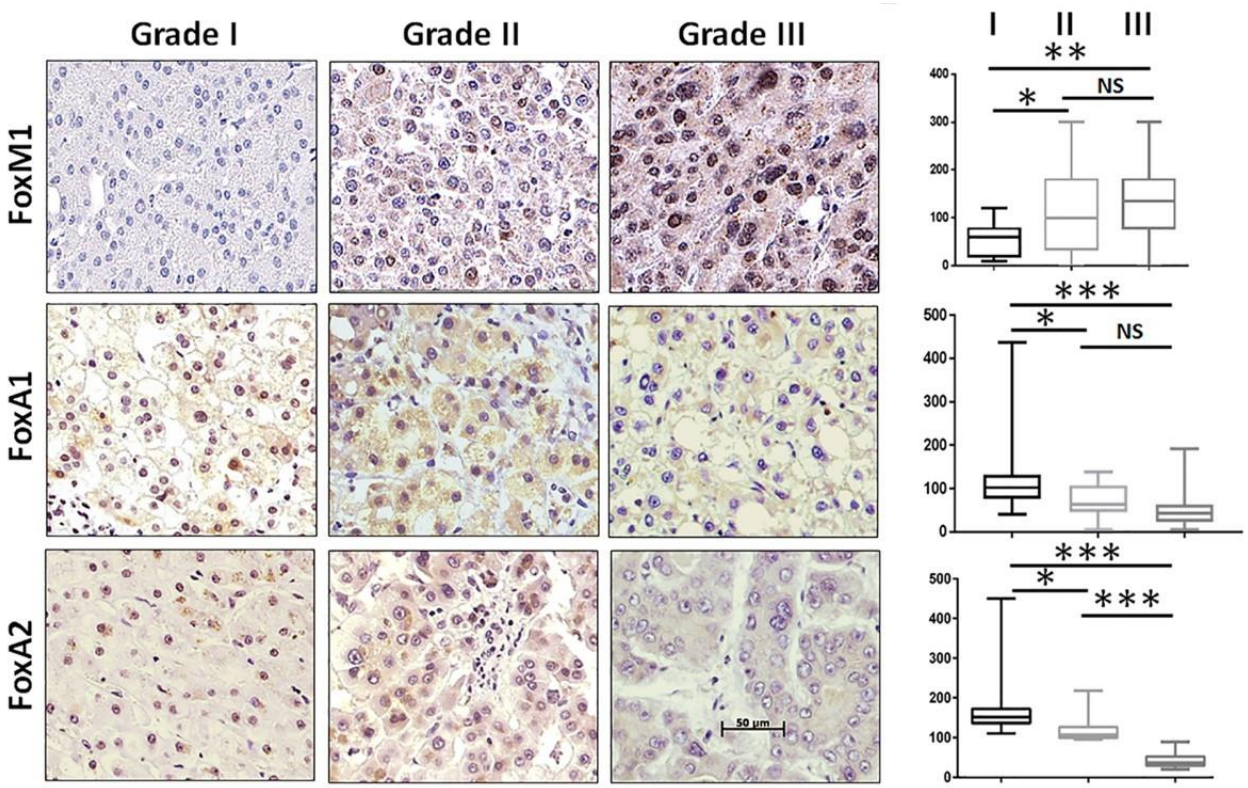
Grade I
Grade II
Grade III
FoxM1
FoxA1
FoxA2
50 µm
I
II
III
**
*
NS
***
*
NS
***
*
***
400
300
200
100
0
500
400
300
200
100
0

**B.**

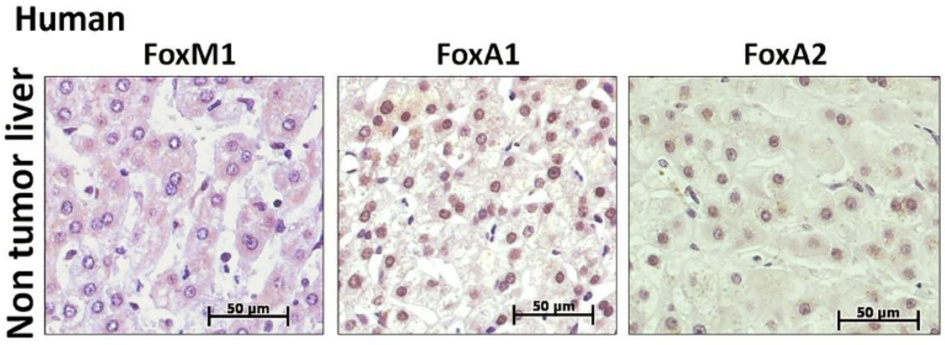
Human
FoxM1
FoxA1
FoxA2
Non tumor liver
50 µm
50 µm
50 µm

### (iii) FoxM1 inhibits FoxA1/A2 in HCC cells

Next we investigated the possibility of a direct role of FoxM1 in suppressing the FoxA1/A2 genes. We determined the effects of FoxM1b over-expression and FoxM1-knockdown on the levels of FoxA1/A2 in HCC cell lines. Expression of T7-tagged FoxM1b in Huh7 (Fig. 25A, B) and HepG2 cells (Fig. 25C, D) inhibited the levels of FoxA1/A2 at both mRNA and protein levels. For the western blots of FoxM1b in Figs. 25B and 25D short exposures of the films are shown, the endogenous FoxM1 was not detected under that condition. FoxM1-siRNAs were used to knockdown the levels of FoxM1 in Huh7 (Fig. 26A, B) and SNU449 (Fig. 26C, D) cells. Consistent with the over-expression results, knockdown of FoxM1 caused increases in the levels of FoxA1/A2 in both Huh7 and SNU449 cells. Increases in expression were detected at both mRNA (Fig. 26A, C) and protein levels (Fig. 26B, D). Also, we developed Huh7 stable cell lines in which FoxM1-shRNA can be expressed in an inducible manner by adding doxycycline in the culture medium. Expression of FoxM1-shRNA in three independent clones increased expression of FoxA1/A2 proteins (Fig. 27). Together, these observations provide evidence for an involvement of FoxM1 in regulation of the levels of FoxA1/A2 in HCC.

**Figure 25**

**FoxM1 regulates the expression of FoxA1 and FoxA2 in human HCC cells.** Huh7 cells (A-B) or HepG2 cells (C-D) were transfected with empty vector (control) or vector expressing T7-FoxM1b. Forty-eight hours after transfection, cells were harvested for protein and RNA assays. Total RNA (1 ug) was analyzed by quantitative real time PCR (qRT-PCR) for expression of FoxA1, FoxA2 and cyclophilin. Relative expressions of FoxA1 and FoxA2 were plotted (A and C). Whole cell extracts (70 ug) were subjected to western blotting for the relative expression of FoxA1 and FoxA2 (B and D). Statistical calculations for the RNA assays were done using GraphPad Prism online tool for t-test and p values stated as *$p \leq 0.05$, **$p \leq 0.001$ and ***$p \leq 0.0001$.

**Figure 25**

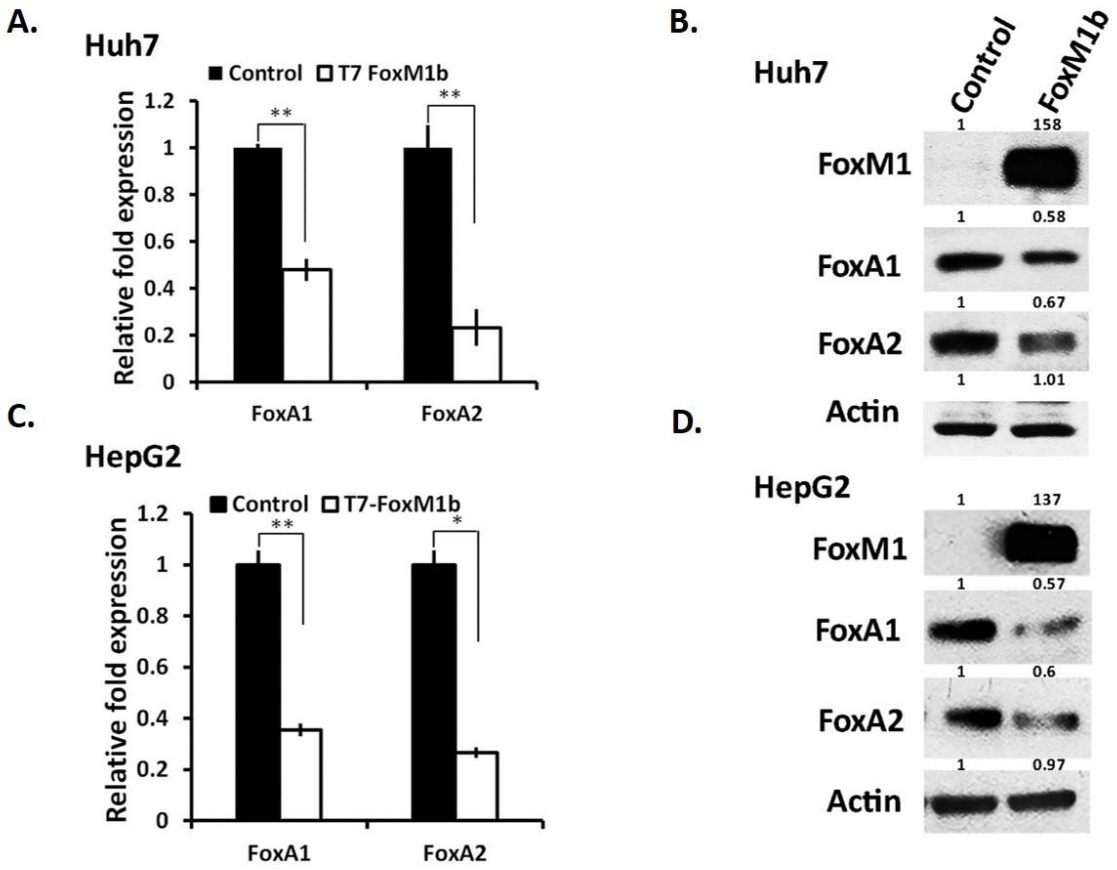
A.
Huh7
Control
T7 FoxM1b
Relative fold expression
1.2
1
0.8
0.6
0.4
0.2
0
**
**
FoxA1
FoxA2
B.
Huh7
Control
FoxM1b
FoxM1
1
158
FoxA1
1
0.58
FoxA2
1
0.67
Actin
1
1.01
C.
HepG2
Control
T7-FoxM1b
Relative fold expression
1.2
1
0.8
0.6
0.4
0.2
0
**
*
FoxA1
FoxA2
D.
HepG2
FoxM1
1
137
FoxA1
1
0.57
FoxA2
1
0.6
Actin
1
0.97

**Figure 26**

**FoxM1 regulates the expression of FoxA1 and FoxA2 in human HCC cells.** Huh7 cells (A, B) or SNU449 cells (C, D) were transfected with control-siRNA or FoxM1-siRNAs. Seventy-two hours after siRNA transfection, cells were harvested for RNA (1 ug) (A and C) and protein (100 ug) (B and D) assays, as described for the panels in A-D. For the western blots, the number above each band represents image J quantification relative to control set at 1. Statistical calculations for the RNA assays were done using GraphPad Prism online tool for t-test and p values stated as *p≤0.05, **p≤0.001 and ***p≤0.0001.

**Figure 26**

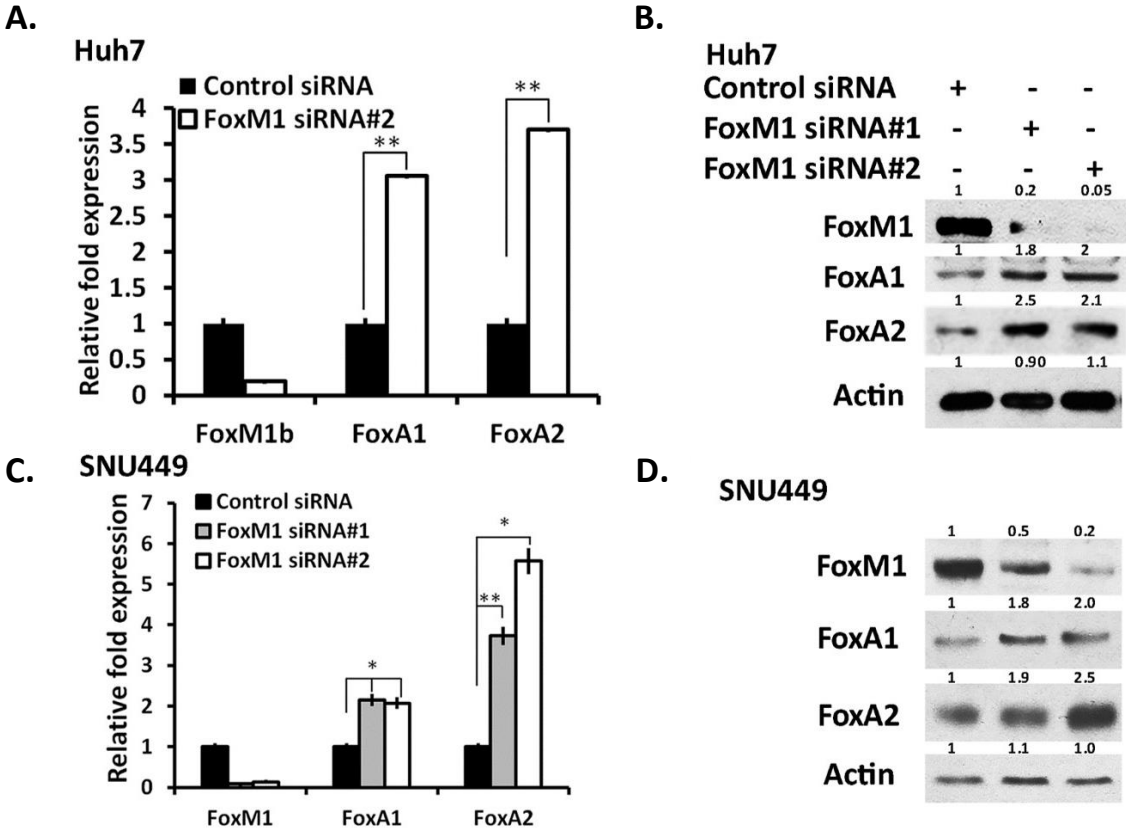
A.
Huh7
Control siRNA
FoxM1 siRNA#2
Relative fold expression
FoxM1b
FoxA1
FoxA2
B.
Huh7
Control siRNA + - -
FoxM1 siRNA#1 - + -
FoxM1 siRNA#2 - - +
FoxM1
FoxA1
FoxA2
Actin
C.
SNU449
Control siRNA
FoxM1 siRNA#1
FoxM1 siRNA#2
Relative fold expression
FoxM1
FoxA1
FoxA2
D.
SNU449
FoxM1
FoxA1
FoxA2
Actin

**Figure 27**

**FoxM1 regulates the expression of FoxA1 and FoxA2 in human HCC cells**. Inducible shFoxM1-HuH7 cell line clones were induced with doxycycline and harvested for protein. Western blot assay was carried out to observe the changes in FoxA1/A2 protein levels upon FoxM1 attenuation.

**Figure 27**

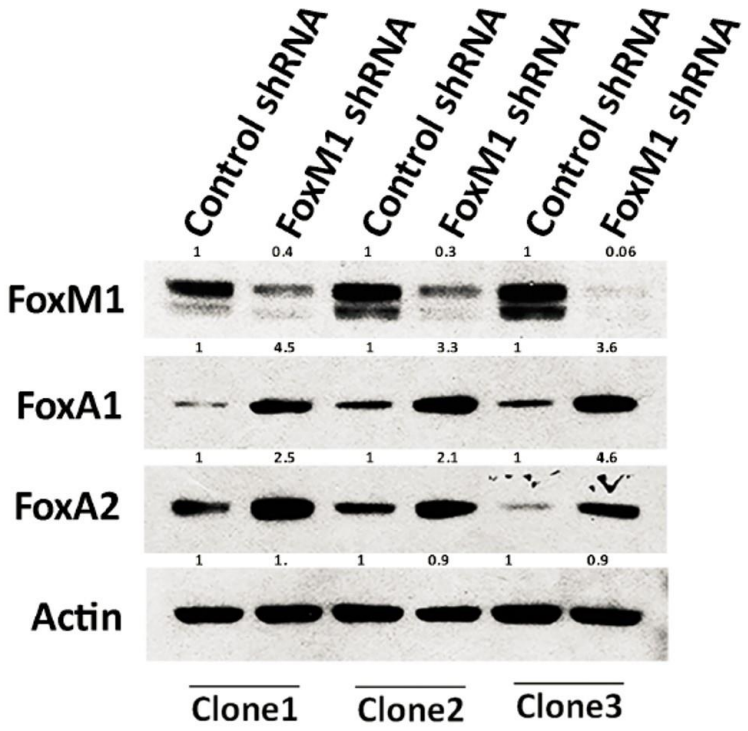
Control shRNA
FoxM1 shRNA
Control shRNA
FoxM1 shRNA
Control shRNA
FoxM1 shRNA
1 0.4 1 0.3 1 0.06
FoxM1
1 4.5 1 3.3 1 3.6
FoxA1
1 2.5 1 2.1 1 4.6
FoxA2
1 1. 1 0.9 1 0.9
Actin
Clone1
Clone2
Clone3

**(iv) FoxM1 recruits DNMT3b and Rb onto the FoxA1/A2 promoters**

Recently, we described a transcriptional repression function of FoxM1 in which it represses the mammary luminal gene GATA3 involving DNMT3b and Rb[112]. Depletion of Rb in vitro and in vivo blocked FoxM1-mediated repression of GATA3. The effects of FoxM1 on FoxA1/A2 are not likely to be related to GATA3, as the HCC cells do not express GATA3 in a detectable level (Fig. 28). To determine whether a more direct mechanism, like repression of GATA3, is in play for repression of FoxA1/A2 in HCC cells, we sought to determine whether FoxM1 directly targets FoxA1/A2 promoters. The human FoxA1 gene – 5 kb upstream region contains two FoxM1-binding sites at around -1391 and -4221, whereas the FoxA2 gene contains at least four putative FoxM1-binding elements (Fig. 29). Chromatin-IP experiments using FoxM1-ab detected enrichment of DNA fragments encompassing the sites at -1391 in the FoxA1 gene (Fig. 30A) and at -1294 and -4156 in the FoxA2 gene (Fig. 30B), providing evidence that FoxM1 binds to the FoxA1/A2 promoters in Huh7 cells. The other sites in the FoxA1/A2 upstream regions did not show any significant enrichment over that with the IgG (Figs. 30A, B).

Previously, we showed that FoxM1 binds to both DNMT3b and Rb, forming a repressor complex in breast cancer cells[112]. Interestingly, that complex could be easily detected in HCC cells. Immunoprecipitation of Huh7 cell extracts with a monoclonal antibody against FoxM1 (Fig. 31A) or a rabbit polyclonal antibody against FoxM1 (Fig. 31B) co-immunoprecipitated DNMT3b and Rb. Next, we investigated whether FoxM1 recruits Rb and DNMT3b onto the upstream regions of FoxA1/A2. We carried out chromatin-IP experiments with Rb and DNMT3b antibodies using the Huh7 cells expressing control-

siRNA or FoxM1-siRNA (Fig. 31C). As shown in Figs. 32 & 33, both Rb and DNMT3b are bound to the same promoter-fragments that were enriched in chromatin-IP with FoxM1-ab. Moreover, knockdown of FoxM1 caused significant reduction in the bindings of Rb and DNMT3b onto the specific sites in the FoxA1/A2 promoters. Together, the results confirm the notion that FoxM1 recruits DNMT3b and Rb onto the FoxA1/A2 promoters.

**Figure 28**

**GATA3 protein levels in human HCC cell lines**. Multiple human HCC cell lines (HepG2, Huh7, Hep3B, and SNU449) were investigated for the expression of GATA3 using western blot assay. 100 μg of protein extract from HCC cell lines and luminal breast cancer cell line MCF7 were compared for GATA3 expression. ImageJ quantifications are also indicated above the lanes.

**Figure 28**

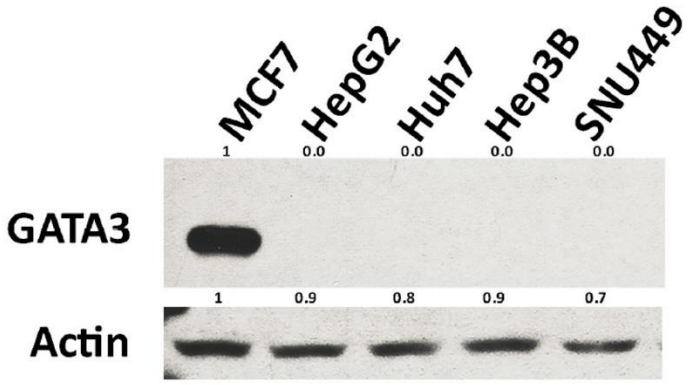
MCF7
HepG2
Huh7
Hep3B
SNU449
1
0.0
0.0
0.0
0.0
GATA3
1
0.9
0.8
0.9
0.7
Actin

**Figure 29**

**Presence of FoxM1 binding sites and CpG islands on human FoxA1 and FoxA2 promoters.** Schematic shows the predicted CpG methylation islands (sky blue) using Methprimer tool (http://www.urogene.org) and FoxM1 binding sites (Red arrow) using Mac Vector promoter consensus sequence finding tool on the FoxA1 and FoxA2 promoters.

**Figure 29**

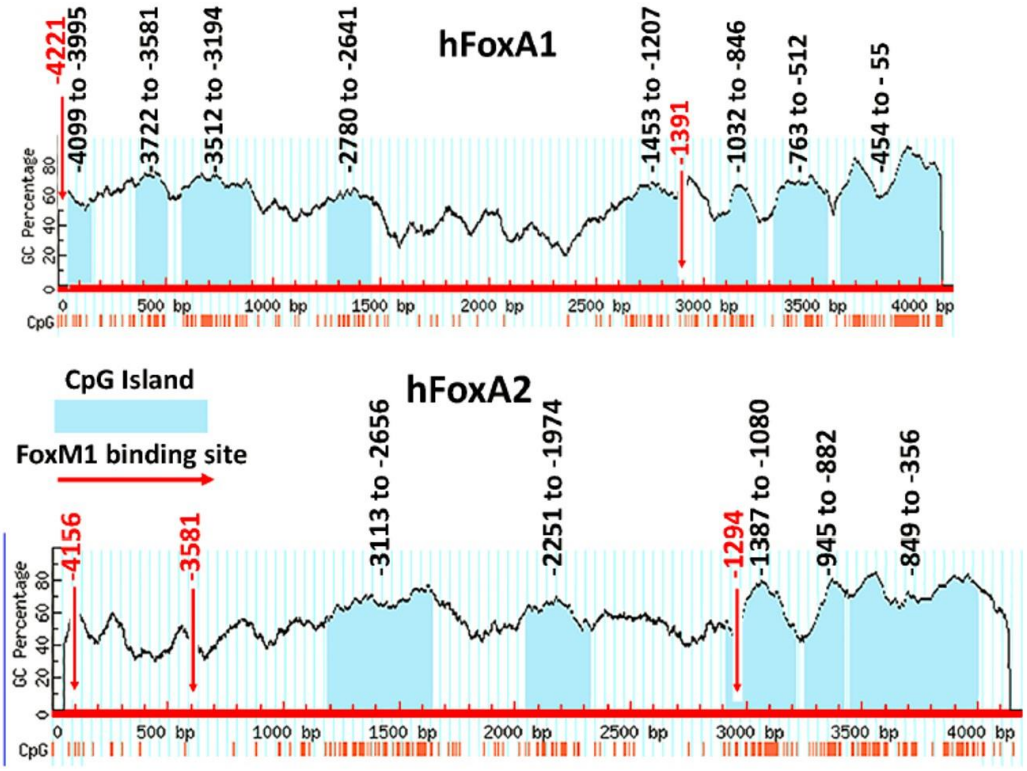
hFoxA1
-4221
-4099 to -3995
-3722 to -3581
-3512 to -3194
-2780 to -2641
-1453 to -1207
-1391
-1032 to -846
-763 to -512
-454 to - 55
GC Percentage
0 20 40 60 80
0 500 bp 1000 bp 1500 bp 2000 bp 2500 bp 3000 bp 3500 bp 4000 bp
CpG
CpG Island
FoxM1 binding site
hFoxA2
-4156
-3581
-3113 to -2656
-2251 to -1974
-1294
-1387 to -1080
-945 to -882
-849 to -356
GC Percentage
0 20 40 60 80
0 500 bp 1000 bp 1500 bp 2000 bp 2500 bp 3000 bp 3500 bp 4000 bp
CpG

**Figure 30**

**FoxM1 binds to FoxA1 and FoxA2 promoter**

Huh7 cells were transfected with control-siRNA or FoxM1-siRNA1. Seventy-two hours after transfection, cells were subjected to crosslinking for chromatin-IP (ChIP). The chromatin preparations were immunoprecipitated with FoxM1-ab or IgG. Enrichments of the FoxA1 (A) and FoxA2 (B) promoter fragments were assayed by quantitative RT-PCR, and the relative enrichments with FoxM1-ab over that with IgG after normalization against a non-specific site are shown. Statistical calculations were done using GraphPad Prism online tool for t-test and p values stated as *$p \leq 0.05$ and **$p \leq 0.001$

**Figure 30**

**A.**

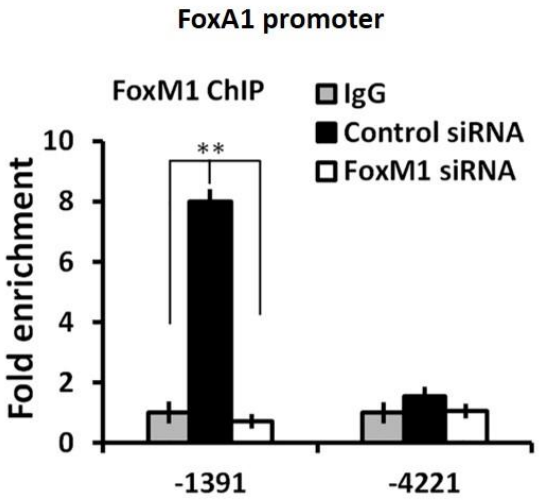
FoxA1 promoter
FoxM1 ChIP
IgG
Control siRNA
FoxM1 siRNA
Fold enrichment
10
8
6
4
2
0
**
-1391
-4221

**B.**

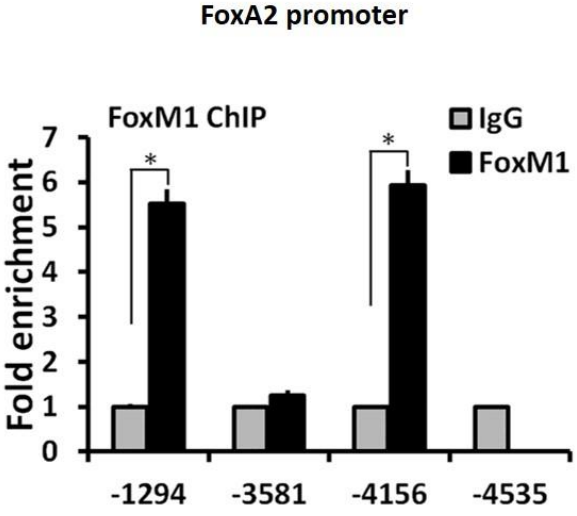
FoxA2 promoter
FoxM1 ChIP
IgG
FoxM1
Fold enrichment
7
6
5
4
3
2
1
0
*
*
-1294
-3581
-4156
-4535

**Figure 31**

**FoxM1 binds to Rb and DNMT3b in human HCC cell line Huh7.** Interactions of FoxM1 with Rb and DNMT3b were analyzed by immunoprecipitating Huh7 cell extracts (1.5 mg) with mouse IgG or a monoclonal FoxM1 antibody (A); rabbit-IgG or Rabbit polyclonal antibody (B). The immunoprecipitates were assayed for the presence of Rb and DNMT3b by western blotting. Huh7 cells transfected with control-siRNA or FoxM1 siRNA for 72h, the transfected cells were harvested 72 hours post transfection and the level of FoxM1 knock down was analyzed by western blotting (0.1 mg cell-extracts) with FoxM1 antibody and actin was used as loading control (C).

**Figure 31**

**A.**

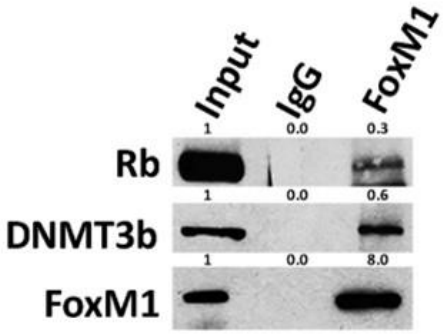


**B.**

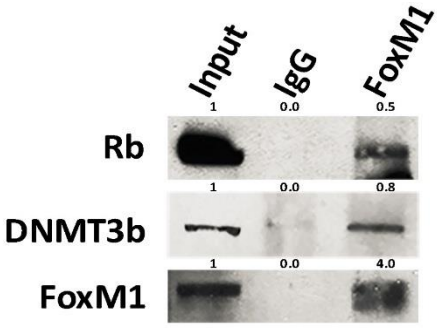


**C.**

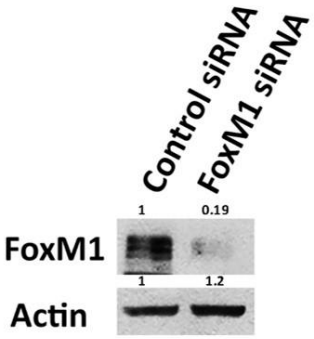

**Figure 32**

**FoxM1 recruits Rb and DNMT3b to FoxA1 promoter.** Huh7 cells transfected with control-siRNA or FoxM1 siRNA for 72h (Fig 31C); the transfected cells were harvested 72 hours post transfection and processed for for ChIP using Rb antibody or DNMT3b-antibod. Relative enrichments of the FoxA1 promoter fragments from control-siRNA transfected cells over those from the FoxM1-siRNA transfected cells are shown. Statistical calculations were done using GraphPad Prism online tool for t-test and p values stated as *p≤0.05 and **p≤0.001

**Figure 32**

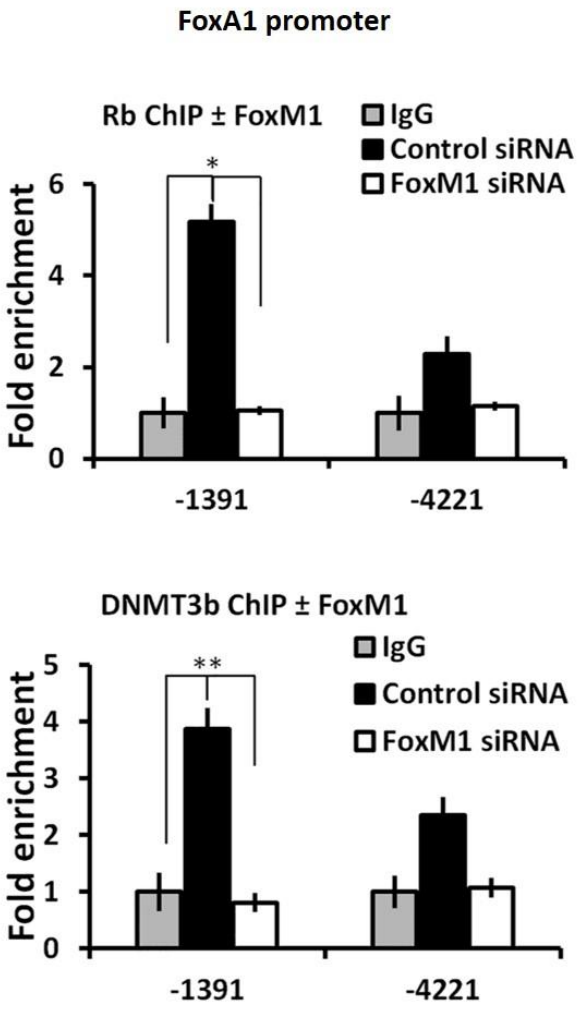
FoxA1 promoter
Rb ChIP ± FoxM1
IgG
Control siRNA
FoxM1 siRNA
Fold enrichment
0
2
4
6
*
-1391
-4221
DNMT3b ChIP ± FoxM1
IgG
Control siRNA
FoxM1 siRNA
Fold enrichment
0
1
2
3
4
5
**
-1391
-4221

**Figure 33**

**FoxM1 recruits Rb and DNMT3b to FoxA2 promoter.** Huh7 cells transfected with control-siRNA or FoxM1 siRNA for 72h (Fig 31C); the transfected cells were harvested 72 hours post transfection and processed for for ChIP using Rb antibody or DNMT3b-antibod. Relative enrichments of the FoxA2 promoter fragments from control-siRNA transfected cells over those from the FoxM1-siRNA transfected cells are shown. Statistical calculations were done using GraphPad Prism online tool for t-test and p values stated as *p≤0.05 and **p≤0.001

**Figure 33**

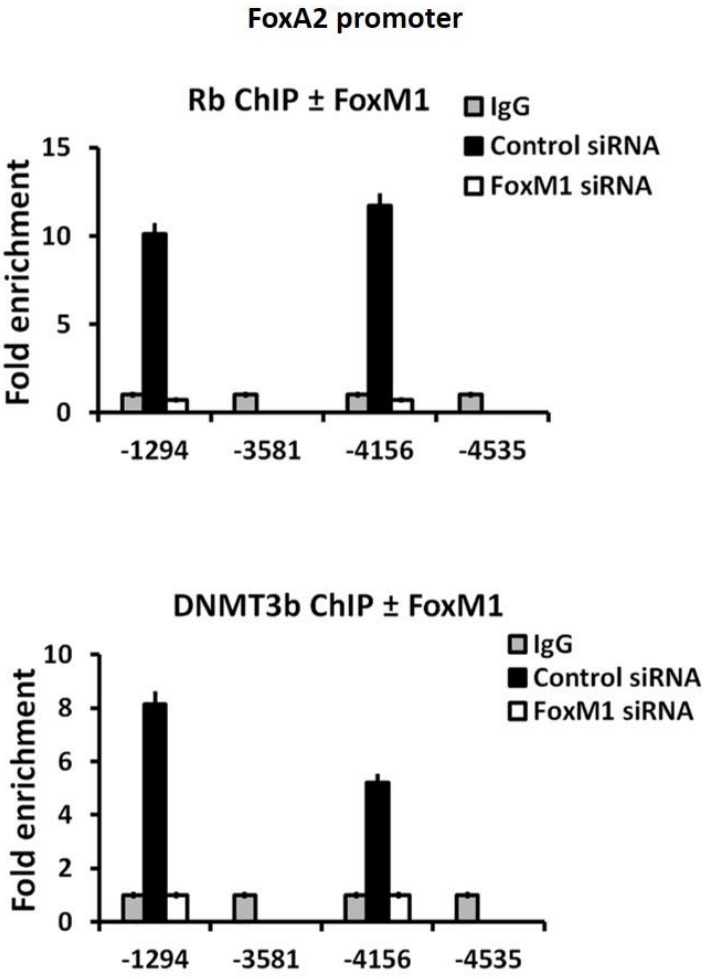
FoxA2 promoter
Rb ChIP ± FoxM1
IgG
Control siRNA
FoxM1 siRNA
Fold enrichment
15
10
5
0
-1294
-3581
-4156
-4535
DNMT3b ChIP ± FoxM1
IgG
Control siRNA
FoxM1 siRNA
Fold enrichment
10
8
6
4
2
0
-1294
-3581
-4156
-4535

### (v) FoxM1 induces methylation of CpGs in the FoxA1/A2 promoters requiring Rb

Recruitment of DNMT3b onto the FoxA1/A2 promoters suggests that the repression by FoxM1 would involve methylation of CpG islands in the FoxA1/A2 promoters. We employed methylation-specific PCR to investigate FoxM1-mediated methylation of the FoxA1/A2 promoters. Huh7 cells were transfected with FoxM1b-expresion vector or FoxM1-siRNA. Genomic DNAs from the transfected cells were treated with bisulfite followed by PCR using primers for the CpG islands in the FoxA1/A2 promoters. Expression of FoxM1b caused an increase in CpG methylation near the FoxM1-binding sites in the FoxA1/A2 gene (Fig. 34A, B and C). Moreover, knockdown of FoxM1 caused a decrease in CpG methylation at those sites in the FoxA1/2 promoters (Fig. 35).

Next, we investigated whether there is any involvement of Rb in the FoxM1-directed methylation of the FoxA1/A2 promoters. We employed an Rb-shRNA construct that allows inducible depletion of Rb in the presence of doxycycline (Fig. 36A). As shown in Fig. 36B, expression of FoxM1 increased methylation of the FoxA1/A2 promoters in the presence of Rb (no doxycycline), but upon depletion of Rb (doxycycline) there was no increase in the CpG methylation at the indicated sites. Moreover, depletion of Rb caused increases in the expression of FoxA1/A2 (Fig. 37, 36A). Expression of FoxM1 in the Rb-depleted cells had very little effect (Fig. 37). These observations demonstrate that the FoxM1/DNMT3b complex methylates and represses the FoxA1/A2 promoters requiring Rb. The extent of FoxA1/A2 repression by FoxM1 varied between 40 and 75%, which is likely due to variations in the levels of active Rb in the transfected cells.

**Figure 34**

**FoxM1 induces methylation of the FoxA1 and FoxA2 promoters.** (A) Huh7 cells were transfected with empty vector (control) and T7-FoxM1b expressing vector. Genomic DNA was isolated and subjected to bisulphite treatment for CT conversion. Methylation of the FoxA1 and FoxA2 upstream regions in control and FoxM1 transfected was assayed using qRT-PCR. Other sites did not show any noticeable change in methylation levels (B, C). Statistical calculations were done using GraphPad Prism online tool for t-test and p values stated as *p≤0.05and **p≤0.001.

**Figure 34**

**A.**

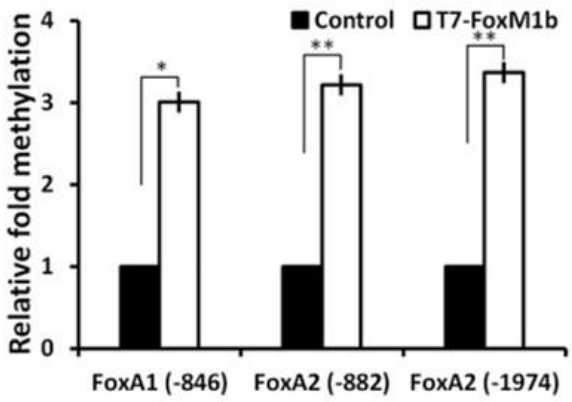


**B.**

**C.**

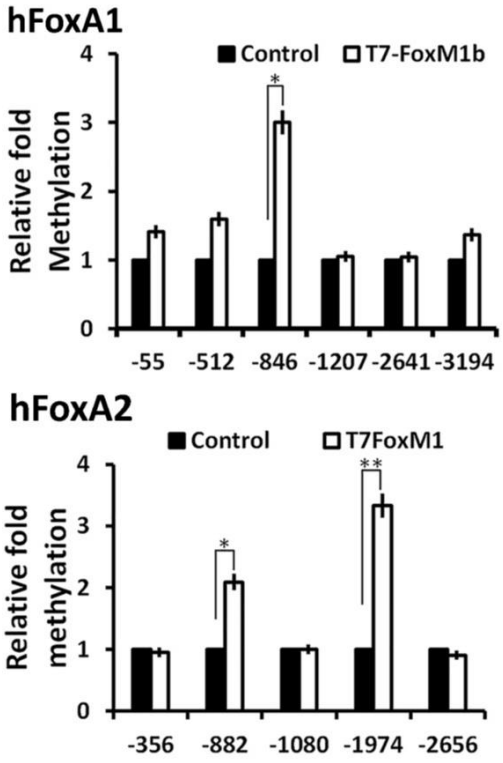

**Figure 35**

**FoxM1 induces methylation of the FoxA1 and FoxA2 promoters.**

Huh7 cells were transfected with either control siRNA or FoxM1 siRNA. Cell were harvested 72 hours post transfection; genomic DNA was isolated and subjected to bisulphite treatment for CT conversion. Methylation of the FoxA1 and FoxA2 upstream regions in control and FoxM1 transfected was assayed using qRT-PCR. Statistical calculations were done using GraphPad Prism online tool for t-test and p values stated as *p≤0.05and **p≤0.001.

**Figure 35**

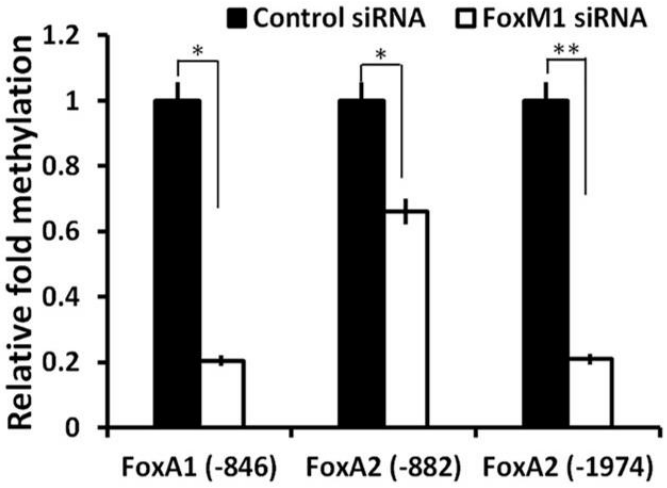
Control siRNA
FoxM1 siRNA
Relative fold methylation
1.2
1
0.8
0.6
0.4
0.2
0
*
*
**
FoxA1 (-846)
FoxA2 (-882)
FoxA2 (-1974)

**Figure 36**

**FoxM1 induces methylation of the FoxA1 and FoxA2 promoters requiring Rb.**

Huh7 cells stably expressing Dox inducible Rb-shRNA (A). Western blot (100 μg of cell-extracts) showing depletion of Rb in doxycycline-induced Huh7 cells and effect of Rb knock down on FoxA1 and FoxA2 expression. Inducible Rb-shRNA Huh7 cells were transfected with control and T7-FoxM1 expression vectors in presence and absence of Dox as depicted (B). The genomic DNAs were isolated for CT conversion using bisulphite method and the difference in the promoter methylation of FoxA1 and FoxA2 was assayed by qRT-PCR. Statistical calculations were done using GraphPad Prism online tool for t-test and p values stated as *$p \leq 0.05$and **$p \leq 0.001$.

**Figure 36**

**A.**

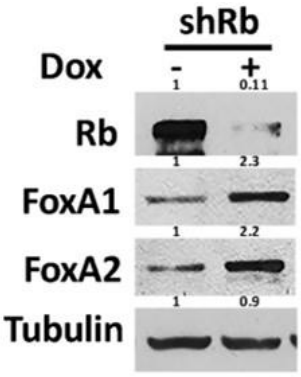
shRb
Dox
-
+
1
0.11
Rb
1
2.3
FoxA1
1
2.2
FoxA2
1
0.9
Tubulin

**B.**

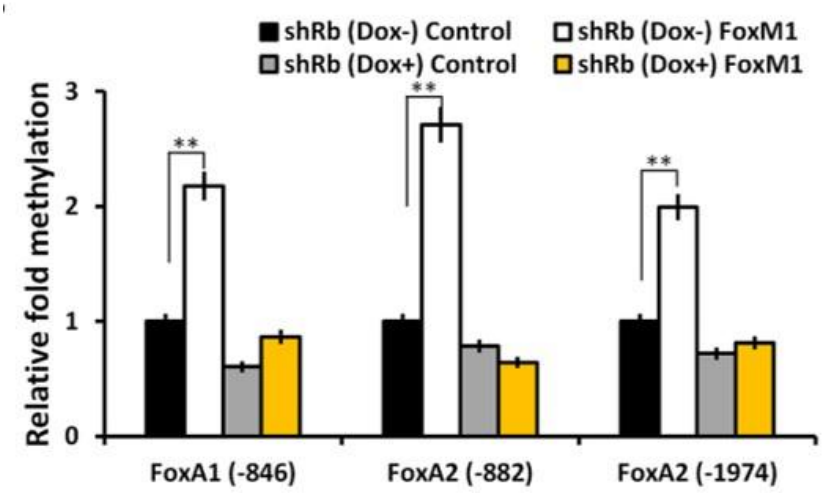
shRb (Dox-) Control
shRb (Dox-) FoxM1
shRb (Dox+) Control
shRb (Dox+) FoxM1
Relative fold methylation
0
1
2
3
**
**
**
FoxA1 (-846)
FoxA2 (-882)
FoxA2 (-1974)

**Figure 37**

**Rb is required for FoxM1 mediated repression of FoxA1 and FoxA2.**

Quantification of FoxA1 and FoxA2 relative mRNA expressions using qRT-PCR in Huh7 cells expressing Dox inducible Rb-shRNA and transfected with either control vector or T7-FoxM1 in absence and presence of Dox. Statistical calculations were done using GraphPad Prism online tool for t-test and p values stated as *p≤0.05and **p≤0.001.

**Figure 37**

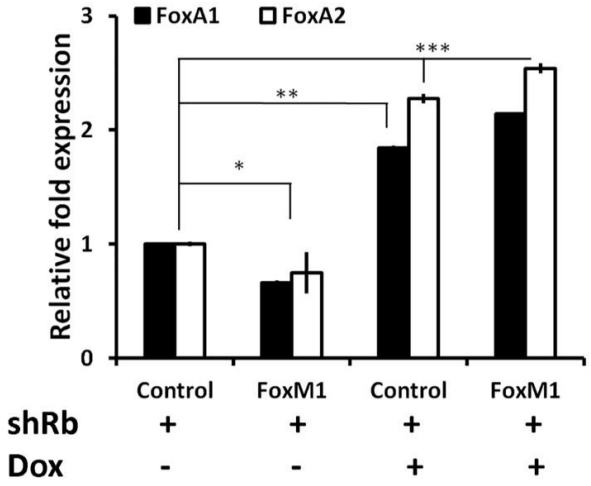
FoxA1
FoxA2
Relative fold expression
3
2
1
0
***
**
*
Control
FoxM1
Control
FoxM1
shRb + + + +
Dox - - + +

### (vi) Deletion of FoxM1 in a Ras-transgenic model for HCC causes accumulation of FoxA1/A2, coinciding with decreased promoter methylation

As described above, we studied the roles of FoxM1 in HCC progression using a transgenic mouse model that expresses oncogenic HRas in the liver. In that study, the floxed alleles of FoxM1 were deleted after HCC development using the MxCre deletion system, which deletes floxed alleles in liver as well as in blood cells[117], and that somewhat mimics what would be expected from a drug that inhibits FoxM1. In those experiments, FoxM1-deletion in the HCC nodules was detected mainly in the HCC cells. Moreover, it is shown above that deletion of FoxM1 after HCC development inhibits HCC progression. Sections from those tumor nodules were analyzed for FoxA1/A2 expression by immunohistochemistry. The HRas-derived tumor nodules without FoxM1-deletion exhibited very little expression of FoxA1/A2 (Figs. 38A, B and 39A, B). But, in the FoxM1-deleted samples there was a significant increase in the FoxA1/A2. The observation was confirmed by western blot assays using extracts from tumor nodules with and without FoxM1-deletion (Figs. 38C and 39C). The increases in the expression of FoxA1/A2 in the FoxM1-deleted samples provides in vivo genetic evidence that FoxM1 plays a role in the inhibition of these FoxA genes in HCC. Expression of FoxM1, FoxA1 and FoxA2 in normal mouse liver is shown in Fig. 40. Changes in CpG methylation was detected also in the mouse HCC samples following deletion of FoxM1. We checked for changes in methylation at the predicted CpG islands (Fig 41A, B) on mFoxA1 and mFoxA2 promoters. As shown in Figs. 42A and 42B, there were decreases in CpG-methylation in the promoters of FoxA1 and FoxA2 in samples derived from FoxM1-deleted livers. Moreover, we show evidence

that mouse FoxM1 binds to Rb and DNMT3b using extracts from the mouse Hepa1-6 cell line (Fig. 42C).

**Figure 38**

**Increase in FoxA1 protein levels in mouse HCC samples upon deletion of FoxM1**

(A) Immunohistochemical staining of mouse HCC sections using FoxA1 antibody with and without deletion of FoxM1. HCC in those mice was driven by expression of oncogenic H-Ras. The mouse strains also harbored floxed alleles of FoxM1 and MxCre. FoxM1 deletion was induced following HCC development by injecting (10 times) the mice with polyIpolyC. (B) Graph showing quantification of FoxA1 +ve from 3 pairs of mice, and 5 random fields were chosen for analyses. $p<0.05$ (C) Comparison (0.1 mg of tumor extracts) of the FoxA1 protein levels between FoxM1+/+ and FoxM1 fl/fl tumor tissue-extracts from mice injected with poly(I)poly(C) five times, using western blots.

**Figure 38**

**A.**

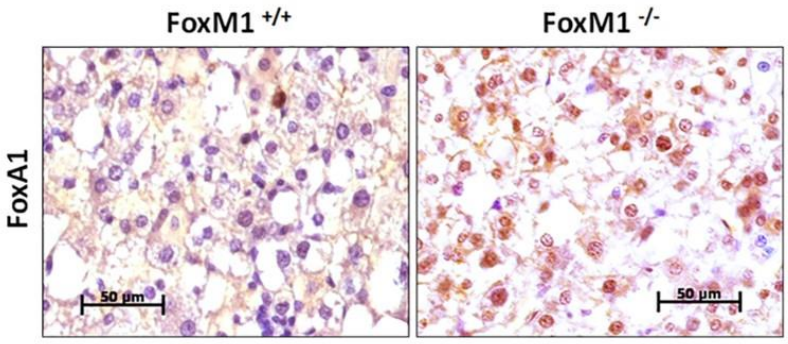


**B.**

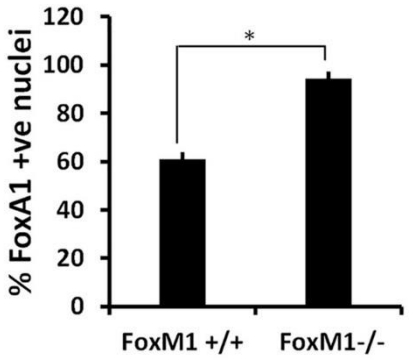


**C.**

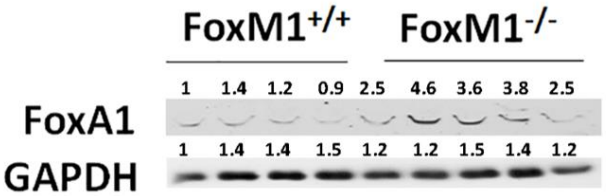

**Figure 39**

**Increase in FoxA2 protein levels in mouse HCC samples upon FoxM1 deletion**

(A) Immunohistochemical staining of mouse HCC sections using FoxA2 antibody with and without deletion of FoxM1. HCC in those mice was driven by expression of oncogenic H-Ras. The mouse strains also harbored floxed alleles of FoxM1 and MxCre. FoxM1 deletion was induced following HCC development by injecting (5 times) the mice with polyIpolyC. (B) Graph showing quantification of FoxA1 +ve from 3 pairs of mice, and 5 random fields were chosen for analyses. $p<0.05$ (C) Comparison (0.1 mg of tumor extracts) of the FoxA2 protein levels between FoxM1+/+ and FoxM1 fl/fl tumor tissue-extracts from mice injected with poly(I)poly(C) five times, using western blots.

**Figure 39**

**A.**

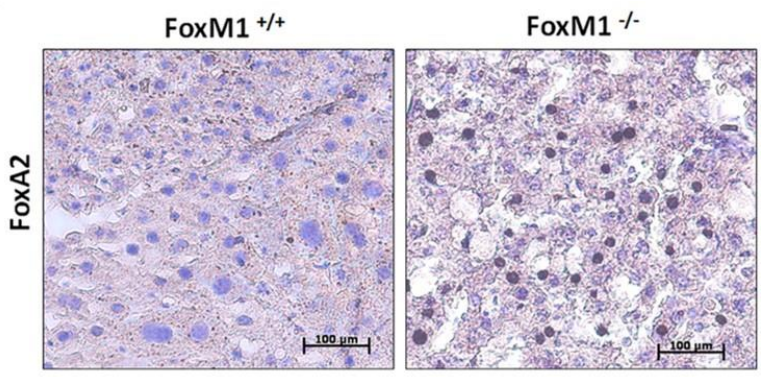


**B.**

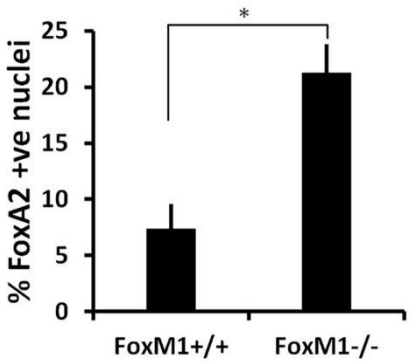


**C.**

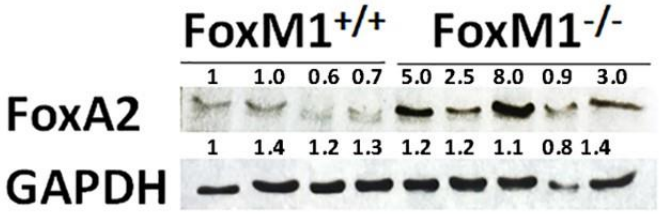

**Figure 40**

Immunohistochemical analysis for checking the expression of FoxM1, FoxA1 and FoxA2 in adult mice non-tumor liver sections of the transgenic mice. Scale bar is set to 100 μm.

**Figure 40**

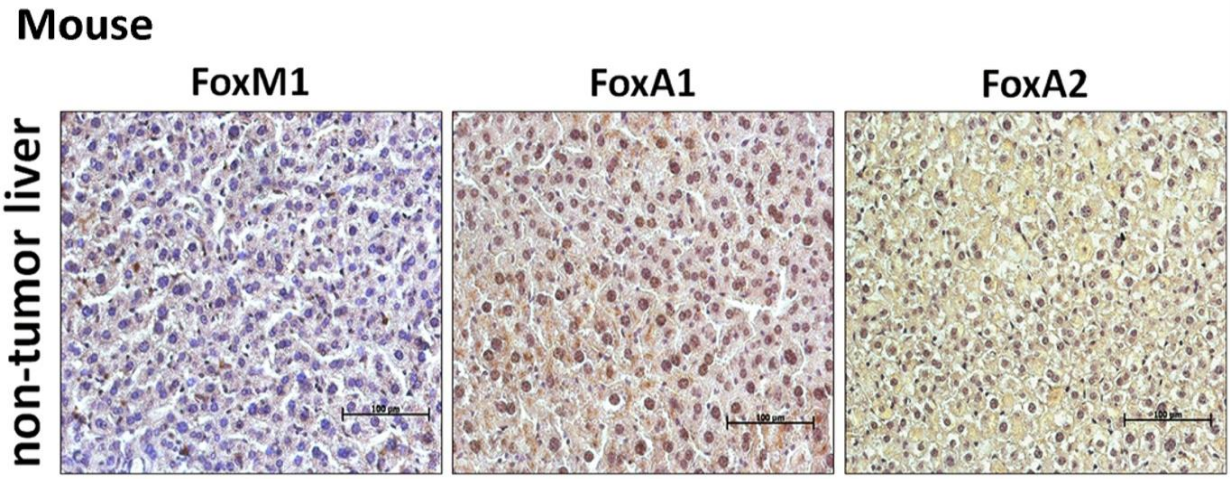

**Figure 41**

**Schematics of mFoxA1 and mFoxA2 promoters and interaction between mFoxM1, mRb and mDNMT3b:** (A-B) Schematic shows the predicted CpG methylation islands (sky blue) using Methprimer tool (http://www.urogene.org) and FoxM1 binding sites (Red arrow) using Mac Vector promoter consensus sequence finding tool on the FoxA1 and FoxA2 promoters.

**Figure 41**

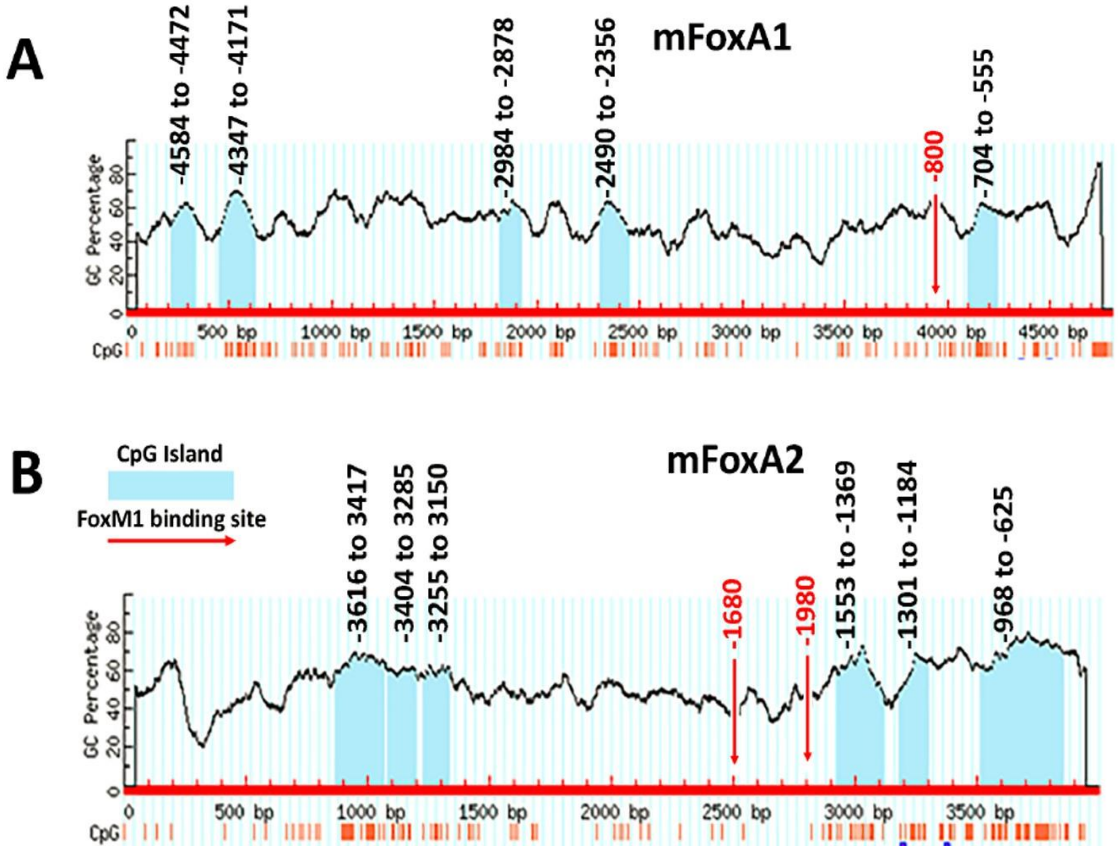
A
mFoxA1
-4584 to -4472
-4347 to -4171
-2984 to -2878
-2490 to -2356
-800
-704 to -555
GC Percentage
0
20
40
60
80
0
500 bp
1000 bp
1500 bp
2000 bp
2500 bp
3000 bp
3500 bp
4000 bp
4500 bp
CpG
B
CpG Island
FoxM1 binding site
mFoxA2
-3616 to 3417
-3404 to 3285
-3255 to 3150
-1680
-1980
-1553 to -1369
-1301 to -1184
-968 to -625
GC Percentage
0
20
40
60
80
0
500 bp
1000 bp
1500 bp
2000 bp
2500 bp
3000 bp
3500 bp
CpG

**Figure 42**

**FoxM1 deletion leads to decrease in promoter methylation on FoxA1 and FoxA2 promoters *invivo.*** (A, B) Genomic DNA was isolated from FoxM1+/+ and FoxM1-/- mouse tumor tissues and bisulphite conversion was performed, quantification of the FoxA1 and FoxA2 promoter methylation was assayed using qRT-PCR and graph shows the average representation of tumor samples from two different mice (Statistical calculation was performed using Graphpad Prism and p value states *p<=0.05). (C) Interactions of mFoxM1 with mRb and mDNMT3b were assayed by immunoprecipitation with FoxM1-ab and 2 mg of mouse cellular extract (Hepa1-6 cells) and interaction was analyzed by western blotting with Rb and DNMT3b antibody.

**Figure 42**

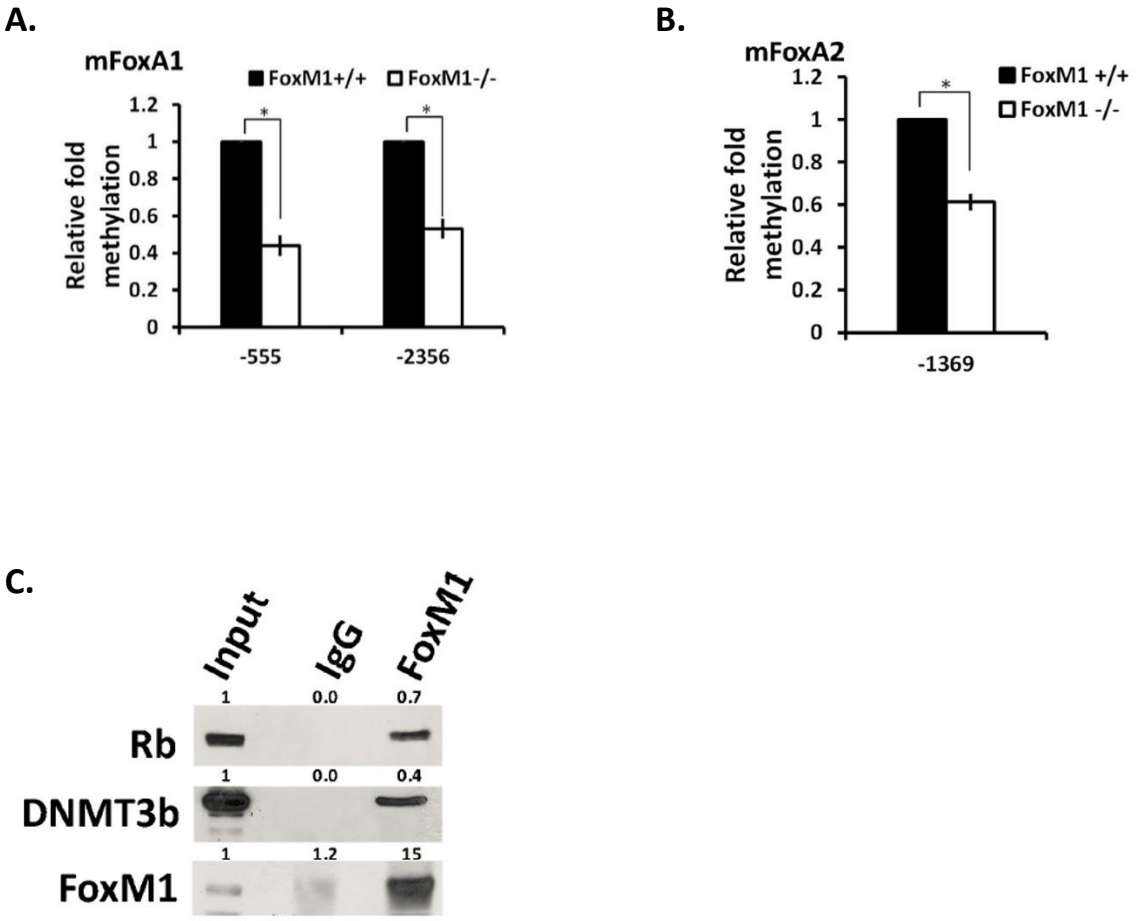
A.
mFoxA1
FoxM1+/+
FoxM1-/-
Relative fold methylation
1.2
1
0.8
0.6
0.4
0.2
0
*
*
-555
-2356
B.
mFoxA2
FoxM1 +/+
FoxM1 -/-
Relative fold methylation
1.2
1
0.8
0.6
0.4
0.2
0
*
-1369
C.
Input
IgG
FoxM1
1
0.0
0.7
Rb
1
0.0
0.4
DNMT3b
1
1.2
15
FoxM1

### (vii) FoxA1/A2 inhibit FoxM1b-induced clonogenicity and soft agar colony formation

FoxM1 is a pro-proliferation transcription factor that also inhibits apoptosis, and drives aggressive progression of cancers when over-expressed[95]. We investigated whether repression of the FoxA genes plays any role in those processes. If repression of FoxAs is important, the prediction is that expression of FoxAs would inhibit the FoxM1 pathways in HCC cells. We investigated whether FoxA1/A2 inhibits FoxM1 functions. We analyzed clonogenicity of Huh7 cells following expression of FoxM1 and FoxA1/A2. Clonogenic growth accounts for both proliferative capacity and viability of cells. As expected, expression of FoxM1 led to significant increases in clonogenicity of the Huh7 cells (Figs. 43A and B). Expression of either FoxA1 or FoxA2 alone did not show any significant effect, but when expressed in combination with FoxM1 they strongly inhibited the FoxM1-induced increased clonogenicity of the Huh7 cells (Figs. 43A and 43B). Expression of FoxM1 also increases soft agar colony formation (Figs. 44A and B). We show that co-expression of FoxA1 or FoxA2 inhibited FoxM1-induced increase in soft agar colonies (Figs. 44A and B). Also, FoxA1 or FoxA2 inhibits FoxM1-mediated increase in cell migration in wound healing assays (Fig. 45). Furthermore, we observed that expression of FoxM1 increased sphere formation in HepG2 cells, and that co-expression of FoxA1 or FoxA2 inhibited the FoxM1-mediated increase in sphere formation (Fig. 46A, B and C).

Interestingly, in the co-expression experiments above, we consistently observed that expression of FoxA1 or FoxA2 affected the levels of total FoxM1. FoxA1/A2 did not have any significant effect on the co-expressed Flag tagged FoxM1b levels (Fig. 47, Flag panel).

However, expression of Flag-FoxM1b increased the levels of the endogenous FoxM1 (Fig. 47, top panel), and that is consistent with a previous report[134]. Co-expression of FoxA1 or FoxA2 appeared to inhibit the increase of the endogenous FoxM1 (Fig. 47, top panel). Therefore, we investigated whether FoxA1/A2 are able to inhibit expression of FoxM1. As shown in Fig. 48, expression of FoxA1 or FoxA2 in Huh7 cells inhibited the mRNA levels of FoxM1 as well as several FoxM1 target genes, including Survivin, Aurora B and CD44. Moreover, in a chromatin-IP experiment, we observed interaction of the endogenous FoxA1 and FoxA2 with an upstream FoxA1/A2 cognate element in the FoxM1 promoter (Fig. 49). Together, these observations indicate that FoxA1/A2 are inhibitors of the FoxM1 pathway, which is related to aggressive cancer progression, and that FoxM1-mediated suppression of FoxA1/A2 is likely an important step towards aggressive progression of HCC.

**Figure 43**

**FoxA1 and FoxA2 inhibits FoxM1-induced clonogenicity and anchorage independent growth of the Huh7 cells.** Huh7 cells were transfected individually with empty vector, Flag-FoxM1, FoxA1, or FoxA2 or a combination of Flag-FoxM1 and FoxA1 or Flag-FoxM1 and FoxA2, along with GFP expression plasmid as transfection control. Clonogenicity assay was performed using these cells. About $1x10^4$ cells were seeded in triplicate in 24-well plate and allowed to grow for one week then cells were fixed and stained with crystal violet and pictures were taken under a light microscope (B). Quantifications are shown in (A).

**Figure 43**

**A.**

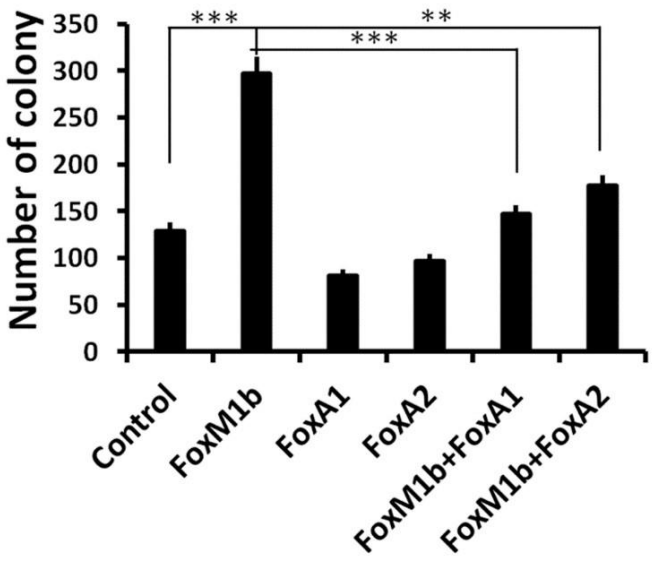
***
**
***
Number of colony
350
300
250
200
150
100
50
0
Control
FoxM1b
FoxA1
FoxA2
FoxM1b+FoxA1
FoxM1b+FoxA2

**B.**

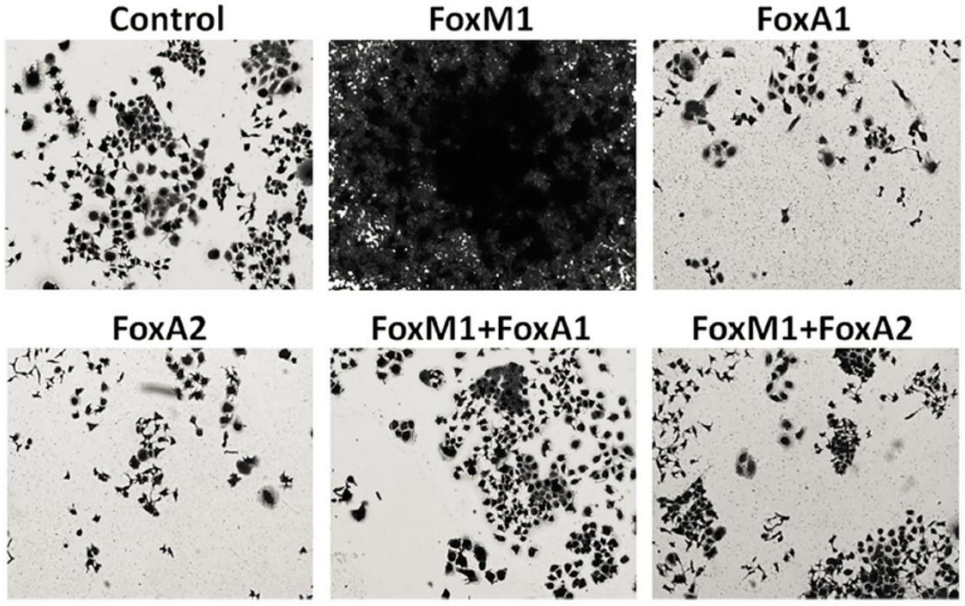
Control
FoxM1
FoxA1
FoxA2
FoxM1+FoxA1
FoxM1+FoxA2

**Figure 44**

**FoxA1 and FoxA2 inhibits FoxM1-induced anchorage independent growth of the Huh7 cells.** Huh7 cells (2 x$10^4$ cells) as described for Figure 43 were seeded in triplicate into soft agar and allowed to grow for 20 days and the quantification (A) and representative pictures of soft agar colonies are shown (B). Statistical calculations were done using GraphPad Prism online tool for t-test and p values stated as *p≤0.05, **p≤0.001 and ***p≤0.0001

**Figure 44**

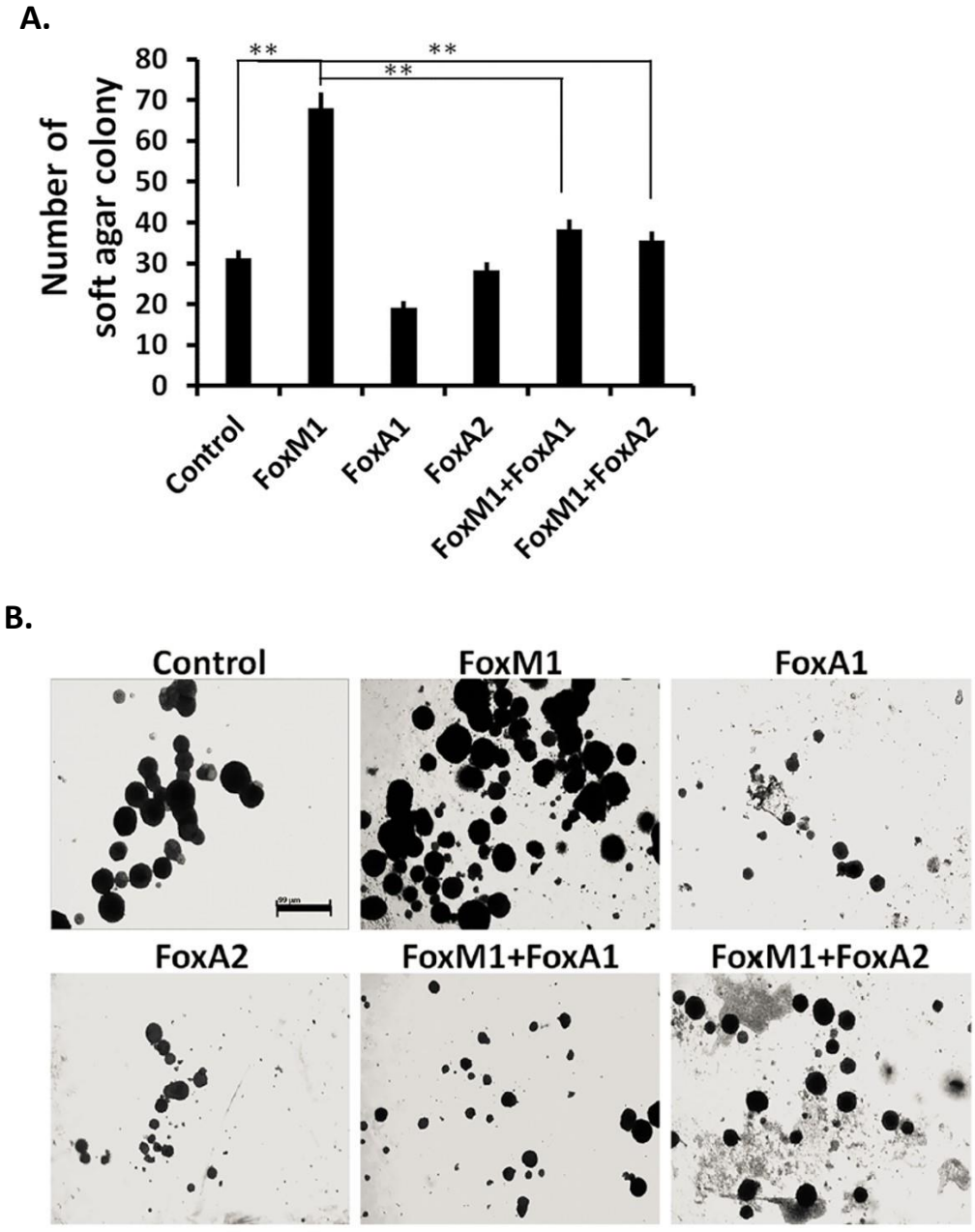
A.
Number of soft agar colony
80
70
60
50
40
30
20
10
0
**
**
**
Control
FoxM1
FoxA1
FoxA2
FoxM1+FoxA1
FoxM1+FoxA2
B.
Control
FoxM1
FoxA1
FoxA2
FoxM1+FoxA1
FoxM1+FoxA2

**Figure 45**

**FoxA1 and FoxA2 inhibit the migration properties of Huh7 cells**. Huh7 cells transfected with control, Flag-FoxM1, FoxA1 and FoxA2, or a combination of FoxM1 and FoxA1 or FoxM1 and FoxA2. Cells ($1x10^6$ cells) were seeded in 6-well plates in triplicate and allowed to reach full confluency. Scratch-wounds were generated using the 200 µl micro tip and debris were washed and the cells were replenished with fresh media and 0h pictures were captured. The wounds were monitored every 24h and representative pictures were captured.

**Figure 45**

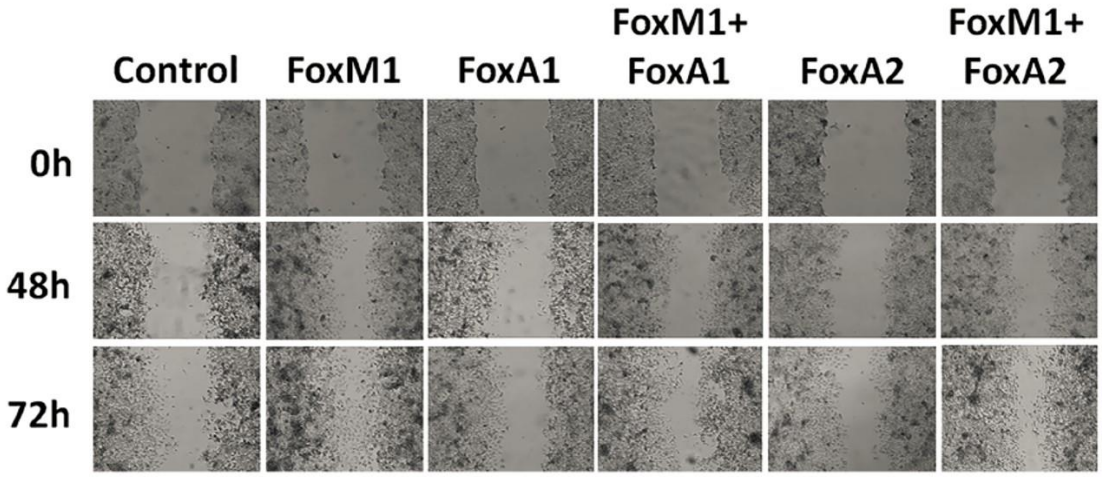
Control
FoxM1
FoxA1
FoxM1+ FoxA1
FoxA2
FoxM1+ FoxA2
0h
48h
72h

**Figure 46**

**FoxA1 and FoxA2 inhibit FoxM1-induced sphere formation by HepG2 cells.** HepG2 cells transfected individually with Flag-FoxM1, FoxA1 and FoxA2 or in combination with Flag-FoxM1 and FoxA1 or Flag-FoxM1 and FoxA2. Forty-eight hours post transfections 200 cells were seeded in spheroid formation medium and allowed to grow for two weeks. Quantification of the spheres in respective conditions in panel (A). Representative images of the spheres in control, FoxM1, FoxA1, FoxA2, FoxM1+FoxA1 and FoxM1+FoxA2 are shown in (B). Western blot (70 ug extract) for protein expression of FoxM1, FoxA1 and FoxA2 (C). **p≤0.001 and ***p≤0.0001.

**Figure 46**

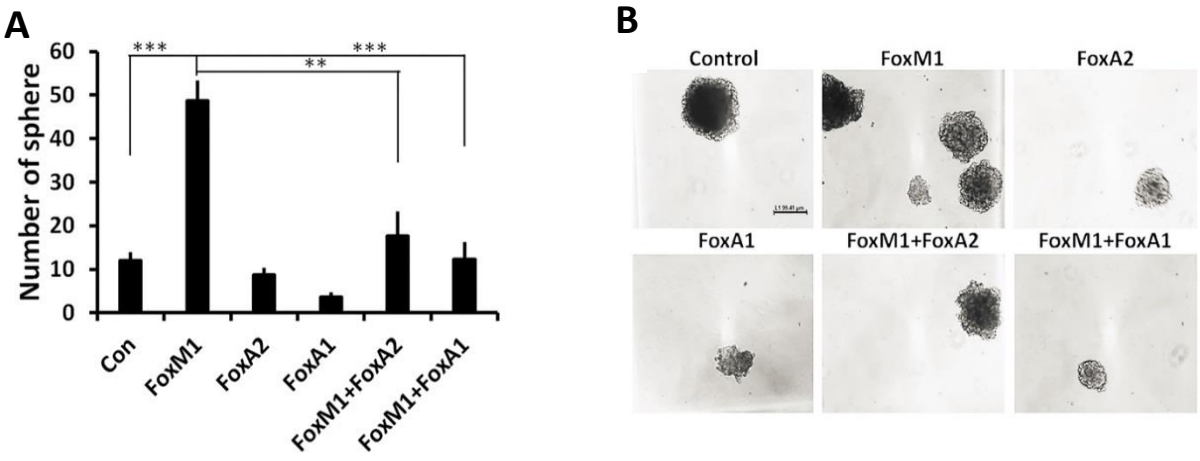
A
Number of sphere
60
50
40
30
20
10
0
***
***
**
Con
FoxM1
FoxA2
FoxA1
FoxM1+FoxA2
FoxM1+FoxA1
B
Control
FoxM1
FoxA2
FoxA1
FoxM1+FoxA2
FoxM1+FoxA1
C
Flag-FoxM1 - + - - + +
FoxA1 - - + - + -
FoxA2 - - - + - +
1.0 25.0 0.7 0.8 2.0 2.2
FoxM1
FoxA1
FoxA2
1.0 1.3 1.3 1.2 1.3 1.2
Actin

**Figure 47**

**FoxA1/A2 attenuate endogenous FoxM1 protein levels.** Huh7 cells were transfected individually with empty vector, Flag-FoxM1, FoxA1, or FoxA2 or a combination of Flag-FoxM1 and FoxA1 or Flag-FoxM1 and FoxA2, along with GFP expression plasmid as transfection control. Cells were harvested for protein extraction forty-eight hours after transfection, and 70 μg of extracts were resolved on SDS-PAGE. Expressions of FoxM1, FoxA1 and FoxA2 were assayed by western blotting with anti-Flag, anti-FoxM1, anti-FoxA1, anti-FoxA2 antibodies. For loading control, actin-ab and anti-GFP antibody were used. For the over-expressed Flag-FoxM1b, FoxA1/A2 short exposure (t<1 sec) of the blots was taken.

**Figure 47**

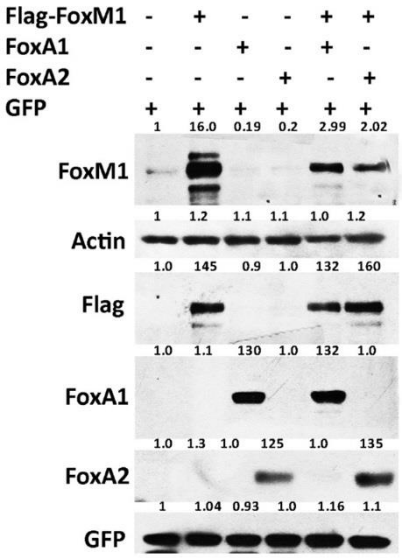
Flag-FoxM1 - + - - + +
FoxA1 - - + - + -
FoxA2 - - - + - +
GFP + + + + + +
1 16.0 0.19 0.2 2.99 2.02
FoxM1
1 1.2 1.1 1.1 1.0 1.2
Actin
1.0 145 0.9 1.0 132 160
Flag
1.0 1.1 130 1.0 132 1.0
FoxA1
1.0 1.3 1.0 125 1.0 135
FoxA2
1 1.04 0.93 1.0 1.16 1.1
GFP

**Figure 48**

**Overexpression of FoxA1 and FoxA2 inhibits FoxM1 mRNA expression.** Huh7 cells were transfected with control vector, FoxA1 or FoxA2 expression vector. Forty-eight hours post transfection cells were harvested. Total RNAs were isolated and effects of FoxA1 or FoxA2 on FoxM1 and its downstream targets were analyzed by qRT-PCR. Statistical calculations were done using GraphPad Prism online tool for t-test and p values stated as *p≤0.05, **p≤0.001 and ***p≤0.0001

**Figure 48**

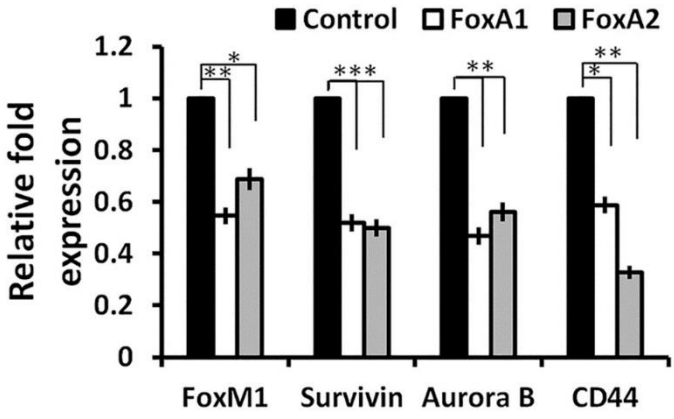
Control
FoxA1
FoxA2
Relative fold expression
1.2
1
0.8
0.6
0.4
0.2
0
**
*
***
**
**
*
FoxM1
Survivin
Aurora B
CD44

**Figure 49**

**Binding of FoxA1 and FoxA2 to the FoxM1 promoter.** Huh7 cells were cross linked and ChIP was performed using anti-FoxA1 or anti-FoxA2 antibody and the binding of FoxA1 and FoxA2 to the FoxM1 promoter was analyzed using the qRT-PCR for the indicated consensus binding sites. Statistical calculations were done using GraphPad Prism online tool for t-test and p values stated as *p≤0.05, **p≤0.001 and ***p≤0.0001.

**Figure 49**

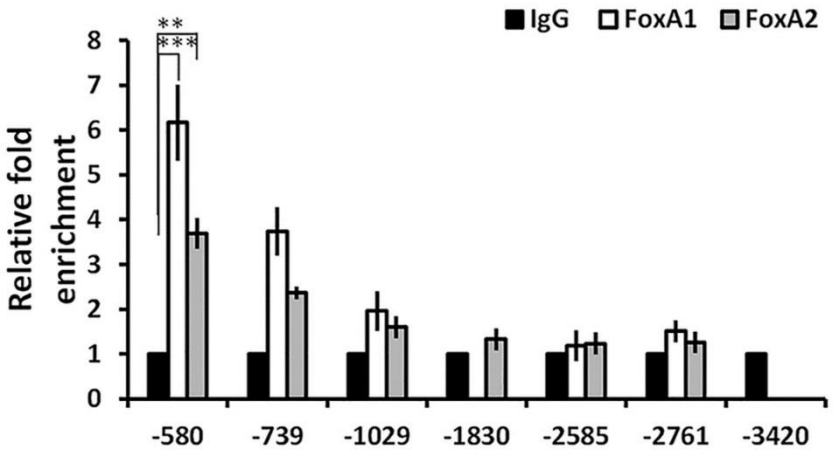
IgG
FoxA1
FoxA2
Relative fold enrichment
0
1
2
3
4
5
6
7
8
**
***
-580
-739
-1029
-1830
-2585
-2761
-3420

## Discussion

The work presented in my thesis is significant in several ways. First, we provide genetic evidence that FoxM1 is essential for H-ras12V-driven liver cancer (HCC) progression. Loss of FoxM1 leads to decreased proliferation and increased apoptosis of HCC cells. Targeting FoxM1 leads to a disproportionate loss of the CD44+ and EpCAM+ HCC cells, in vivo. Moreover, FoxM1 plays important roles in the maintenance of the cancer cells with stem-like features ($CD90^+$ cells), at least partly, through its ability to regulate the levels of ROS.

High-grade progression of HCC coincides with over-expression of FoxM1. Our observations provide evidence for a causal role of FoxM1 in the high-grade progression of HCC, as it suppresses expression of the hepatocyte-differentiation genes FoxA1/A2. Mechanistically, it involves FoxM1-directed methylation of the promoters of those genes. Surprisingly, suppression of the FoxA1/A2 genes by FoxM1 involves Rb, a tumor suppressor protein.

Nonalcoholic fatty liver disease (NAFLD), including nonalcoholic steatohepatitis (NASH) is a significant risk factor for liver cirrhosis, and becoming a major cause of hepatocellular carcinoma[7,8]. Recent studies also indicated almost ubiquitous activation of the Ras-signaling pathway in hepatocellular carcinoma through silencing expression of the Ras regulatory GAP proteins[28]. A transgenic mouse model that expresses H-ras12V in the liver was shown to develop steatosis, linking activated Ras-signaling to steatosis[135]. Moreover, the male mice in that strain develop hepatocellular carcinoma. Interestingly, we observed that FoxM1 is expressed at a high level in those tumors (HCCs), and it is critical for the

survival of the tumors. The genetically engineered mouse model for HCC used in this study is significant because of its relatedness to human HCC. Our observation that inhibition of FoxM1 inhibits HCC progression in that model further supports the notion that FoxM1 is a key molecular target for HCC. It is noteworthy that deletion of FoxM1 also inhibits initiation of lung cancer[136].

We employed the MxCre transgene and double stranded RNA to induce expression of Cre recombinase conditionally to delete FoxM1 after tumor development. Surprisingly, we observed loss of FoxM1 mainly in the HCC cells, but not in other fibroblast-like cells within the tumor nodules. Nevertheless, the reduction in FoxM1 expression caused a decrease in cell proliferation and an increase in apoptosis of the HCC cells, which coincided with a reduction in the number of tumor nodules. Some of the mice with longer induction of the Cre recombinase (10 injections of pIpC) exhibited a total loss of the tumor nodules. The deletion of FoxM1 resulted in inhibition of HCC progression, however we did not observe any significant loss in the expression of HRasV12 driver oncogene. This suggests that Ras signaling pathway is dependent on FoxM1's expression to drive the progression of the disease. There was a significant increase in the levels of ROS in the HCC nodules following deletion of FoxM1. It is likely that the increased ROS might be an important factor in increasing apoptosis of the HCC cells that is likely related to the loss of the tumor nodules.

The disproportionate loss of the EpCAM+ and CD44+ HCC cells in H-ras12V induced HCC is interesting because it is likely related to the mechanism by which FoxM1 deletion inhibits HCC progression. These markers were shown to be present in the HCC precursor cells[137]. Moreover, the liver cancer cells with stem cell features were shown to express

these markers. Importantly, CD44 has been shown to protect cancer cells with stem cell properties from ROS-induced apoptosis by increasing the cellular levels of anti-oxidants[138]. Also, it was shown that CD44 is important for survival of the liver cancer cells with stem cell features[69]. We observed that both human and mouse CD44 promoters contain FoxM1 binding sites, and that FoxM1 interacts with those sites in the human gene promoter to activate expression of CD44. Since expression of CD44 is under the regulation by FoxM1 and is required by the HCC precursor cells, this could potentially explain why FoxM1 is essential for HCC development[137]. However, we did not observe dependence of CD90 expression on FoxM1 in the human liver cancer cell lines. Our observations on the liver cancer cells with stem cell features provide further insights into the mechanism by which FoxM1 supports HCC progression. The $CD90^+$, $CD44^+$ and the $CD133^+/CD44^+$ cells in culture were induced to apoptosis by transient depletion of FoxM1, which had only marginal effect on the majority of the cells in culture. Moreover, subcutaneous injections of $10^6$ FoxM1-depleted Huh7 cells did not form tumors indicating that FoxM1 is required for tumorigenicity, also this observation would be consistent with a loss of the cancer stem-like cells. We observed increased ROS accumulation following depletion of FoxM1 in those cells. Moreover, inhibition of ROS decreased the apoptosis of the CD90+ cells. While some, but not all, of the CD90+ cells were also positive for CD44, we observed that expression of the antioxidant gene MnSOD in the CD90+ cells was dependent upon FoxM1. Loss of the FoxM1-activated antioxidant gene expression could explain the loss of the CD90+ cells. However, since FoxM1 deletion also inhibits the ‘‘stemness’’ genes in

these HCC cells, it is possible that a significant population of those also undergo differentiation upon transient loss of FoxM1.

Our data suggest that MnSOD expression strongly depends upon FoxM1 in the CD90+ cells, but not in the CD90- cell population. MnSOD expression is activated by a variety of transcription factors, including p53[139–141]. It is likely that in the CD90- cells one or more of those transcription factor(s) participate in the expression of MnSOD. Together, these observations are highly significant with regards to development of new therapeutic strategies against HCC focusing on the FoxM1 pathway.

The FoxA genes are critical for liver development. FoxA1/A2 knockout embryos failed to develop liver bud from the gut endoderm that is also associated with a loss of the hepatoblast marker alpha-fetoprotein[130]. These genes are important also for hepatocyte differentiation[142]. In chemical carcinogenesis (Diethylnitrosamine or DEN)-induced HCC model, the FoxA1/A2 genes were shown to play important roles in the sexual dimorphism in HCC development[132]. Male mice are more susceptible to HCC development than females, and that is related to the sex hormones androgen and estrogen. A previous study linked estrogen to IL-6 expression to explain sexual dimorphism of HCC development[137]. However, studies by Li et al. [132] suggested that genes co-regulated by FoxA1/A2 and AR (androgen receptor) are responsible for the susceptibility to HCC in male mice, whereas genes co-regulated by FoxA1/A2 and ER (estrogen receptor) in female liver are responsible for the resistance to DEN-induced HCC development. That study also implied a need for FoxA1/A2 in the development of HCC in male mice. FoxM1 is not linked to sexual dimorphism with regards to HCC development because, unlike the FoxA1/A2 liver

knockout female mice, the FoxM1 liver knockout male or female mice fail to develop HCC. This apparent discrepancy in the observations on FoxM1 and FoxA1/A2 is most likely related to the context in which FoxM1 regulates FoxA1/A2. Based on analyses of human HCC specimens we think that the FoxM1/Rb/DNMT3 pathway of FoxA1/A2 repression is operative only when FoxM1 is over-expressed. The need for over-expression of FoxM1 might be related to low-abundance of active Rb in HCC cells. High levels of FoxM1 would be needed to seek out active under-phosphorylated Rb protein because it is the under-phosphorylated Rb that binds to FoxM1[143] (Fig. 50). We suspect that the FoxM1 mediated inhibition of FoxA1/A2 might be involved in de-differentiation of the HCC cells or maintenance of poorly differentiated HCC cells. Alternatively, in the event that the low- and high-grade HCCs develop from different progenitors, we speculate that the FoxM1 mediated repression of FoxA1/A2 is important for the progenitors that give rise to high-grade HCC. It is noteworthy that studies by another group also indicated that, in human specimens, FoxA2 expression is down-regulated in metastatic HCC[133]. Moreover, expression of FoxA2 inhibits expression of MMP9, leading to an inhibition of invasiveness of HCC cells. Therefore, it appears that, while the FoxA genes are required for HCC development in male mice subjected to DEN chemical carcinogenesis they have opposite effects on metastatic progression of HCC.

Importantly, over-expression of FoxM1 in the high-grade HCC specimens coincides with reduced expression of FoxA1/A2. Moreover, deletion of FoxM1 in HRasV12-induced HCC, which expresses FoxM1 at high levels, led to increased expression of FoxA1/A2. These observations provide genetic evidence that FoxM1 is involved in suppression of the FoxA

genes in high-grade HCC. It is noteworthy that deletion of FoxM1 in the HRasV12 mouse HCC model was associated with a preferential loss of the EpCAM+ve and CD44+ve cells. Those cell-surface markers are found on liver cancer stem cells (). It is possible that increased expression of the FoxA genes, upon FoxM1 deletion, increases differentiation of those cells. Consistent with that we show that expression of FoxA1/A2 inhibits FoxM1-induced sphere formation in HepG2 cells (Fig. 46). These observations also are consistent with the notion that suppression of the FoxA genes is important in the mechanism by which FoxM1 supports maintenance or progression to poorly differentiated HCC cells. That would be consistent also with a previous study, which indicated that FoxA2 inhibits epithelial to mesenchymal transition of HCC cells[133].

Inhibition of FoxM1-induced increase in clonogenicity and soft-agar colony formation by FoxA1/A2 further explains why expression of the FoxA genes needs to be repressed by FoxM1. Interestingly, we also provide evidence for a feedback loop in which over-expression of FoxA1 or FoxA2 inhibits expression of FoxM1 and the FoxM1 target genes in HCC cells. Inhibition of FoxM1 expression coincides with binding of FoxA1 and FoxA2 to the promoter of FoxM1 in HCC cells. FoxM1 was shown to activate its own expression in a positive feedback loop[134]. We think that over-expressed FoxA1 or FoxA2 disrupts that positive feedback, resulting in an inhibition of FoxM1 expression. That would further explain the opposite expression patterns of FoxM1 and FoxA1/A2 in HCCs (Fig. 24). Moreover, the inhibition of FoxM1 would explain how FoxA1/A2 inhibits clonogenicity and soft agar colonies induced by FoxM1. A recent study showed that in HCC cells FoxA1/A2 bind to the promoters of G6Pase and IGFBP1 in a FoxO-dependent manner[144].

That study also showed that FoxA1/A2 promotes promoter binding of the FoxO factors that are known to stimulate genes involved in growth arrest[145]. Therefore, it is possible that FoxA1/A2 antagonize FoxM1 also by enhancing the activities of the FoxO factors. Soft-agar colony formation is a reflection of tumorigenic properties of cancer cells, and that is related also to the presence of cancer stem cells or tumor initiating cells. FoxM1 increases tumorigenicity of HCC cells by supporting the population of cancer stem cells as observed above. Inhibition of the FoxM1-mediated increase in the soft-agar colony by FoxA1/A2 further supports the notion that suppression of FoxA1/A2 is important for FoxM1-driven aggressive HCC progression.

The involvement of Rb in the suppression of the FoxA1/A2 genes is surprising because it suggests that Rb participates in progression of high-grade HCC. We show that FoxM1 recruits Rb and DNMT3b onto the promoters of FoxA1/A2, and increases methylation of the CpG islands in those promoters. Moreover, depletion of Rb blocks FoxM1-mediated increase in promoter-methylation and suppression of the FoxA1/A2 genes. Promoter CpG-methylation strongly correlates with gene silencing[146]. Often, following methylation, MeCpG-binding proteins bind to the methylated sites and recruit co-repressor complexes, including HDACs. Therefore, it is likely that the repression of FoxA1/A2 also involves the co-repressor complex and HDACs[147]. Other histone modifications, such as H3K9 tri-methylation and H3K27 tri-methylation, also have been reported to associate with CpG-methylation[148]. We think that the methylation of the FoxA1/A2 promoters is the primary event directed by FoxM1 because we could detect abundant interaction between FoxM1 and DNMT3b.

Rb has previously been shown to participate in cell lineage fate decision making[149,150]. It depends on the differentiation factor and the cellular context, whether Rb activates or represses its expression[150]. For example, in mesenchymal progenitors, Rb represses PPARγ in association with E2F to suppress adipogenesis (Fig 51). In another study, Rb has been shown to be crucial for switch between white and brown adipose tissue, deletion of Rb from adult adipose tissue results higher accumulation of brown adipose tissue[151]. This suggests that Rb plays a role in cell lineage commitment decisions at multiple hierarchal levels as well.

The involvement of Rb in the suppression of FoxA1/A2 also suggests that the mechanism might be more active in G1 phase where under-phosphorylated Rb is abundant. Interestingly, studies on embryonic stem (ES) cell differentiation indicated that G1 phase is the phase in which the chromatin is available for the differentiation mechanisms, and that the ES cells retain pluripotency by suppressing differentiation mechanisms in G1 and increasing expression of the pluripotency genes in the S/G2 phases[152]. In the light of those observations in ES cells, our observations that FoxA1/A2 inhibit expression of the pluripotency genes and that FoxM1/Rb/DNMT3b inhibit FoxA1/A2 are interesting because that could be important in the mechanism by which FoxM1 over-expression maintain poorly differentiated state of cells in high-grade HCC. Together, the results suggest that, in the context of over-expressed FoxM1, there is a gain of function for Rb, and that function is related to the suppression of differentiation genes, which is likely involved in high-grade progression of HCC.

**Figure 50**

**Tumorigenic bypass by Rb.**

Rb is a classical tumor suppressor, however, tumorigenic bypass of Rb suppression can lead to high grade progression of liver cancer in context of high FoxM1 expression. High levels of FoxM1 are needed to seek out the active Rb from cells and repress the differentiation genes FoxA1 and FoxA2.

**Figure 50**

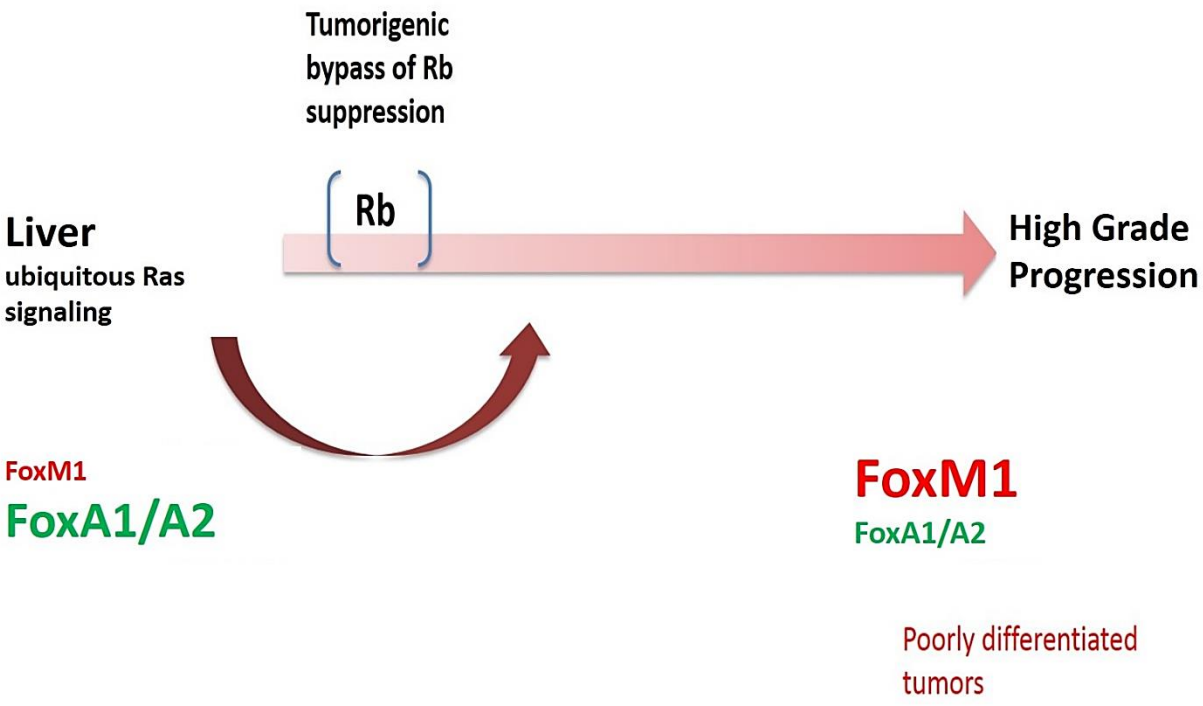
Tumorigenic
bypass of Rb
suppression
Rb
Liver
ubiquitous Ras
signaling
High Grade
Progression
FoxM1
FoxA1/A2
FoxM1
FoxA1/A2
Poorly differentiated
tumors

**Figure 51**

Rb inhibits adipogenesis of mesenchymal progenitor cells by inhibiting the expression of PPARγ.

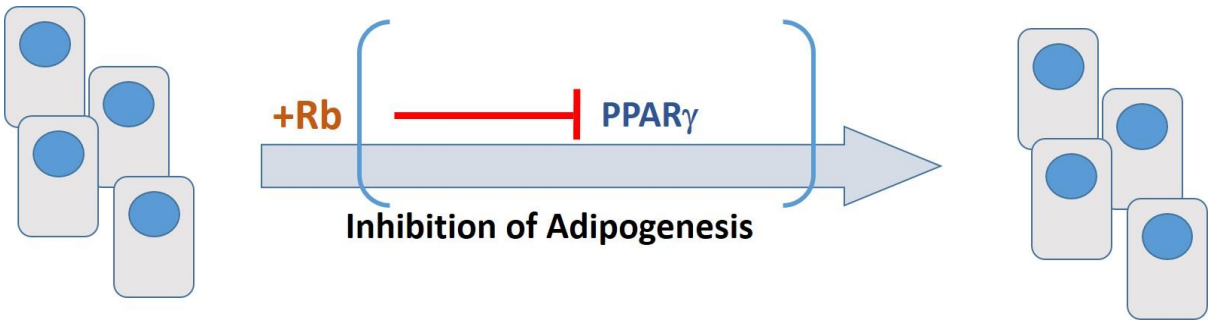


**Mesenchymal progenitors**

## Materials and Methods

### Cell Culture and Transfections

Human hepatocellular carcinoma Huh7 cells (American Type Culture Collection) were maintained in Dulbecco's modified Eagle's medium supplemented with 10% fetal bovine serum (HyClone Laboratories Inc.) and 100 units of penicillin/ streptomycin at 37 °C with 5% $CO_2$. Cells were transfected with plasmid DNA or siRNA using LipofectamineTM 2000 (Invitrogen) in serum-free tissue culture medium following the manufacturer's protocol. Six hours after transfection, cells were fed with complete Dulbecco's modified Eagle's medium containing 10% fetal bovine serum.

### Animal studies

All animal experiments were pre-approved by the UIC institutional animal care and use committee. Previously described H-ras12V mice were crossed with FoxM1fl/fl MxCre C57/BL6 mice to obtain $FoxM1^{fl/fl}$ MxCre H-ras12V and $FoxM1^{+/+}$ MxCre H-ras12V mice. For deletion studies, eight months old male mice ($FoxM1^{+/+}$ MxCre H-ras12V and $FoxM1^{fl/fl}$ MxCre H-ras12V) were subjected to five or ten intraperitoneal (i.p.) injections (every other day) with 250 μg of synthetic polyinosinic-polycytidylic acid (polyIpolyC) (Sigma-Aldrich, St. Louis, MO) to induce expression of the Mx-Cre transgene. The mice were sacrificed three weeks following the last injection, and the liver tissues and HCC nodules were harvested. For xenograft tumor, male $^{Nu/Nu}$ strain mice were purchased from Charles River Laboratories (USA). Huh7 cells were transfected with control or FoxM1 siRNA. Twenty-four hours post transfection, cells (total of $1 \times 10^6$) were subcutaneously injected.

**Immunohistochemistry and human tissue micro array**

Immunohistochemical stainings were performed following standard procedure. Antigen retrieval was done using sodium citrate buffer and sections were then treated with antibodies overnight. Additional blocking step was performed using Avidin/biotin Vectastain kit following manufacturer's protocol. Visualization was done using DAB and counterstained using Hematoxylin (Polyscientific, Bay Shore, NY). For antibodies of mouse origin, mouse on mouse (MOM) kit was used. All used reagents are from Vector Labs (Burlingame, CA). Information about the antibodies is included in Table 1. Visualization was done using DAB and counterstained using Hematoxylin (Polyscientific, Bay Shore, NY). For antibodies of mouse origin, mouse on mouse (MOM) kit was used. All used reagents are from Vector Labs (Burlingame, CA) unless otherwise indicated.

**RT-PCR, Western Blot, and Chromatin Immunoprecipitation**

RNA was Trizol extracted (Invitrogen, Carlsbad, CA) and cDNA was synthesized using Bio-Rad reverse transcriptase (Bio-Rad, Hercules, CA). cDNA was amplified using SYBR Green (Bio-Rad, Hercules, CA) and analyzed via iCycler software. Western blots and chromatin-IPs were performed following previously described procedures[112]. For chromatin-IPs, signals obtained with IgG and specific-antibodies were first normalized with signals obtained with those antibodies on a non-specific site in the GATA3 promoter[112]. The normalized values were used to plot the fold enrichment with FoxM1-ab over IgG. For Rb-ChIP and DNMT3b-ChIP, we compared enrichments with same antibody, after normalization, in the presence and absence of FoxM1-siRNA, and the fold enrichments in

control-siRNA over FoxM1-siRNA were plotted. All antibodies and primer sequences are included in Table 1 and Table 2 respectively.

**FACS analysis and cell sorting**

Antibodies used for FLOW analysis are listed in Table 1. Cells (re-suspended in PBS with 2%FBS and 2 mM EDTA) were incubated with PE and/ or FITC-conjugated antibodies for 20 min on ice. To analyze apoptosis of CD90+ versus CD90- cell population, cells were collected by trypsinization and incubated in pre-warmed complete medium with DEVD-FMK-FITC (CaspGLOW™ Fluorescein Active Caspase Staining Kit, eBioscience, San Diego, CA) for 20 min, at 37°C, 5% CO2 as recommended by the manufacturer. After incubation cells were washed with provided washing buffer, resuspended in 2% FBS, 2mM EDTA PBS and stained with CD90-PE antibody as described.

To analyze apoptosis of tumor cells, collected tumors were dissociated by collagenase, single cell suspension was made and incubated with DEVD-FMK-FITC as described.

To measure ROS in CD90+ and CD90- cells, cells were incubated with 10 μM 5-(6)-chloromethyl-2-dichlorodihydrofluorescein diacetate (CM-H2DCFDA) (Invitrogen, Carlsbad, CA,) for 20 min at 37°C. Cells were then washed with PBS, collected by trypsinization and immediately stained with CD90-PE antibody. The samples were analyzed using a Cyan ADP flow cytometer (Beckman Coulter, Fullerton, CA) and Summit software. To sort CD90+ vs. CD90- cell population, Huh7 cells were incubated with CD90-PE antibody as described above and sorted by a Mo-Flo instrument (Beckman Coulter, Fullerton, CA).

**Isolation of genomic DNA**

Genomic DNA (gDNA) was obtained from Huh7 cells and mouse tissue using Wizard™ Genomic DNA Purification kit as instructed by the manufacturers manual.

**Bisulfite treatment and Quantitative methylation-specific PCR assay (qMSP)**

Genomic DNA samples were treated with EZ DNA methylation™ kit (Zymo Research, Orange, CA) as per the manufacturer's recommendation. The extent of methylation of desired gene was then measured by qPCR amplification with pairs of specific primers as mentioned in Table 3 which were designed using MethPrimer MSP/BSP prediction and primer designing tool. Quantitative MSP was performed with using SYBR Green (Bio-Rad, Hercules, CA) and analyzed via iCycler software. Each reaction contained 20 ng of bisulfite-treated DNA as a template, 6.25 µl SYBR Green PCR (Bio-Rad, Hercules, CA) and 50 nM each forward and reverse primers in a total volume of 12.5 µl. The quantification cycle ($C_q$) was determined for each reaction with methylation-specific primers (MSP) the ratio of unmethylated to total amplifiable bisulfite-treated DNA was calculated.

**Wound Healing (Cell Culture) Assay**

For wound healing assay, cells were seeded at a density of $1x10^5$ cells in 24 well plates and allowed to grow up to full confluence in a monolayer. A single linear scratch of approximately 1mm was introduced in each well using a sterile micro-tip. The debris was washed with PBS and replaced with fresh growth medium containing appropriate drug. Wound closure was monitored by capturing images at different time intervals after scratching. The experiments were carried out in triplicate.

**Soft Agar Assay**

For transformation and anchorage independent colony formation ability, soft agar assay was performed. Cells ($2\times10^4$) were suspended in a medium containing 0.4% agarose and then poured onto 60mm culture dish coated with 0.8% agarose. The top agar surface was layered with complete medium every third day and cells were allowed to grow for 20 days. Colonies larger than 1mm in soft agar were stained with 0.1% crystal violet for counting and capturing images.

**Clonogenic assay**

To check the effect of the FoxA2 on FoxM1 expressing cell line proliferation, clonogenic assay was performed with Huh7 cells transfected with Control, T7-FoxM1, CMV-FoxA2 and co-transfected with T7-FoxM1 and FoxA2 were seeded at the density of $1X10^4$ cell in 24 well plate. Cells were feed with fresh medium every third day and were allowed to grow for 6 days. At the end of the assay, pictures of the cells were captured under bright field microscope after staining with crystal violet solution (0.1% crystal violet in 10% ethanol). Stained colonies were counted.

| **Table 1. Antibodies** | | |
|---|---|---|
| **Protein** | **Company** | **Catalogue number** |
| FoxM1 | Santa Cruz | SC-500 |
| FoxM1 | Santa Cruz | SC-376471 |
| CD44 | Abcam | Ab 65829 |
| PCNA | Neomarkers | MS-106-P0 |
| EpCAM | Abcam | Ab71916 |
| Bmi1 | Cell Signaling | CS#2830 |
| Sox2 | Cell Signaling | CS#3579 |
| Oct4 | Cell Signaling | CS#2840 |
| c-myc | SantaCruz Biotechnology | sc-764 |
| Survivin | Novus Biologicals | NB500-201 |
| Cyclin E | Santa Cruz | sc-481 |
| Plk-1 | Upstate | 05-844 |
| CD90-PE | BD Biosciences | #555596 |
| CD44-FIITC | BD biosciences | #555478 |
| CD133-PE | MACS Miltenyl Biotec | AC133 |
| FoxA1 | Abcam | Ab23738 |
| FoxA2 | Santa Cruz | SC-374376 |
| FoxA2 | Rabbit Ab produced in lab | |
| Rb | Cell Signaling | CST9309 |
| DNMT3b | Imgenex | 52A1018 |
| Tubulin | Sigma | T9026 |
| Actin | Sigma | AC-40 |
| GAPDH | Cell Signaling | CST5174 |

| **Table 2. Primer sequences** | | |
|---|---|---|
| **Gene name** | **Sense (5'→3')** | **Antisense (5'→3')** |
| **RT-PCR** | | |
| hFoxM1 | GGAGGAAATGCCACACTTAGCG | TAGGACTTCTTGGGTCTTGGGGTG |
| hcyclophilin | GCAGACAAGGTCCCAAAGACAG | CACCCTGACACATAAACCCTGG |
| hCD44 | CGGACACCATGGACAAGTTT | GAAAGCCTTGCAGAGGTCAG |
| hSOX2 | TGAATGCCTTCATGGTGTGGTC | CCGTCTCCGACAAAAGTTTCC |
| hBmi1 | TGATGTGTGTGCTTTGTGGAGG | GTGGTCTGGTCTTGTGAACTTGG |
| hNanog | CCAGTCCCAAAGGCAAACAAC | TGGAGGCTGAGGTATTTCTGTCTC |
| hOct4 | GGGGTTCTATTTGGGAAGGTATTC | GGTTCGCTTTCTCTTTCGGG |
| hc-myc | TAGTGGAAAACCAGCAGCCTCC | CCTCGTCGCAGTAGAAATACGG |
| hAFP | GGTGGTGGATGAAACATATG | TTGCTTTTGCTTCACAAGGTTA |
| hMnSOD | GGCTTGGTTTCAATAAGGAACGG | ATCCCCAGCAGTGGAATAAGG |
| hGAPDH | ACACCCACTCCTCCACCTTT | TTCCTCTTGTGCTCTTGCTG |
| mFoxM1 | GAGGAAAGAGCACCTTCAGC | AGGCAATGTCTCCTTGATGG |
| mGAPDH | AACTTTGGCATTGTGGAAGG | CCATCCACAGTCTTCTGGGT |
| mHRasV12 | CCTTTCCTATCAACCCCACTA | GGATCAACTGAATGGTCAGC |
| mBmi1 | AGAGGGATGGACTACGAATGC | AACAGGAAGAGGTGGAGGGAAC |
| mNanog | AGCCCTGATTCTTCTACCAGTCCC | ACAGTCCGCATCTTCTGCTTCC |
| mc-myc | TAATCGAGGAGGAGCTGGA | ACCAAGGTTGTGAGGTTAGG |

| | | |
|---|---|---|
| mCdc25B | CCCTTCCCTGTTTTCCTTTC | ACACACACTCCTGCCATAGG |
| mAuroraB | CAGAAGGAGAACGCCTACCC | GAGAGCAAGCGCAGATGTC |
| mPlk1 | CCCAGCTACTACGAAAGGGTG | CAACATACGTCTGGACACATTCA |
| hFoxA1 | CAATGACTGCTTCGTCAAGG | TAGCAGCCGTTCTCGAACAT |
| hFoxA2 | CTTCAAGCACCTGCAGATTC | AGACCTGGATTTCACCGTGT |
| **ChIP primers** | | |
| CD44 (-1180) | TTTCTGTGTAACTCACCAGGCAAG | TCTCCCATCTTTCCTACCCAGC |
| CD44 (-4714, -4698) | GACTGTTTTGCTTGTGTTCCTTCC | GGTTTTACGCAGACCTTTGGAGG |
| CD44 (-16487) | TACTTTCTGCTTTGTTTCGGGG | ACTGCCAAGGGATAACTCACTCC |
| FoxA1 (-1391) | ACAAAGCACAGGGAAAAAGG | GATGGTGCGTGTGTTTTGAG |
| FoxA1 (-4221) | AGGCAGGAGTAGGGGAAAAG | CGTGTGCTTGTGTCTGTGTG |
| FoxA1 (-6846) | GGAGGGCAGGGCTCAGTT | CTATGGACCACAGAGCAAAACTACT |
| FoxA2 (-1294) | GGACAGAGACGCTCTTGAA | AAACAGGGCAGGAGGTG |
| FoxA2 (-3581) | CATATCTGCCTTATGTTGC | CACATGAAACCAACCAGTGC |
| FoxA2 (-4156) | CTGGTCTTTTGACCATCCAAGAAC | GGCCCATGCCTATAATCCCAGCTAC |
| FoxA2 (-4535) | GAGAATGTAATAATAAAGTAGTG | GGGGGAGGCAAGGTGCAACATT |
| Non-Specific | TTTTACGGGGCAACTACGGC | CAGTGGCATTAGCAGGTC |
| **MSP primers (human)** | | |
| FoxA1 (-55) | TTGTAAATAAAGTGAGGGTTTCGT | AAACTAATATAAATCTTACGTCGCT |

| | | |
|---|---|---|
| FoxA1 (-512) | GTATTTTTGGGGAGGGATTTC | ACGAACGAACTAAAACTCTAAATCG |
| FoxA1 (-846) | GTATTTTTGGGGAGGGATTTC | ACTAAAACTCTAAATCGAAACCTCG |
| FoxA1 (-1207) | GTTTAGGATCGATTAGGAATTAAGC | AAAAAAACATCTCCCATAACACG |
| FoxA1 (-2641) | AATTTAAATTTTTGATTGGGATGC | CAAAATAAACTCTACCAACTTCGAA |
| FoxA1 (-3194) | TACGGGTGTAGTAAGGGTAGTTTTC | GAACTCCTCAAATAAAAAATCCG |
| FoxA2 (-356) | CGCGTTATATTATTAGTTTTTTACGT | CAATACCGAACTACCCCGAA |
| FoxA2 (-882) | GGTTTTTATAGGGATTTGTCGG | AAAAAAAACCACCCTCTAAAACG |
| FoxA2 (-1080) | AATTTTAGTTTTTTAATCGTCGGTC | CCTATTACAATTCAAACCCGAA |
| FoxA2 (-1974) | GAGTTTTTAGTATTCGGGGGATC | CATAAAAAAAAACATTAATAAACCCG |
| FoxA2 (-2656) | GTATTTTTATGGGTAGGCGTGTC | CTAACGAAATTCTAAAAACTCCGAT |
| Non-Specific | ATTTAATACGATTTTGTTGATTCGT | AAAAAAAACTAAATTTTCCCGC |
| **MSP primers (mouse)** | | |
| FoxA1 | GGTTTAATTTAGTTTAGTTCGTCGG | CCCTTTAAAACCTTAATCCGAA |
| FoxA1 | AGAGGTAGGTTTGATTAGGATTCGT | CTAAATCAACCGAACAAAATAACGT |
| FoxA2 | TTAGAAAGAGGATTGAGGTAATTGAC | CAAATAACAACCAATTTACAAAACG |
| Non-Specific | TTCAGTCCAAAAGGATGCTG | GGATACAGTCCCAAACTCTTC |
| **siRNA sequences** | | |
| FoxM1 siRNA#1 | CAACAGGAGUCUAAUCAAG | |
| FoxM1 siRNA#2 | GGACCACUUUCCCUACUUUUU | |

**References**


1. Global, regional, and national comparative risk assessment of 79 behavioural, environmental and occupational, and metabolic risks or clusters of risks, 1990-2015: a systematic analysis for the Global Burden of Disease Study 2015. *Lancet (London, England)* **388,** 1659–1724 (2016).

2. Chuang, S.-C., Vecchia, C. La & Boffetta, P. Liver cancer: Descriptive epidemiology and risk factors other than HBV and HCV infection. *Cancer Lett.* **286,** 9–14 (2017).

3. HB, E.-S. & AC, M. Risk factors for the rising rates of primary liver cancer in the united states. *Arch. Intern. Med.* **160,** 3227–3230 (2000).

4. Levrero, M. Viral hepatitis and liver cancer: the case of hepatitis C. *Oncogene* **25,** 3834–3847 (2006).

5. Lin, H. *et al.* Both HCV and HBV are major causes of liver cancer in Southeast Asians. *J. Immigr. Minor. Heal.* **15,** 1023–1029 (2013).

6. Arzumanyan, a, Reis, H. M. & Feitelson, M. a. Pathogenic mechanisms in HBV- and HCV-associated hepatocellular carcinoma. *Nat Rev Cancer* **13,** 123–135 (2013).

7. Page, J. M. & Harrison, S. A. NASH and HCC. *Clinics in Liver Disease* **13,** 631–647 (2009).

8. De Minicis, S., Day, C. & Svegliati-Baroni, G. From NAFLD to NASH and HCC: Pathogenetic Mechanisms and Therapeutic Insights. *Curr Pharm Des* 5239–5249 (2013). doi:CPD-EPUB-20130204-12 [pii]

9. Wang, F. S., Fan, J. G., Zhang, Z., Gao, B. & Wang, H. Y. The global burden of liver disease: The major impact of China. *Hepatology* **60,** 2099–2108 (2014).

10. Tominaga, S. Major avoidable risk factors of cancer. *Cancer Lett.* **143 Suppl,** S19-23 (1999).

11. Liu, Y. & Wu, F. Global burden of Aflatoxin-induced hepatocellular carcinoma: A risk assessment. *Environ. Health Perspect.* **118,** 818–824 (2010).

12. Jackson, P. E. & Groopman, J. D. Aflatoxin and liver cancer. *Bailliere's Best Practice and Research in Clinical Gastroenterology* **13,** 545–555 (1999).

13. Kitya, D., Bbosa, G. S. & Mulogo, E. Aflatoxin levels in common foods of South Western Uganda: A risk factor to hepatocellular carcinoma. *Eur. J. Cancer Care (Engl).* **19,** 516–521 (2010).

14. Gupta, G. P. & Massagué, J. Cancer Metastasis: Building a Framework. *Cell* **127,** 679–695 (2006).

15. Keating, G. M. & Santoro, A. Sorafenib. *Drugs* **69,** 223–240 (2009).

16. Hasskarl, J. Sorafenib. *Recent Results Cancer Res.* **184,** 61–70 (2010).

17. Gauthier, A. & Ho, M. Role of sorafenib in the treatment of advanced hepatocellular carcinoma: An update. *Hepatology Research* **43,** 147–154 (2013).

18. Llovet, J. M. *et al.* Sorafenib in advanced hepatocellular carcinoma. *N. Engl. J. Med.* **359,** 378–90 (2008).

19. Cox, A. D. & Der, C. J. Ras history: The saga continues. *Small GTPases* **1,** 2–27 (2010).

20. Settleman, J., Albright, C. F., Foster, L. C. & Weinberg, R. A. Association between GTPase activators for Rho and Ras families. *Nature* **359,** 153–154 (1992).

21. Tocque, B. *et al.* Ras-GTPase activating protein (GAP): A putative effector for Ras. *Cellular Signalling* **9,** 153–158 (1997).

22. Scheffzek, K., Ahmadian, M. R. & Wittinghofer, A. GTPase-activating proteins: Helping hands to complement an active site. *Trends in Biochemical Sciences* **23,** 257–262 (1998).

23. Calvisi, D. F. *et al.* Ubiquitous Activation of Ras and Jak/Stat Pathways in Human HCC. *Gastroenterology* **130,** 1117–1128 (2006).

24. Fernández-Medarde, A. & Santos, E. Ras in cancer and developmental diseases. *Genes Cancer* **2,** 344–58 (2011).

25. Bos, J. L. Ras Oncogenes in Human Cancer: A Review. *Cancer Res.* **49,** 4682–4689 (1989).

26. Brunner, T. B. *et al.* Pancreatic cancer cell radiation survival and prenyltransferase inhibition: The role of K-ras. *Cancer Res.* **65,** 8433–8441 (2005).

27. Calcagno, S. R. *et al.* Oncogenic K-ras promotes early carcinogenesis in the mouse proximal colon. *Int. J. Cancer* **122,** 2462–2470 (2008).

28. Calvisi, D. F. *et al.* Inactivation of Ras GTPase-activating proteins promotes unrestrained activity of wild-type Ras in human liver cancer. *J. Hepatol.* **54,** 311–319 (2011).

29. Donninger, H., Vos, M. D. & Clark, G. J. The RASSF1A tumor suppressor. *J. Cell Sci.* **120,** 3163–72 (2007).

30. Macheiner, D. *et al.* NORE1B is a putative tumor suppressor in hepatocarcinogenesis and may act via RASSF1A. *Cancer Res.* **69,** 235–242 (2009).

31. Macheiner, D. *et al.* NORE1B, a candidate tumor suppressor, is epigenetically silenced in human hepatocellular carcinoma. *J. Hepatol.* **45,** 81–89 (2006).

32. Palakurthy, R. K. *et al.* Epigenetic Silencing of the RASSF1A Tumor Suppressor Gene through HOXB3-Mediated Induction of DNMT3B Expression. *Mol. Cell* **36,**

219–230 (2009).

33. Hesson, L. B., Cooper, W. N. & Latif, F. The role of RASSF1A methylation in cancer. *Dis. Markers* **23,** 73–87 (2007).

34. Pfeifer, G. P. & Dammann, R. Methylation of the tumor suppressor gene RASSF1A in human tumors. *Biochem.* **70,** 576–583 (2005).

35. Sui, G., Ma, X., Liu, S., Niu, H. & Dong, Q. Study of the correlation between H-ras mutation and primary hepatocellular carcinoma. *Oncol. Lett.* **4,** 779–782 (2012).

36. Ohta, M. *et al.* Decreased Expression of the RAS-GTPase Activating Protein RASAL1 Is Associated With Colorectal Tumor Progression. *Gastroenterology* **136,** 206–216 (2009).

37. Gao, W. *et al.* Variable DNA methylation patterns associated with progression of disease in hepatocellular carcinomas. *Carcinogenesis* **29,** 1901–1910 (2008).

38. Robertson, K. D. DNA methylation and human disease. *Nat. Rev. Genet.* **6,** 597–610 (2005).

39. Schubbert, S., Shannon, K. & Bollag, G. Hyperactive Ras in developmental disorders and cancer. *Nat. Rev. Cancer* **7,** 295–308 (2007).

40. Reiss, Y., Goldstein, J. L., Seabra, M. C., Casey, P. J. & Brown, M. S. Inhibition of purified p21ras farnesyl:protein transferase by Cys-AAX tetrapeptides. *Cell* **62,** 81–88 (1990).

41. Whyte, D. B. *et al.* K- and N-Ras are geranylgeranylated in cells treated with farnesyl protein transferase inhibitors. *J. Biol. Chem.* **272,** 14459–14464 (1997).

42. Cox, A. D., Fesik, S. W., Kimmelman, A. C., Luo, J. & Der, C. J. Drugging the undruggable RAS: Mission Possible? *Nat. Rev. Drug Discov.* **13,** 828–51 (2014).

43. Downward, J. Targeting RAS signalling pathways in cancer therapy. *Nat Rev Cancer* **3,** 11–22 (2003).

44. Gattermann, N. Imatinib Glivec. *Tagliche Praxis* **44,** 149–154 (2003).

45. Capdeville, R., Buchdunger, E., Zimmermann, J. & Matter, A. Glivec (STI571, imatinib), a rationally developed, targeted anticancer drug. *Nat. Rev. Drug Discov.* **1,** 493–502 (2002).

46. Saglio, G., Cilloni, D., Rancati, F. & Boano, L. Glivec and CML: a lucky date. *Journal of biological regulators and homeostatic agents* **18,** 246–251 (2004).

47. Dudley, D. T., Pang, L., Decker, S. J., Bridges, a J. & Saltiel, a R. A synthetic inhibitor of the mitogen-activated protein kinase cascade. *Proc. Natl. Acad. Sci. U. S. A.* **92,** 7686–7689 (1995).

48. De Bono, J. S. & Rowinsky, E. K. The ErbB receptor family: A therapeutic target for

cancer. *Trends in Molecular Medicine* **8,** (2002).

49. Ranson, M. Epidermal growth factor receptor tyrosine kinase inhibitors. *Br. J. Cancer* **2,** 2250–2255 (2004).

50. Fabbro, D., Parkinson, D. & Matter, A. Protein tyrosine kinase inhibitors: New treatment modalities? *Curr. Opin. Pharmacol.* **2,** 374–381 (2002).

51. Crooke, S. T. Review Article: Potential roles of antisense technology in cancer chemotherapy. *Oncogene* **19,** 6651–6659 (2000).

52. Chen, G., Oh, S., Monia, B. P. & Stacey, D. W. Antisense oligonucleotides demonstrate a dominant role of c-Ki-RAS proteins in regulating the proliferation of diploid human fibroblasts. *J. Biol. Chem.* **271,** 28259–28265 (1996).

53. Gleave, M. E. & B.P. Monia. Antisense therapy for cancer. *Nat. Rev. Cancer* **5,** 468–479 (2005).

54. Moore, K. a & Lemischka, I. R. Stem cells and their niches. *Science* **311,** 1880–1885 (2006).

55. Morrison, S. J. & Spradling, A. C. Stem Cells and Niches: Mechanisms That Promote Stem Cell Maintenance throughout Life. *Cell* **132,** 598–611 (2008).

56. Li, L. & Clevers, H. Coexistence of quiescent and active adult stem cells in mammals. *Science* **327,** 542–5 (2010).

57. Reya, T., Morrison, S. J., Clarke, M. F. & Weissman, I. L. Stem cells, cancer, and cancer stem cells. *Nature* **414,** 105–111 (2001).

58. Lee, T. K. W. *et al.* CD24 + Liver Tumor-Initiating Cells Drive Self-Renewal and Tumor Initiation through STAT3-Mediated NANOG Regulation. *Cell Stem Cell* **9,** 50–63 (2011).

59. Dieter, S. M. *et al.* Distinct types of tumor-initiating cells form human colon cancer tumors and metastases. *Cell Stem Cell* **9,** 357–365 (2011).

60. Ishizawa, K. *et al.* Tumor-initiating cells are rare in many human tumors. *Cell Stem Cell* **7,** 279–282 (2010).

61. Sampieri, K. & Fodde, R. Cancer stem cells and metastasis. *Seminars in Cancer Biology* **22,** 187–193 (2012).

62. Bonnet, D. & Dick, J. E. Human acute myeloid leukemia is organized as a hierarchy that originates from a primitive hematopoietic cell. *Nat. Med.* **3,** 730–737 (1997).

63. Schneider, M. *et al.* Characterization of colon cancer cells: a functional approach characterizing CD133 as a potential stem cell marker. *BMC Cancer* **12,** 96 (2012).

64. Kreso, A. & Obrien, C. A. Colon cancer stem cells. *Current Protocols in Stem Cell Biology* (2008). doi:10.1002/9780470151808.sc0301s7

65. Li, C. *et al.* Identification of pancreatic cancer stem cells. *Cancer Res.* **67,** 1030–1037 (2007).

66. Velasco-Velázquez, M. A., Homsi, N., De La Fuente, M. & Pestell, R. G. Breast cancer stem cells. *Int. J. Biochem. Cell Biol.* **44,** 573–7 (2012).

67. Morrison, B. J., Schmidt, C. W., Lakhani, S. R., Reynolds, B. a & Lopez, J. A. Breast cancer stem cells: implications for therapy of breast cancer. *Breast cancer Res. BCR* **10,** 210 (2008).

68. Bozorgi, A., Khazaei, M. & Khazaei, M. R. New findings on breast cancer stem cells: A review. *Journal of Breast Cancer* **18,** 303–312 (2015).

69. Yang, Z. F. *et al.* Significance of CD90+ Cancer Stem Cells in Human Liver Cancer. *Cancer Cell* **13,** 153–166 (2008).

70. Li, F., Tiede, B., Massagué, J. & Kang, Y. Beyond tumorigenesis: cancer stem cells in metastasis. *Cell Res.* **17,** 3–14 (2007).

71. Hill, R. P., Marie-Egyptienne, D. T. & Hedley, D. W. Cancer Stem Cells, Hypoxia and Metastasis. *Seminars in Radiation Oncology* **19,** 106–111 (2009).

72. Ma, S. *et al.* Identification and Characterization of Tumorigenic Liver Cancer Stem/Progenitor Cells. *Gastroenterology* **132,** 2542–2556 (2007).

73. Hermann, P. C. *et al.* Distinct populations of cancer stem cells determine tumor growth and metastatic activity in human pancreatic cancer. *Cell Stem Cell* **1,** 313–23 (2007).

74. Chen, K., Huang, Y. & Chen, J. Understanding and targeting cancer stem cells: therapeutic implications and challenges. *Acta Pharmacol. Sin.* **34,** 732–740 (2013).

75. Hu, Y. & Fu, L. Targeting cancer stem cells: a new therapy to cure cancer patients. *Am. J. Cancer Res.* **2,** 340–56 (2012).

76. McDermott, S. P. & Wicha, M. S. Targeting breast cancer stem cells. *Molecular Oncology* **4,** 404–419 (2010).

77. Krause, M., Dubrovska, A., Linge, A. & Baumann, M. Cancer stem cells: Radioresistance, prediction of radiotherapy outcome and specific targets for combined treatments. *Advanced Drug Delivery Reviews* (2015). doi:10.1016/j.addr.2016.02.002

78. Maugeri-Saccà, M., Bartucci, M. & De Maria, R. DNA damage repair pathways in cancer stem cells. *Mol. Cancer Ther.* **11,** 1627–36 (2012).

79. Lord, C. The DNA damage response and cancer therapy. *Nature* **481,** 287–94 (2012).

80. Kalin, T. V., Ustiyan, V. & Kalinichenko, V. V. Multiple faces of FoxM1 transcription factor: Lessons from transgenic mouse models. *Cell Cycle* **10,** 396–405 (2011).

81. Laoukili, J. *et al.* FoxM1 is required for execution of the mitotic programme and chromosome stability. *Nat. Cell Biol.* **7,** 126–136 (2005).

82. Laoukili, J., Stahl, M. & Medema, R. H. FoxM1: At the crossroads of ageing and cancer. *Biochimica et Biophysica Acta - Reviews on Cancer* **1775,** 92–102 (2007).

83. Krupczak-Hollis, K. *et al.* The mouse Forkhead Box m1 transcription factor is essential for hepatoblast mitosis and development of intrahepatic bile ducts and vessels during liver morphogenesis. *Dev. Biol.* **276,** 74–88 (2004).

84. Wang, I.-C. *et al.* Forkhead box M1 regulates the transcriptional network of genes essential for mitotic progression and genes encoding the SCF (Skp2-Cks1) ubiquitin ligase. *Mol. Cell. Biol.* **25,** 10875–94 (2005).

85. Wierstra, I. The transcription factor FOXM1 (Forkhead box M1): Proliferation-specific expression, transcription factor function, target genes, mouse models, and normal biological roles. *Adv. Cancer Res.* **118,** 97–398 (2013).

86. Zhang, H. *et al.* The FoxM1 transcription factor is required to maintain pancreatic beta-cell mass. *Mol. Endocrinol.* **20,** 1853–1866 (2006).

87. Tan, Y., Yoshida, Y., Hughes, D. E. & Costa, R. H. Increased Expression of Hepatocyte Nuclear Factor 6 Stimulates Hepatocyte Proliferation During Mouse Liver Regeneration. *Gastroenterology* **130,** 1283–1300 (2006).

88. Zhao, Y. Y. *et al.* Endothelial cell-restricted disruption of FoxM1 impairs endothelial repair following LPS-induced vascular injury. *J. Clin. Invest.* **116,** 2333–2343 (2006).

89. Kalinichenko, V. V. *et al.* Ubiquitous expression of the Forkhead Box M1B transgene accelerates proliferation of distinct pulmonary cell types following lung injury. *J. Biol. Chem.* **278,** 37888–37894 (2003).

90. Wang, X. *et al.* Increased levels of forkhead box M1B transcription factor in transgenic mouse hepatocytes prevent age-related proliferation defects in regenerating liver. *Proc. Natl. Acad. Sci. U. S. A.* **98,** 11468–11473 (2001).

91. Park, H. J. *et al.* FoxM1, a critical regulator of oxidative stress during oncogenesis. *EMBO J* **28,** 2908–2918 (2009).

92. Droge, W. Free radicals in the physiological control of cell function. *Physiol. Rev.* **82,** 47–95 (2002).

93. Le Belle, J. E. *et al.* Proliferative neural stem cells have high endogenous ROS levels that regulate self-renewal and neurogenesis in a PI3K/Akt-dependant manner. *Cell Stem Cell* **8,** 59–71 (2011).

94. Bigarella, C. L., Liang, R. & Ghaffari, S. Stem cells and the impact of ROS signaling. *Development* **141,** 4206–18 (2014).

95. Raychaudhuri, P. & Park, H. J. FoxM1: A master regulator of tumor metastasis. *Cancer Research* **71,** 4329–4333 (2011).

96. Pandit, B., Halasi, M. & Gartel, A. L. p53 negatively regulates expression of FoxM1. *Cell Cycle* **8,** 3425–3427 (2009).

97. Barsotti, A. M. & Prives, C. Pro-proliferative FoxM1 is a target of p53-mediated repression. *Oncogene* **28,** 4295–305 (2009).

98. Wierstra, I. & Alves, J. Transcription factor FOXM1c is repressed by RB and activated by cyclin D1/Cdk4. *Biol. Chem.* **387,** 949–962 (2006).

99. Gusarova, G. A. *et al.* A cell-penetrating ARF peptide inhibitor of FoxM1 in mouse hepatocellular carcinoma treatment. *J. Clin. Invest.* **117,** 99–111 (2007).

100. Wang, Z. *et al.* FoxM1 in tumorigenicity of the neuroblastoma cells and renewal of the neural progenitors. *Cancer Res.* **71,** 4292–4302 (2011).

101. Gong, A. H. *et al.* FoxM1 drives a feed-forward STAT3-activation signaling loop that promotes the self-renewal and tumorigenicity of glioblastoma stem-like cells. *Cancer Res.* **75,** 2337–2348 (2015).

102. Yang, C. *et al.* Inhibition of FOXM1 transcription factor suppresses cell proliferation and tumor growth of breast cancer. *Cancer Gene Ther.* **20,** 117–24 (2013).

103. Carr, J. R., Park, H. J., Wang, Z., Kiefer, M. M. & Raychaudhuri, P. FoxM1 mediates resistance to herceptin and paclitaxel. *Cancer Res.* **70,** 5054–5063 (2010).

104. Wang, I. C. *et al.* FoxM1 regulates transcription of JNK1 to promote the G1/S transition and tumor cell invasiveness. *J. Biol. Chem.* **283,** 20770–20778 (2008).

105. Yang, C. *et al.* FOXM1 promotes the epithelial to mesenchymal transition by stimulating the transcription of Slug in human breast cancer. *Cancer Lett.* **340,** 104–112 (2013).

106. Balli, D. *et al.* Foxm1 transcription factor is required for lung fibrosis and epithelial-to-mesenchymal transition. *Embo J* **32,** 231–244 (2013).

107. Meng, F. Di *et al.* FoxM1 overexpression promotes epithelial-mesenchymal transition and metastasis of hepatocellular carcinoma. *World J. Gastroenterol.* **21,** 196–213 (2015).

108. Bao, B. *et al.* Over-expression of FoxM1 leads to epithelial-mesenchymal transition and cancer stem cell phenotype in pancreatic cancer cells. *J. Cell. Biochem.* **112,** 2296–2306 (2011).

109. Park, H. J. *et al.* Deregulation of FoxM1b leads to tumour metastasis. *EMBO Mol. Med.* **3,** 21–34 (2011).

110. Alexander, D. *et al.* High-grade tumor differentiation is an indicator of poor

prognosis in African Americans with colonic adenocarcinomas. *Cancer* **103,** 2163–2170 (2005).

111. HAKYEMEZ, B. *et al.* High-grade and low-grade gliomas: differentiation by using perfusion MR imaging. *Clin. Radiol.* **60,** 493–502 (2005).

112. Carr, J. R. *et al.* FoxM1 Regulates Mammary Luminal Cell Fate. *Cell Rep.* **1,** 715–729 (2012).

113. Chou, J., Provot, S. & Werb, Z. GATA3 in development and cancer differentiation: Cells GATA have it! *Journal of Cellular Physiology* **222,** 42–49 (2010).

114. Usary, J. *et al.* Mutation of GATA3 in human breast tumors. *Oncogene* **23,** 7669–7678 (2004).

115. Asselin-Labat, M. L. *et al.* Gata-3 is an essential regulator of mammary-gland morphogenesis and luminal-cell differentiation. *Nat Cell Biol* **9,** 201–209 (2007).

116. Wang, A. G. *et al.* Gender-dependent hepatic alterations in H-ras12V transgenic mice. *J. Hepatol.* **43,** 836–844 (2005).

117. Feil, S., Valtcheva, N. & Feil, R. Inducible cre mice. *Methods Mol. Biol.* **530,** 343–363 (2009).

118. Ghosh, K. & Van Duyne, G. D. Cre-loxp biochemistry. *Methods* **28,** 374–383 (2002).

119. He, G. *et al.* Identification of Liver Cancer Progenitors Whose Malignant Progression Depends on Autocrine IL-6 Signaling. *Cell* **155,** 384–396 (2017).

120. Ma, S. *et al.* miR-130b Promotes CD133(+) liver tumor-initiating cell growth and self-renewal via tumor protein 53-induced nuclear protein 1. *Cell Stem Cell* **7,** 694–707 (2010).

121. Charette, N. *et al.* Salirasib inhibits the growth of hepatocarcinoma cell lines in vitro and tumor growth in vivo through ras and mTOR inhibition. *Mol. Cancer* **9,** 256 (2010).

122. Gemenetzidis, E. *et al.* Induction of human epithelial stem/progenitor expansion by FOXM1. *Cancer Res.* **70,** 9515–9526 (2010).

123. Liu, L. L., Fu, D., Ma, Y. & Shen, X. Z. The power and the promise of liver cancer stem cell markers. *Stem Cells Dev* **20,** 2023–2030 (2011).

124. Sun, H. *et al.* FOXM1 expression predicts the prognosis in hepatocellular carcinoma patients after orthotopic liver transplantation combined with the Milan criteria. *Cancer Lett.* **306,** 214–222 (2011).

125. Sun, H.-C. *et al.* Overexpression of Forkhead box M1 protein associates with aggressive tumor features and poor prognosis of hepatocellular carcinoma. *Oncol. Rep.* **25,** 1533–1539 (2011).

126. Kalinichenko, V. V *et al.* Foxm1b transcription factor is essential for development of hepatocellular carcinomas and is negatively regulated by the p19ARF tumor suppressor. *Genes Dev.* **18,** 830–850 (2004).

127. Gong, A. & Huang, S. FoxM1 and Wnt/beta-catenin signaling in glioma stem cells. *Cancer Res.* **72,** 5658–5662 (2012).

128. Xie, Z. *et al.* Foxm1 transcription factor is required for maintenance of pluripotency of P19 embryonal carcinoma cells. *Nucleic Acids Res.* **38,** 8027–8038 (2010).

129. Bella, L., Zona, S., Nestal de Moraes, G. & Lam, E. W. F. FOXM1: A key oncofoetal transcription factor in health and disease. *Seminars in Cancer Biology* **29,** 32–39 (2014).

130. Lee, C. S., Friedman, J. R., Fulmer, J. T. & Kaestner, K. H. The initiation of liver development is dependent on Foxa transcription factors. *Nature* **435,** 944–947 (2005).

131. Gordillo, M., Evans, T. & Gouon-Evans, V. Orchestrating liver development. *Development* **142,** 2094–2108 (2015).

132. Li, Z., Tuteja, G., Schug, J. & Kaestner, K. H. Foxa1 and Foxa2 are essential for sexual dimorphism in liver cancer. *Cell* **148,** 72–83 (2012).

133. Wang, J. *et al.* FOXA2 suppresses the metastasis of hepatocellular carcinoma partially through matrix metalloproteinase-9 inhibition. *Carcinogenesis* **35,** 2576–2583 (2014).

134. Halasi, M. & Gartel, A. L. A novel mode of FoxM1 regulation: Positive auto-regulatory loop. *Cell Cycle* **8,** 1966–1967 (2009).

135. Wang, A.-G. *et al.* Steatosis induced by the accumulation of apolipoprotein A-I and elevated ROS levels in H-ras12V transgenic mice contributes to hepatic lesions. *Biochem. Biophys. Res. Commun.* **409,** 532–538 (2011).

136. Wang, I.-C. *et al.* Foxm1 transcription factor is required for the initiation of lung tumorigenesis by oncogenic Kras(G12D.). *Oncogene* **33,** 1–6 (2013).

137. He, G. *et al.* XIdentification of liver cancer progenitors whose malignant progression depends on autocrine IL-6 signaling. *Cell* **155,** (2013).

138. Lin, C. H., Hung, P. H. & Chen, Y. J. CD44 is associated with the aggressive phenotype of nasopharyngeal carcinoma through redox regulation. *Int. J. Mol. Sci.* **14,** 13266–13281 (2013).

139. Dhar, S. K., Tangpong, J. & Chaiswing, L. Manganese Superoxide Dismutase Is a p53 -Regulated Gene That Switches Cancers between Early and Advanced Stages Manganese Superoxide Dismutase Is a p53-Regulated Gene. *Cancer Res.* **71,** 6684–6695 (2011).

140. Holley, A. K., Dhar, S. K. & Clair, D. K. S. Manganese superoxide dismutase versus p53: The mitochondrial center. in *Annals of the New York Academy of Sciences* **1201,** 72–78 (2010).

141. Holley, A. K., Dhar, S. K. & St. Clair, D. K. Manganese superoxide dismutase vs. p53: Regulation of mitochondrial ROS. *Mitochondrion* **10,** 649–661 (2010).

142. Alder, O. *et al.* Hippo signaling influences HNF4A and FOXA2 enhancer switching during hepatocyte differentiation. *Cell Rep.* **9,** 261–271 (2014).

143. Major, M. L., Lepe, R. & Costa, R. H. Forkhead box M1B transcriptional activity requires binding of Cdk-cyclin complexes for phosphorylation-dependent recruitment of p300/CBP coactivators. *Mol. Cell. Biol.* **24,** 2649–2661 (2004).

144. Yalley, A., Schill, D., Hatta, M., Johnson, N. & Cirillo, L. A. Loss of Interdependent Binding by the FoxO1 and FoxA1/A2 Forkhead Transcription Factors Culminates in Perturbation of Active Chromatin Marks and Binding of Transcriptional Regulators at Insulin-sensitive Genes. *J. Biol. Chem.* **291,** 8848–8861 (2016).

145. Alloatti, G., Montrucchio, G., Lembo, G. & Hirsch, E. Phosphoinositide 3-kinase and Forkhead, a switch f... [Biochem Soc Trans. 2004] - PubMed result. *Biochem. Soc. Trans.* **32,** 383–6 (2004).

146. Schübeler, D. Function and information content of DNA methylation. *Nature* **517,** 321–326 (2015).

147. Feng, Q. & Zhang, Y. The MeCP1 complex represses transcription through preferential binding, remodeling, and deacetylating methylated nucleosomes. *Genes Dev.* **15,** 827–832 (2001).

148. Mendenhall, E. M. *et al.* GC-rich sequence elements recruit PRC2 in mammalian ES cells. *PLoS Genet.* **6,** 1–10 (2010).

149. Fajas, L., Debril, M. B. & Auwerx, J. Peroxisome proliferator-activated receptor-gamma: from adipogenesis to carcinogenesis. *J. Mol. Endocrinol.* **27,** 1–9 (2001).

150. Calo, E. *et al.* Rb regulates fate choice and lineage commitment in vivo. *Nature* **466,** 1110–1114 (2010).

151. Dali-Youcef, N. *et al.* Adipose tissue-specific inactivation of the retinoblastoma protein protects against diabesity because of increased energy expenditure. *Proc. Natl. Acad. Sci. U. S. A.* **104,** 10703–8 (2007).

152. Gonzales, K. A. U. *et al.* Deterministic Restriction on Pluripotent State Dissolution by Cell-Cycle Pathways. *Cell* **162,** 564–579 (2015).

# VITA

**NAME** Akshay Pandey

**EDUCATION** B.Tech, Biotechnology, Vellore Institute of Technology, Vellore, India

**PUBLICATIONS**

**p19Arf Inhibits H-Ras induced aggressive progression of hepatocellular carcinoma**, Carcinogenesis (under review), Dragana Kopanja, **Akshay Pandey**, Shuo Huang, Grace Guzman, Mohamed Rizwan Haroon Al Raheed, Grace Guzman, Pradip Raychaudhuri

**Epigenetic suppression of the hepatic specification genes FoxA1/A2 by FoxM1 in high-grade liver cancer**, Nature Communications (revised and re-submitted), Vaibhav Chand#, **Akshay Pandey#**, Dragana Kopanja, Grace Guzman, Pradip Raychaudhuri (# - equal contribution)

**Plk1 regulates the repressor function of FoxM1b by inhibiting its interaction with Retinoblastoma**, Nature Scientific Reports, 2017, Nishit K Mukhopadhyay, Vaibhav Chand, **Akshay Pandey**, Dragana Kopanja, Janai R. Carr, Yi-Ju Chen, Xiubei Liao, Pradip Rayhaudhuri.

**Essential roles of FoxM1 in Ras-induced liver cancer progression and in cancer cells with stem cell features, Journal of Hepatology**, 2015, Kopanja D, **Pandey A**, Kiefer M, Wang Z, Chandan N, Carr JR, Franks R, Yu DY, Guzman G, Maker A, Raychaudhuri P.

**Radioresistant Sf9 insect cells undergo an atypical form of Bax-dependent apoptosis at very high doses of γ-radiation**, Int J Radiat Biol., 2013, Chandna S, Suman S, Chandna M, **Pandey A**, Singh V, Kumar A, Dwarakanath BS, Seth RK.

**An improved non-enzymatic "DNA ladder assay" for more sensitive and early detection of apoptosis**, Cytotechnology, 2012, Suman S, **Pandey A**, Chandna S.

**Predictive role of mitochondrial genome in the stress resistance of insects and nematodes**, Bioinformation, 2010, **Akshay Pandey**, Shubankar Suman and Sudhir Chandna.

ELSEVIER LICENSE
TERMS AND CONDITIONS
Jun 14, 2017

---

This Agreement between Akshay Pandey ("You") and Elsevier ("Elsevier") consists of your license details and the terms and conditions provided by Elsevier and Copyright Clearance Center.

| | |
|---|---|
| License Number | 4085960691438 |
| License date | Apr 11, 2017 |
| Licensed Content Publisher | Elsevier |
| Licensed Content Publication | Journal of Hepatology |
| Licensed Content Title | Essential roles of FoxM1 in Ras-induced liver cancer progression and in cancer cells with stem cell features |
| Licensed Content Author | Dragana Kopanja,Akshay Pandey,Megan Kiefer,Zebin Wang,Neha Chandan,Janai R. Carr,Roberta Franks,Dae-Yeul Yu,Grace Guzman,Ajay Maker,Pradip Raychaudhuri |
| Licensed Content Date | Aug 1, 2015 |
| Licensed Content Volume | 63 |
| Licensed Content Issue | 2 |
| Licensed Content Pages | 8 |
| Start Page | 429 |
| End Page | 436 |
| Type of Use | reuse in a thesis/dissertation |
| Portion | full article |
| Format | both print and electronic |
| Are you the author of this Elsevier article? | Yes |
| Will you be translating? | No |
| Order reference number | |
| Title of your thesis/dissertation | Role of FoxM1 in Ras induced HCC |
| Expected completion date | May 2017 |
| Estimated size (number of pages) | 150 |
| Elsevier VAT | GB 494 6272 12 |

| | |
|---|---|
| number | GB 494 6272 12 |
| Requestor Location | Akshay Pandey<br>900 S Ashland<br>room # 2218<br>Molecular Biology Research Building<br>CHICAGO, IL 60607<br>United States<br>Attn: Akshay Pandey |
| Publisher Tax ID | 98-0397604 |
| Billing Type | Invoice |
| Billing Address | Akshay Pandey<br>900 S Ashland<br>room # 2218<br>Molecular Biology Research Building<br>CHICAGO, IL 60607<br>United States<br>Attn: Akshay Pandey |
| Total | 0.00 USD |

Terms and Conditions

## INTRODUCTION

1. The publisher for this copyrighted material is Elsevier. By clicking "accept" in connection with completing this licensing transaction, you agree that the following terms and conditions apply to this transaction (along with the Billing and Payment terms and conditions established by Copyright Clearance Center, Inc. ("CCC"), at the time that you opened your Rightslink account and that are available at any time at http://myaccount.copyright.com).

## GENERAL TERMS

2. Elsevier hereby grants you permission to reproduce the aforementioned material subject to the terms and conditions indicated.

3. Acknowledgement: If any part of the material to be used (for example, figures) has appeared in our publication with credit or acknowledgement to another source, permission must also be sought from that source. If such permission is not obtained then that material may not be included in your publication/copies. Suitable acknowledgement to the source must be made, either as a footnote or in a reference list at the end of your publication, as follows:

"Reprinted from Publication title, Vol /edition number, Author(s), Title of article / title of chapter, Pages No., Copyright (Year), with permission from Elsevier [OR APPLICABLE SOCIETY COPYRIGHT OWNER]." Also Lancet special credit - "Reprinted from The Lancet, Vol. number, Author(s), Title of article, Pages No., Copyright (Year), with permission from Elsevier."

4. Reproduction of this material is confined to the purpose and/or media for which permission is hereby given.

5. Altering/Modifying Material: Not Permitted. However figures and illustrations may be altered/adapted minimally to serve your work. Any other abbreviations, additions, deletions and/or any other alterations shall be made only with prior written authorization of Elsevier Ltd. (Please contact Elsevier at permissions@elsevier.com). No modifications can be made

to any Lancet figures/tables and they must be reproduced in full.

6. If the permission fee for the requested use of our material is waived in this instance, please be advised that your future requests for Elsevier materials may attract a fee.

7. Reservation of Rights: Publisher reserves all rights not specifically granted in the combination of (i) the license details provided by you and accepted in the course of this licensing transaction, (ii) these terms and conditions and (iii) CCC's Billing and Payment terms and conditions.

8. License Contingent Upon Payment: While you may exercise the rights licensed immediately upon issuance of the license at the end of the licensing process for the transaction, provided that you have disclosed complete and accurate details of your proposed use, no license is finally effective unless and until full payment is received from you (either by publisher or by CCC) as provided in CCC's Billing and Payment terms and conditions. If full payment is not received on a timely basis, then any license preliminarily granted shall be deemed automatically revoked and shall be void as if never granted. Further, in the event that you breach any of these terms and conditions or any of CCC's Billing and Payment terms and conditions, the license is automatically revoked and shall be void as if never granted. Use of materials as described in a revoked license, as well as any use of the materials beyond the scope of an unrevoked license, may constitute copyright infringement and publisher reserves the right to take any and all action to protect its copyright in the materials.

9. Warranties: Publisher makes no representations or warranties with respect to the licensed material.

10. Indemnity: You hereby indemnify and agree to hold harmless publisher and CCC, and their respective officers, directors, employees and agents, from and against any and all claims arising out of your use of the licensed material other than as specifically authorized pursuant to this license.

11. No Transfer of License: This license is personal to you and may not be sublicensed, assigned, or transferred by you to any other person without publisher's written permission.

12. No Amendment Except in Writing: This license may not be amended except in a writing signed by both parties (or, in the case of publisher, by CCC on publisher's behalf).

13. Objection to Contrary Terms: Publisher hereby objects to any terms contained in any purchase order, acknowledgment, check endorsement or other writing prepared by you, which terms are inconsistent with these terms and conditions or CCC's Billing and Payment terms and conditions. These terms and conditions, together with CCC's Billing and Payment terms and conditions (which are incorporated herein), comprise the entire agreement between you and publisher (and CCC) concerning this licensing transaction. In the event of any conflict between your obligations established by these terms and conditions and those established by CCC's Billing and Payment terms and conditions, these terms and conditions shall control.

14. Revocation: Elsevier or Copyright Clearance Center may deny the permissions described in this License at their sole discretion, for any reason or no reason, with a full refund payable to you. Notice of such denial will be made using the contact information provided by you. Failure to receive such notice will not alter or invalidate the denial. In no event will Elsevier or Copyright Clearance Center be responsible or liable for any costs, expenses or damage incurred by you as a result of a denial of your permission request, other than a refund of the amount(s) paid by you to Elsevier and/or Copyright Clearance Center for denied

permissions.

**LIMITED LICENSE**

The following terms and conditions apply only to specific license types:

15. **Translation**: This permission is granted for non-exclusive world **English** rights only unless your license was granted for translation rights. If you licensed translation rights you may only translate this content into the languages you requested. A professional translator must perform all translations and reproduce the content word for word preserving the integrity of the article.

16. **Posting licensed content on any Website**: The following terms and conditions apply as follows: Licensing material from an Elsevier journal: All content posted to the web site must maintain the copyright information line on the bottom of each image; A hyper-text must be included to the Homepage of the journal from which you are licensing at http://www.sciencedirect.com/science/journal/xxxxx or the Elsevier homepage for books at http://www.elsevier.com; Central Storage: This license does not include permission for a scanned version of the material to be stored in a central repository such as that provided by Heron/XanEdu.

Licensing material from an Elsevier book: A hyper-text link must be included to the Elsevier homepage at http://www.elsevier.com . All content posted to the web site must maintain the copyright information line on the bottom of each image.

**Posting licensed content on Electronic reserve**: In addition to the above the following clauses are applicable: The web site must be password-protected and made available only to bona fide students registered on a relevant course. This permission is granted for 1 year only. You may obtain a new license for future website posting.

17. **For journal authors:** the following clauses are applicable in addition to the above:

**Preprints:**

A preprint is an author's own write-up of research results and analysis, it has not been peer-reviewed, nor has it had any other value added to it by a publisher (such as formatting, copyright, technical enhancement etc.).

Authors can share their preprints anywhere at any time. Preprints should not be added to or enhanced in any way in order to appear more like, or to substitute for, the final versions of articles however authors can update their preprints on arXiv or RePEc with their Accepted Author Manuscript (see below).

If accepted for publication, we encourage authors to link from the preprint to their formal publication via its DOI. Millions of researchers have access to the formal publications on ScienceDirect, and so links will help users to find, access, cite and use the best available version. Please note that Cell Press, The Lancet and some society-owned have different preprint policies. Information on these policies is available on the journal homepage.

**Accepted Author Manuscripts:** An accepted author manuscript is the manuscript of an article that has been accepted for publication and which typically includes author-incorporated changes suggested during submission, peer review and editor-author communications.

Authors can share their accepted author manuscript:

- immediately
    - via their non-commercial person homepage or blog
    - by updating a preprint in arXiv or RePEc with the accepted manuscript
    - via their research institute or institutional repository for internal institutional uses or as part of an invitation-only research collaboration work-group
    - directly by providing copies to their students or to research collaborators for their personal use
    - for private scholarly sharing as part of an invitation-only work group on commercial sites with which Elsevier has an agreement
- After the embargo period
    - via non-commercial hosting platforms such as their institutional repository
    - via commercial sites with which Elsevier has an agreement

In all cases accepted manuscripts should:

- link to the formal publication via its DOI
- bear a CC-BY-NC-ND license - this is easy to do
- if aggregated with other manuscripts, for example in a repository or other site, be shared in alignment with our hosting policy not be added to or enhanced in any way to appear more like, or to substitute for, the published journal article.

**Published journal article (JPA):** A published journal article (PJA) is the definitive final record of published research that appears or will appear in the journal and embodies all value-adding publishing activities including peer review co-ordination, copy-editing, formatting, (if relevant) pagination and online enrichment.

Policies for sharing publishing journal articles differ for subscription and gold open access articles:

**Subscription Articles:** If you are an author, please share a link to your article rather than the full-text. Millions of researchers have access to the formal publications on ScienceDirect, and so links will help your users to find, access, cite, and use the best available version.

Theses and dissertations which contain embedded PJAs as part of the formal submission can be posted publicly by the awarding institution with DOI links back to the formal publications on ScienceDirect.

If you are affiliated with a library that subscribes to ScienceDirect you have additional private sharing rights for others' research accessed under that agreement. This includes use for classroom teaching and internal training at the institution (including use in course packs and courseware programs), and inclusion of the article for grant funding purposes.

**Gold Open Access Articles:** May be shared according to the author-selected end-user license and should contain a CrossMark logo, the end user license, and a DOI link to the formal publication on ScienceDirect.

Please refer to Elsevier's posting policy for further information.

18. **For book authors** the following clauses are applicable in addition to the above: Authors are permitted to place a brief summary of their work online only. You are not allowed to download and post the published electronic version of your chapter, nor may you scan the printed edition to create an electronic version. **Posting to a repository:** Authors are

permitted to post a summary of their chapter only in their institution's repository.

19. **Thesis/Dissertation**: If your license is for use in a thesis/dissertation your thesis may be submitted to your institution in either print or electronic form. Should your thesis be published commercially, please reapply for permission. These requirements include permission for the Library and Archives of Canada to supply single copies, on demand, of the complete thesis and include permission for Proquest/UMI to supply single copies, on demand, of the complete thesis. Should your thesis be published commercially, please reapply for permission. Theses and dissertations which contain embedded PJAs as part of the formal submission can be posted publicly by the awarding institution with DOI links back to the formal publications on ScienceDirect.

## Elsevier Open Access Terms and Conditions

You can publish open access with Elsevier in hundreds of open access journals or in nearly 2000 established subscription journals that support open access publishing. Permitted third party re-use of these open access articles is defined by the author's choice of Creative Commons user license. See our open access license policy for more information.

**Terms & Conditions applicable to all Open Access articles published with Elsevier:**

Any reuse of the article must not represent the author as endorsing the adaptation of the article nor should the article be modified in such a way as to damage the author's honour or reputation. If any changes have been made, such changes must be clearly indicated.

The author(s) must be appropriately credited and we ask that you include the end user license and a DOI link to the formal publication on ScienceDirect.

If any part of the material to be used (for example, figures) has appeared in our publication with credit or acknowledgement to another source it is the responsibility of the user to ensure their reuse complies with the terms and conditions determined by the rights holder.

**Additional Terms & Conditions applicable to each Creative Commons user license:**

**CC BY:** The CC-BY license allows users to copy, to create extracts, abstracts and new works from the Article, to alter and revise the Article and to make commercial use of the Article (including reuse and/or resale of the Article by commercial entities), provided the user gives appropriate credit (with a link to the formal publication through the relevant DOI), provides a link to the license, indicates if changes were made and the licensor is not represented as endorsing the use made of the work. The full details of the license are available at http://creativecommons.org/licenses/by/4.0.

**CC BY NC SA:** The CC BY-NC-SA license allows users to copy, to create extracts, abstracts and new works from the Article, to alter and revise the Article, provided this is not done for commercial purposes, and that the user gives appropriate credit (with a link to the formal publication through the relevant DOI), provides a link to the license, indicates if changes were made and the licensor is not represented as endorsing the use made of the work. Further, any new works must be made available on the same conditions. The full details of the license are available at http://creativecommons.org/licenses/by-nc-sa/4.0.

**CC BY NC ND:** The CC BY-NC-ND license allows users to copy and distribute the Article, provided this is not done for commercial purposes and further does not permit distribution of the Article if it is changed or edited in any way, and provided the user gives appropriate

credit (with a link to the formal publication through the relevant DOI), provides a link to the license, and that the licensor is not represented as endorsing the use made of the work. The full details of the license are available at http://creativecommons.org/licenses/by-nc-nd/4.0. Any commercial reuse of Open Access articles published with a CC BY NC SA or CC BY NC ND license requires permission from Elsevier and will be subject to a fee.

Commercial reuse includes:

- Associating advertising with the full text of the Article
- Charging fees for document delivery or access
- Article aggregation
- Systematic distribution via e-mail lists or share buttons

Posting or linking by commercial companies for use by customers of those companies.

20. **Other Conditions**:

v1.9

**Questions? customercare@copyright.com or +1-855-239-3415 (toll free in the US) or +1-978-646-2777.**